ACTA UNIVERSITATIS SZEGEDIENSIS

ACTA MINERALOGICA-PETROGRAPHICA

TOMUS XXV, Fasc. 2

SZEGED, HUNGARIA
1982

ACTA UNIVERSITATIS SZEGEDIENSIS

ACTA MINERALOGICA-PETROGRAPHICA

TOMUS XXV, Fasc. 2

SZEGED, HUNGARIA
1982

HU ISSN 0365—8066

Adjuvantibus

BÉLA MOLNÁR et TIBOR SZEDERKÉNYI

Redigit

GYULA GRASSELLY

Edit

Institutum Mineralogicum, Geochimicum et Petrographicum
Universitatis Szegediensis de Attila József nominatae
Egyetem u. 2—6., H—6722 Szeged, Hungary

Nota

Acta Miner. Petr., Szeged

Szerkeszti

GRASSELLY GYULA

a szerkesztő bizottság tagjai

MOLNÁR BÉLA és SZEDERKÉNYI TIBOR

Kiadja

a József Attila Tudományegyetem Ásványtani, Geokémiai és Kőzettani Tanszéke
H-6722 Szeged, Egyetem u. 2—6.

Kiadványunk címének rövidítése
Acta Miner. Petr., Szeged

Acta Mineralogica-Petrographica, Szeged, XXV/2, 131—145, 1982

ON THE ROLE OF TEMPERATURE AND PRESSURE IN THE ARTIFICIAL EVOLUTION OF ORGANIC MATTER OF THE PULA OIL SHALE (HUNGARY)

M. HETÉNYI, J. TÓTH and GY. MILLEY

INTRODUCTION

The Upper Pannonian oil shale of Pula (Hungary, Transdanubia) provides advantageous material for the experiments investigating the evolution of the sedimentary organic matter since it contains considerable amount of organic matter of algal origin being in the initial stage of evolution.

Factors determining the evolution of organic matter are the environmental conditions being changed during sedimentation and subsidence, the increase of pressure and temperature, as well as the geological time during which the degradation of organic matter proceeds just on the effect of above parameters. Under natural conditions the three influences cannot be separated from each other, moreover other factors (*e.g.* mineral components, water) should also be taken into account. Only the laboratory experiments make possible to study the independent effects of these parameters. In order to study the possible widest interval of evolution process, kerogen of early evolutionary stage is to be used as raw material.

The physical and chemical analysis of samples of great number taken from different depths of sedimentary basins, as well as the laboratory experiments showed that the process of degradation is determined primarily by the temperature. Temperature plays such an important role that the economically most important stage of kerogen evolution, i.e. the catagenesis can be simulated by means of thermal degradation. This artificially produced process provides possibility to follow the change of kerogen during evolution. The chemical composition of products and of oil formed during the laboratory and natural degradation, slightly differs just because of temperature differences [TISSOT and WELTE, 1978]. Higher temperatures favour the formation of products of smaller C-number. The basis of this simulation is the reaction kinetics of the process. According to most of researchers the transformation of the organic matter is a first-order or at least a pseudo-first-order reaction [DI RICCO, 1956; CANE, 1948, 1976; CONNAN, 1974; WEITKAMP *et al.* 1970; CUMMINS and ROBINSON, 1972; TISSOT and WELTE, 1978].

In accordance to the ARRHENIUS-equation the temperature and the reaction time may mathematically compensate each other. This makes possible to approach certain stages of natural processes by means of model experiments of much shorter time but at somewhat higher temperature.

As it was emphasized by TISSOT and WELTE [1978] and STRAKHOV [1962], temperature is of decisive role in the first stage of evolution of organic matter (called diagenesis after STRAKHOV), but it is only one and not the primary parameter. Having studied the role of pressure in the degradation of kerogen, temperature values were chosen with changing pressures, which fall to the temperature range of experimental

simulation of diagenesis. It seems to be expedient to study the effect of pressure in the stage of diagenesis where temperature plays less important role, since according to the uniform view of researchers pressure plays subordinate role as compared to that of the temperature concerning the whole process. Within the given stage, however, relatively high temperature was chosen in order to observe the changes. At low temperature the preformed hydrocarbon of the sample is released, the gases however, produced at about 150—200°C are undoubtedly the degradation products of kerogen [ABELSON, 1967]. At this temperature the carbon dioxide production exceeds that of the hydrocarbons, at 300°C, however, the hydrocarbon production is considerably accelerated, too.

The limit of experimental simulation of diagenesis and catagenesis, as well as the upper limit of catagenesis were determined by TISSOT and WELTE [1978] at about 350°C and between 470 and 500°C, respectively. The validity of these values were experimentally verified in case of Pula oil shale used as raw material in the measurements to be discussed below [HETÉNYI, 1980].

Taking into account these facts, measurements aiming the investigation of the effect of temperature were carried out between 325 and 500°C at different temperatures, starting somewhat lower temperatures than the lower limit. The effect of pressure was studied at 260°C at overpressure 0, 200, 300, 400 bars. In the case of latter experiments special attention was taken to the gaseous products. In all measurements the unconverted organic matter was characterized and the quantity of bitumen was determined which is usually believed to be an intermediate product produced during the evolution of kerogen [ABELSON, 1967; VITOROVIĆ and JOVANOVIĆ, 1968; CARLSON *et al.*, 1937; CANE, 1951]. The role of degradation time was studied and kinetic calculations were also made.

EXPERIMENTAL

The air-dried oil shale sample was ground to the grain size of 0.05—0.15 mm, then the bitumen was extracted in Soxhlet extractor in two stages: first by chloroform (Bit-A), then by benzene:acetone:methanol mixture of 70:15:15 ratio (BAM-bitumen). After the extraction kerogen was izolated from the inorganic components by means of physical enrichment, *i.e.* by specific gravity separation.

The thermal degradation was carried out in a furnace provided by programmed heating, in an ignition glass tube, in nitrogen stream. The oil was collected in an air-cooled and adjoining trap cooled with salted ice.

The investigation of the effect of pressure was carried out in a special GEOTERD equipment *(Fig. 1)*. During measurements the required pressure was assured by a hydraulic compressor and a suitably processed membrane. The sample was diluted with glass beads in order to eliminate the compaction of the sample caused by the pressure effect.

The most important parts of GEOTERD device are as follows:

— the GEOTERD cell with a hot trap mounted to the output;

— air thermostate with „kaowool" isolation (only indicated on the figure),

— hydraulic compressor (adjoining the pressing rod „15", not indicated in the figure),

— gas flow meter and the liquid air-cooled cold trap (not indicated in the figure).

Between the conical piston and the pressing rod, between the upper margin of the cell and the top cover an elastic gas-insulating membrane is built in which en-

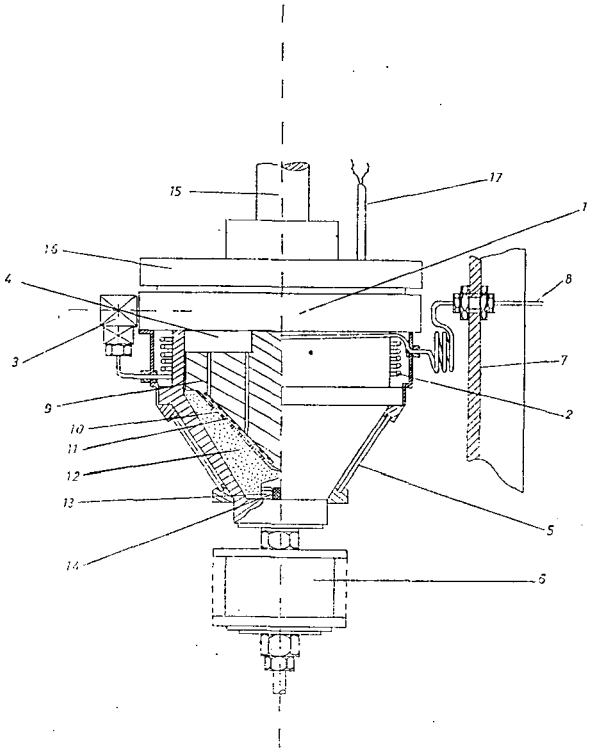

Fig. 1. Sketch of the GEOTERD device

1. Cell of GEOTERD
2. Preheating tube-coil (stainless steel, i.d. 2.2 mm)
3. Gas inlet port
4. Space filled with the eluent gas
5. Cell heating elements
6. Hot trap
7. Steel frame of the device
8. Gas inlet tube
9. Conical pressing pistone
10. Perforated stainless steel cover
11. Stainless steel mesh (45 μm)
12. Test sample mixed with glass beads
13. Gas outlet port
14. Sintered glass filter
15. Pressing rod
16. Cover flange
17. Pt thermometer

sures the flushing gas to flow only through the bores of the piston. The temperature is controlled by a two-stage electronic thermoregulator operated by a Pt-resistivity thermometer. The high temperature gas when leaving the cell, flows through the labyrinth-like hot-trap then gets the liquid air cooled special cold-trap where the hydrocarbons heavier than methane will be released. The cooled gas flows through

a rotameter which serves to control and state the 7—9 litre/min velocity of the flushing gas.

According to *Fig. 1* the device operates as follows: the moisture-free flushing gas is directed first through the adsorber, than through the (8) inlet tube into the (2) tube coil, which is dimensioned that the gas should reach the experimental temperature up to the (3) gas inlet port. The flushing gas gets the (4) gas space, from here it passes the vertical bores of the conical pressing piston, the (11) mesh tissue, the (10) perforated steel cover through the (12) mixture of powdered sample and glass beads, the (13) outlet port and (14) glass filter and finally gets into the hot and cold traps. In the sample the pressure is assured by the hydraulic compressor joining the (15) pressing rod. The heating elements are found at the lower conical part of the cell, their on and off stages are controlled by the electronic thermoregulator according to the sign of the Pt resistivity thermometer.

The bitumen formed during degradation was extracted in solvent mixture in Soxhlet extractor.

The hydrogen and carbon contents were determined by CHN—1 analysator.

The degradation factor denotes the carbon content (C_R) of the sample after thermal treatment at 500°C for 30 minutes in inert atmosphere, as compared to the carbon content before thermal treatment (Standard Methods of Laboratory Sampling and Analysis of Coal and Coke D 271—48, in 1952, Book of ASTM Standard, 1952).

The gas chromatographic analyses were made with a Hewlett—Packard 5750 GC equipped with flame ionization detector, electronic integrator and gas feeding apparatus. The column packing: Porapack Q, 100—120 mesh, length: 2 m, diameter 3,2 mm. Temperature: 120—170°C, 8°C/min programmed heating velocity, then at 170°C isothermal conditions. Base gas: helium 30 ml/min, auxiliary gas: helium 20 ml/min. To determine qualitatively and quantitatively the desorbed hydrocarbons external or absolute calibration method was used. Natural gas sample of known composition served as standard.

RESULTS

Characterization of the kerogen

Kerogen used in the measurements was isolated from the Pliocene (Upper Pannonian) oil shale of Pula (Hungary, Transdanubia). This oil shale was generated as a filling material of a volcanic crater lake, at 10 to 12°C, in semi-haline water. Its biological precursor proved to be the *Botryococcus braunii* KÜTZ alga [JÁMBOR and SOLTI, 1976; NAGY, 1976]. It is rich in organic matter and proves to be a near-surface alginite. According to the palynological investigations carried out on the kerogen, the preservation state of the microscopic plant remnants is excellent. The *Botryococcus* alga predominates, in addition small amount of *fungi* is found. The preservation state of *Botryococcus* coloniae and sporomorphs relates to biologically inactive sedimentation conditions.

The composition of sporomorphs according to the personal communication of M. KEDVES is as follows:

Pteridophyta

Polypodiaceae 0.8%

some perisporium specimen also occurred supporting the favourable sedimentation conditions.

Gymnospermatophyta

Abietaceae	
Pinus haploxylon type	17.7%
Pinus diploxylon type	18.7%
Tsuga	10.0%
Picea	26.3%
Pseudotsuga-Larix	0.8%
Abies	18.7%
Taxodiaceae-Cupressaceae	1.4%

Angiospermatophyta

Dicotyleodonopsida

Tiliaceae	
Tilia	0.4%
Ulmaceae	0.4%
Betulaceae	
Corylus	2.6%
Fagaceae	
cf. Quercus	0.8%
Juglandaceae	
Carya	1.4%

Only a few sporomorphs relate to shallow bog or bog forest vegetation (Taxodiaceae-Cupressaceae, Polypodiaceae with underwood). *Monocotyledons,* the *Cyperaceae, Gramineae,* as well as the dicotyledons of this biotope, e.g. *Nymphaeaceae,* the Alnus or Salix referring to bog forest, are absent. The proportion of dicotyledons are negligible, in general.

The predominance of pines is conspicuous. Among others, the pollen grains of *Tsuga, Picea, Pseudotsuga-Larix* and *Abies* relate to mountain forests [KEDVES, 1981, personal communication].

According to the technological tests, the oil shale can be qualified as an oil shale of progressed polymerization and of high kerogen content (according to the ratio of bitumen of the Fisher-distillation to that of the bitumen is greater than 2; [ARATÓ and BELLA 1976]. The organic carbon content of the average sample is 27.4%, Bit-A=3.3%, BAM-bitumen=1.3%.

Based on the behaviour during the gradual $KMnO_4$ oxidation the organic matter is an "A_1-type kerogen" according to the CANE [1976] classification [HETÉNYI and SIROKMÁN, 1978] which probably developed from algal fatty acids.

The H/C atomic ratio (1.76), the degradation factor (T_D<0.10) as well as the results of IR and NMR analyses relate to the fact that the studied kerogen is in rather immature state at the initial stage of evolution and it consists mainly of long-chain paraffin hydrocarbons built up by organic polymers.

Thermal degradation of kerogen

At low temperature (325 and 350°C) medium quantity of gas and water, small quantity (<40 mg/g organic carbon) of oil were formed during 1,5 and 10 hours. The two temperature values fall to the I stage of experimental simulation of kerogen evolution, *i.e.* to the range of diagenesis, and represent the boundary between dia-

TABLE 1

Results of thermal degradation of kerogen from Pula

Temperature (°C)	Temperature (K)	Time (hr)	Oil	BAM-bit.	Gas + water	Unconverted matter
			(mg/1 g organic carbon)			
		1	—	19	—	1329
325	598	5	28	21	86	1288
		10	28	20	114	1267
		1	—	26	—	1270
350	623	5	37	30	177	1180
		10	—	29	—	1111
		1	11	44	174	1197
375	648	5	67	51	246	1063
		10	87	31	367	981
		1	24	64	246	1089
400	673	2	83	86	245	1011
		5	145	63	282	852
		1	251	449	461	264
450	723	2	413	339	522	~150
		5	616	133	522	~150
		1	466	20	716	222
500	773	2	541	29	641	214
		5	688	4	492	224

genesis, and represent the boundary between diagenesis and catagenesis, respectively. Above 350°C the oil formation becomes more intense (Table 1). The amount of oil formed during the 5 hours of thermal treatment suddenly increases as a function of temperature between 375 and 450°C. The increase of temperature of 50°C between 450 and 500°C promotes the oil production only to a restricted extent.

Oil, gas and water are the products of the degradation of organic matter and bitumen of changing quantity can be extracted after experimental evolution in addition to the more coalified kerogen. This bitumen is probably an intermediate product according to the basic scheme of kerogen → bitumen → oil + gas + more coalified organic matter. In case of investigating the oil shale itself the verification is hindered by the fact that in the sample there is also soluble organic matter and in case of the oil shale of Pula its quantity represents high amount, *i.e.* about 4.6%. When degrading the kerogen, however, bitumen may have formed obviously during the thermal treatment of the insoluble organic matter (Table 1).

When comparing thermal treatments of same duration (5 hours), the quantity of the unconverted organic matter decreased up to 400°C. Between 400 and 500°C the degradation proved to be more intense, while between 450 and 500°C equilibrium followed *(Fig. 2)*.

The range of diagenesis is characterized mainly by the diminishing of oxygen-containing groups, thus the H/C atomic ratio expressing the relation of H- and C-content of the organic matter, slightly changed between 325 and 350°C. Above 350°C, in the range of catagenesis the release of hydrocarbons follows consequently the H/C ratio of remaining matter which considerably decreased between 375 and 500°C *(Fig. 2)*. When comparing the results comprehended in Table 2 with the data obtained by TISSOT *et al.* [1974] in the experimental simulation of kerogen of type-II, it was observed that the H/C ratios of the kerogen of type-I degraded by ourselves are somewhat higher at all temperatures, but the difference is not remarkable.

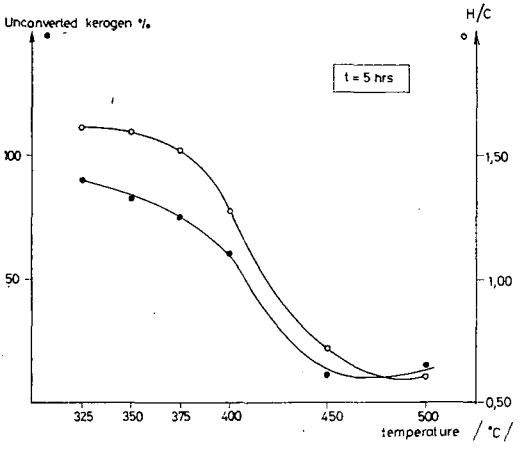

Fig. 2. Changes in the quantity and H/C atomic ratio of unconverted kerogen upon the thermal degradation

E.g. the H/C ratio of the kerogen of type-II is 0.50 and 0.61 at 500°C, at 400°C the difference is greater, *i.e.* 1.07 and 1.27.

The temporal change of the H/C atomic ratio during the experimental degradation indicates that at higher temperature the hydrocarbon production starts only after certain time interval, and this is valid also for the absolute and relative decrease of hydrogen content of remaining organic matter. At 375 and 400°C the H/C ratio scarcely changed after 1 or 2 hours, at higher temperatures not only the measure

TABLE 2

Characterization of unconverted kerogen

Temperature (°C)	(K)	Time (hr)	Quantity (%)	H/C	T_D
Unheated kerogen			—	1.76	<0.10
		1	93.4	1.76	
325	598	5	90.5	1.72	
		10	89.0	1.70	
		1	89.2	1.75	
350	623	5	82.9	1.70	
		10	81.6	1.65	
		1	84.1	1.71	0.16
375	648	5	74.7	1.63	0.21
		10	68.9	1.45	0.41
		1	76.5	1.71	0.19
400	673	2	71.0	1.70	0.44
		5	59.8	1.27	0.53
		1	18.5	1.64	0.42
450	723	2	~10.7	1.28	0.70
		5	~10.7	0.73	0.72
		1	15.6	0.67	0.67
500	773	2	15.0	0.64	1.00
		5	15.7	0.61	1.00

but the rate of the change proved to be also greater. At lower temperature, *i.e.* in the temperature range of experimental simulation of diagenesis, the chemical change of the unconverted organic matter proceeded during much longer time but showed the same tendency (Table 2). At 300°C and during 336 hours the H/C atomic ratio is the same as at 375°C during 10 hours, i.e. H/C=1.45 [HETÉNYI, 1979].

The change of degradation factor expressing the degree of degradation of organic matter ($T_D=C_R/C_T$ at 500°C) as a function of degradation time and temperature, is in accordance to the data above and indicates the development of thermal transformation.

TABLE 3

Kinetical data on thermal degradation of kerogen from Pula

Temperature (°C)	(K)	Time (hr)	$-\log(1-x)$	r^2	-10^2 m	k (per hr)
		1	0.0246			
325	598	5	0.0400	0.97	0.29	$6.7\cdot10^{-3}$
		10	0.0506			
		1	0.0453			
350	623	5	0.0783	0.95	0.57	$1.3\cdot10^{-2}$
		10	0.0969			
		1	0.0670			
375	648	5	0.1203	0.99	1.10	$2.5\cdot10^{-2}$
		10	0.1669			
		1	0.1118			
400	673	2	0.1267	0.99	1.75	$4.03\cdot10^{-2}$
		5	0.1739			
		1	0.3468			
450	723	2	0.5607	0.98	13.7	$3.16\cdot10^{-1}$
		5	0.9172			

The thermal degradation of kerogen, the quantity of the products as well as the chemical features of unconverted organic matter depend also on the duration of degradation and in addition to the temperature. The two parameters may compensate each other to a certain extent. From kinetic point of view the process assumed to be a first order one. Data concerning the degradation between 325 and 450°C are shown in Table 3. The quantity of the original material is taken as unit, x denotes the quantity of gas+water+oil produced during the conversion. In calculations bitumen was regarded as an intermediate product. The degradation time *vs.* $\log(1-x)$ relation is linear at all temperatures with good approximation *(Fig. 3)*, the correlation coefficient (r^2) is 0.95—0.99. Knowing the temperature dependence of specific reaction constants (k) computed from the slopes of curves, the apparent activation energy can be calculated from the Arrhenius-equation.

Regarding the apparent activation energy, the literature data extend over a rather wide range, *i.e.* from kJ up to 251.0—334.7 kJ. Its value may change between the low energy necessary to the decomposition of the weak, *e.g.* adsorption bonds and the 251.0—334.7 kJ required to the break of C—C bonds. It depends on the applied temperature as well as on the type of kerogen. 41.8—62.8 kJ is the apparent activation energy of the start of oil formation [TISSOT, 1969; CONNAN, 1974]. Concerning the Green River kerogen and its experimental degradation between 150 and 350°C CUMMINS and ROBINSON [1972] calculated 79.5 kJ. In case of the kerogen

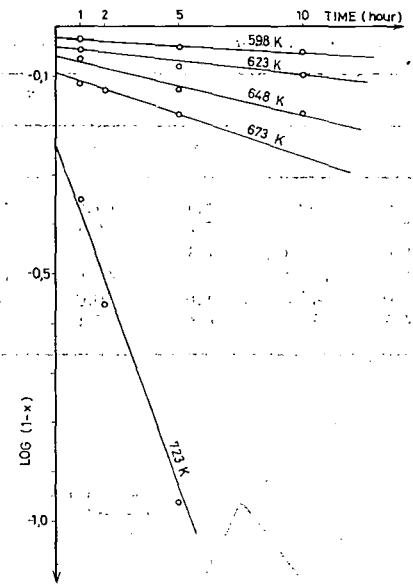

Fig. 3. First-order plot for 598 and 723 K (325°—450°C) data

of type-I according to the VAN KREVELEN diagram, TISSOT and WELTE [1978] found 125.5 and 292.8 kJ for the apparent activation energy, in addition to the 41.8—62.8 kJ mentioned above.

The values calculated for the degradation in wider temperature interval are the average values of the activation energy of different types of processes. Together with the data obtained at 300°C, the measurement results produced $E=92.0$ kJ average activation energy for the temperature range of from 300 to 450°C. Based on the same data $E=50.2$ kJ and 146.4 kJ at from 300 to 350 and from 375 to 400°C, respectively. The lower value agrees fairly well with the $E=41.8$—62.8 kJ apparent activation energy of TISSOT [1969] and CONNAN [1972] for the start of oil formation. The $E=146.4$ kJ determined at higher temperature slightly exceeds the value concerning the kerogen type-I (125.5 kJ) and is somewhat lower than the $E=167.4$ kJ determined by ABELSON [1967] in the course of experimental degradation of Green River oil shale between 185 and 400°C.

Effect of pressure on the kerogen degradation

When studying the role of pressure in the experimental evolution of diagenesis, the kerogen was degraded at 260°C at overpressure 0, 200, 300 and 400 bars. In this process considerable amount of gas was developed, and its hydrocarbon content was determined by means of gas chromatography (C_2—C_6 hydrocarbons).

The degradation time of first series was 8 hours, gas sample was taken in the 5th and 8th hours. The C_2—C_6 hydrocarbon quantities produced from 1 g kerogen are shown in Table 4, the change as a function of pressure is seen in *Fig. 4.*

The hydrocarbon production proved to be more intense during the first five hours than between the 5th and 8th hours. In the first sampling the quantity of the C_2—C_6 hydrocarbons changed according to a maximum curve as a function of pressure. The maximum is more conspicuous in case of higher carbon number, it

TABLE 4

Hydrocarbons yielded by degradation of kerogen from Pula at 260°C

PRESSURE (bar	0		200		300		400	
TIME (hr)	5	8	5	8	5	8	5	8
C_2 (ppm)	64.5	12.0	69.5	5.1	61.9	12.5	31.1	10.6
C_3	44.7	7.8	57.6	7.6	40.1	6.1	11.3	7.4
C_4	49.4	9.6	73.1	8.1	46.2	7.8	12.2	9.0
C_5	34.7	18.6	101.4	11.2	48.6	17.9	5.8	16.7
C_6	12.2	12.0	47.0	1.6	20.6	6.5	7.6	8.0
$>C_6$	1.8	6.3	37.5	0.6	5.1	4.0	2.1	4.0

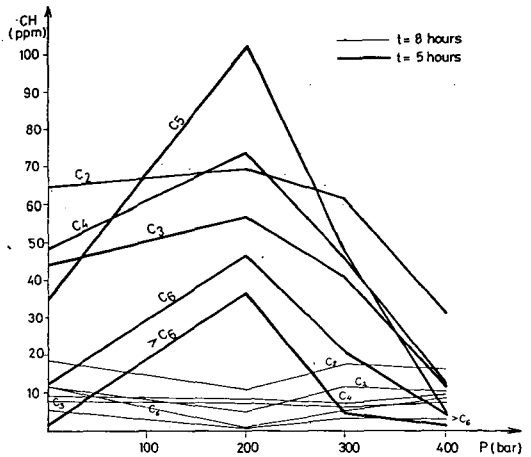

Fig. 4. Changes in the quantity of hydrocarbons (C_2—C_6) as a function of the pressure

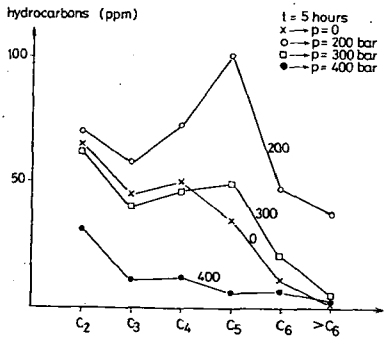

Fig. 5. The quantity of hydrocarbons (C_2—C_6) yielded by degradation of kerogen at different pressures and T = 260°C

can be hardly observed in the lower carbon number range. The quantity of hydrocarbons produced at 300 and 0 bar proved to be nearly the same *(Fig. 5)*, the pressure of 200 bar was especially favourable to the formation of C_2—C_6 hydrocarbons, while their quantity decreased to minimum at high pressure (400 bar).

In the given range, the hydrocarbon content of gas sample taken in the 8th hour proved to be much lower and scarcely changed as a function of pressure. The change is so slight *(Fig. 4)* that the quantity of hydrocarbons is practically independent of the pressure or concerning its tendency is opposite to that of the previous sampling.

TABLE 5

Hydrocarbons yielded by degradation of kerogen from Pula at P=200 bar T=260°C

HC (ppm) / TIME (hr)	C_2	C_3	C_4	C_5	C_6	$>C_6$
5	66.5	24.7	26.0	8.2	0.5	0
8	34.8	28.1	28.6	31.7	8.5	3.2
11	14.0	11.2	13.4	18.5	12.5	5.5
14	10.3	8.9	9.8	12.1	3.2	0.7
29	126.0	112.3	73.1	32.3	7.9	0.4
37	23.3	21.1	17.0	12.3	29.7	—
53	8.5	7.8	8.2	12.0	8.2	0.9
61	5.2	3.4	3.9	8.9	2.4	0.2
77	16.7	16.1	16.6	23.0	10.6	3.6
85	7.4	10.1	9.8	12.5	5.4	0.5
101	13.6	14.3	14.4	21.8	13.2	4.0
109	2.1	0.8	0.8	4.1	0.8	—
114	16.7	10.5	11.9	18.8	8.9	1.7
122	28.2	31.3	20.6	26.1	14.1	1.4
138	68.1	78.6	66.5	53.8	29.3	5.3
146	77.1	94.6	68.9	34.5	4.0	0.3
162	94.8	127.4	98.7	37.5	1.7	1.9
170	43.5	58.4	50.6	39.7	23.5	3.4
186	26.3	31.9	25.5	24.8	9.1	0.7
193	5.1	6.6	9.7	13.8	7.7	1.1

The difference observed in the quantities of hydrocarbons taken in the 5th and 8th hour rose the question how this value will change as a function of degradation time. At 200 bar producing extreme value in the first series, the kerogen was degraded in the second series at 260°C and during 193 hours. Gas samples were taken 20 times and the quantities of C_2—C_6 hydrocarbons were determined (Table 5; *Fig. 6*). Their quantity and its change as a function of time seems to be independent of the carbon number. It is a low value, in general, in the given time interval with two maxima in the 29th and 162nd hours, in case of C_2, C_3 and C_4. The quantity of C_5 and C_6 is less than that of the lighter hydrocarbons, during the whole process. This difference could be observed also in the tendency of change: the maximum is much lower, the average values proved to be somewhat higher, especially in case of C_5. In order to control the results, the first phase of the experiment series above was repeated and though some difference could be detected between the two series regarding the absolute value, the tendency was the same and the maximum observed in the 29th hour could be reproduced. Under the given experimental conditions the formation of C_2, C_3 and C_4 hydrocarbons is periodical.

The dependence on pressure of the intermediate bitumen was also followed (Table 6, *Fig. 7*). When comparing the character of the *Fig. 7* with the data of the Table it is obvious that the increase of pressure and temperature produced increased bitumen quantity up to a certain value, then the bitumen quantity decreased presumably due to the increased rate of further transformation.

Similarly to these two parameters, the increase of degradation time also affected the change of bitumen quantity. At P=300 bar it proved to be 1.9% after 4 hours degradation, and 2.2% after 8 hours degradation. At P=200 bar the reaction time of 8, 33 and 193 hours produced 2.0, 1.5 and 1% bitumen.

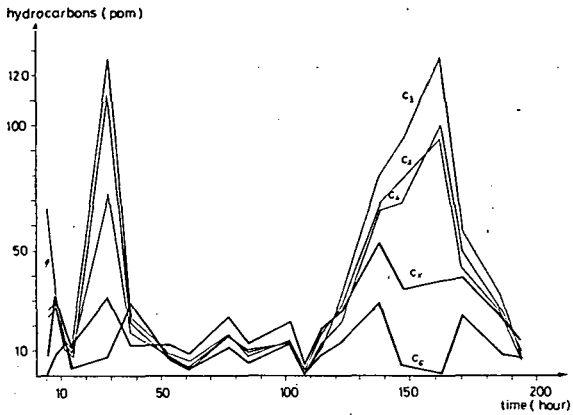

Fig. 6. The quantity of hydrocarbons (C_2—C_6) as a function of the time of degradation at T=260°C and p=200 bar

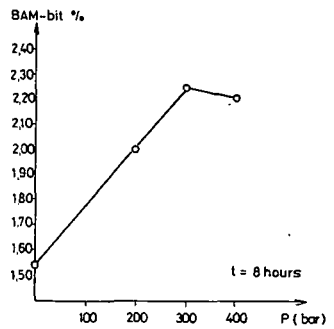

Fig. 7. The quantity of BAM-bitumen extracted from kerogen degraded at T=260°C and at different pressures

The value of the $T_D=C_R/C_T$ expressing the degree of degradation of the unconverted matter relates to the fact that when comparing with the effect of degradation temperature and time, the role of pressure is less significant. The value of this quotient (Table 6) indicates "immature" kerogen even after degradation at 400 bar. The insoluble organic matter seemed to be unchanged even after 33 hours as a

TABLE 6

Effect of the change of pressure and degradation period on the soluble and insoluble organic material

Temperature (°C)	Pressure (bar)	Time (hr)	BAM-bit. %	T_D	H/C
260	0	8	1.5	0.11	1.73
	200	8	2.0	0.13	1.70
	300	8	2.3	0.13	1.68
	400	8	2.2	0.14	1.68
	200	33	1.5	0.14	1.65
	200	193	1.0	0.24	1.54
	300	4	1.9	0.14	1.71

function of degradation time, only the considerable increase of time (193 hours) produced fairly well observable progress in the experimental evolution.

The H/C atomic ratio corresponded to the experimental temperature (260°C), its change as a function pressure can be neglected.

SUMMARY

The oil shale of Pula was generated in a special geological environment, in a Pliocene crater lake surrounded by tuff rings. The organic matter, the precursor of which is the *Botryococcus braunii*, accumulated in a biologically less active environment. The kerogen isolated from the oil shale is an immature geopolymer being in the initial stage of evolution, thus it proved to be suitable to the experimental study of effect of evolution parameters.

In the course of transformation of the insoluble organic matter soluble bitumen was formed as an intermediary product. Its quantity first increased, then decreased as a function of increasing temperature and pressure. The effect of pressure is negligible, that of temperature proved to be significant.

The process of degradation started in all cases by fairly well observable gas development. The concentration of C_2—C_6 hydrocarbons showed periodicity as a function of degradation time, with definite maxima in case of hydrocarbons of C=2—4, and with less variance in case of those of C=5—6. Maxima occurred in the 29th and 162nd hours. The increase of pressure promoted the formation of C_2—C_6 hydrocarbons in the first phase (P=200 bar), the further increase of pressure resulted in minimum quantity of hydrocarbons.

In the experimental temperature range of diagenesis the shale oil production proved to be small, increased above 350°C and intense increase could be observed between 400 and 450°C. At given temperature the quantity of shale oil increased as a function of increasing degradation time.

The quantity of unconverted kerogen decreased practically linearly as a function of temperature between 325—400 and 400—450°C, during 5 hours degradation time, but the change was steeper in the latter interval. Between 450 and 500°C the progressing oil production with constant unconverted matter is verified by the progress of bitumen transformation. In addition to the temperature defining the process of conversion, the role of degradation time cannot be neglected, and difference could

be observed especially in the temperature dependence of degradation of 1 and 5 hours.

When comparing the qualitative change of the unconverted kerogen in the process of degradation produced by the temperature and pressure, the widely accepted view, *i.e.* pressure plays subordinate role against temperature during the evolution of organic matter, can be fairly well illustrated. The value of the degradation factor, being $T_D<0.10$ in the starting material, slightly changed as a function of increasing pressure (between 1 and 400 bar $T_D=0.11$—0.14), but showed considerable increase as a function of increasing temperature (e.g. at 500°C $T_D=0.67$ after degradation of 1 hour).

On the basis of the values of H/C atomic ratio of unconverted kerogen determined in the course of experimental thermal degradation the zones of diagenesis and catagenesis of experimental evolution were simulated between 325 and 500°C during the maximum 10 hours, at higher temperature 5 hours thermal treatment. According to this quotient, the sample degraded at 350°C represents the zone of diagenesis, the sample degraded at 375°C during 10 hours belongs to the zone of catagenesis.

The apparent activation energy of thermal degradation is 50.2 kJ within the temperature range of 300—350°C, and 146.4 kJ between 365 and 450°C.

ACKNOWLEDGEMENTS

Authors express their thanks to DR. Á. JÁMBOR, Head of Department of Hydrocarbon Prognosis for making available the sample, to DR. M. KEDVES, for carrying out the pollen investigations, and DR. J. LAKATOS for making the gas chromatographic analyses.

REFERENCES

ABELSON, P. H. [1967]: Conversion of biochemicals to kerogen and n-paraffins. In: ABELSON, P. H.: Researches in Geochemistry, Vol. 2, p. 63—86.

ARATÓ, K. and BELLA, M. [1976]: Results of technological and chemical analyses of the oil-shale of Pula and Gérce (Transdanubia, Hungary). Annual Report of the Hungarian Geological Institute of 1974, p. 287—300.

CANE, R. F. [1948]: The chemistry of the pyrolysis of torbanite. Aust. Chem. Inst. J. and Proc., **15** p. 62—68.

CANE, R. F. [1951]: The mechanism of the pyrolysis of torbanite. In: Oil shale and cannel coal, **2**, Institute of Petroleum, London.

CANE, R. F. [1976]: The origin and formation of oil shales. In: Oil shale, edited by T. F. YEN G. V. CHILINGARIAN. Elsevier Scientific Publishing Company, p. 27—61.

CARLSON, A. J. [1937]: Inorganic environment in kerogen transformation. In: W. E. ROBINSON and K. E. STANFIELD: Constitution of oil shale kerogen. Bibliography and Notes on Bureau of Mines Research, 7968, p. 39—40.

CONNAN, J. [1974]: Time-temperature relation in oil genesis. AAPG Bulletin **58**, No. 12, p. 2516—2521.

CUMMINS, J. J., DOOLITTLE, F. G. and ROBINSON, W. E. [1974]: Thermal degradation of Green River kerogen at 150° to 350°C. Composition of products. BuMines RI 7924, p. 18.

CUMMINS, J. J. and ROBINSON, W. E. [1972]: Thermal degradation of Green River kerogen at 150° to 350°C. Rate of product formation. BuMines RI 7620, p. 15.

DIRICCO, L. and BARRICK, P. L. [1956]: Pyrolysis of oil shale. Industrial and Engineering Chemistry **48**, No. 8, p. 1316—1319.

GIRAUD, A. [1970]: Application of pyrolysis and gas chromatography to geochemical characterization of kerogen in sedimentary rock. AAPG Bulletin **54**, No. 3, p. 439—455.

HETÉNYI, M. [1979]: Thermal degradation of the oil shale kerogen of Pula (Hungary) at 473 and 573 K. Acta Miner. Petr., Univ., Szeged, XXIV/1, p. 99—111.

HETÉNYI, M. [1980]: Thermal degradation of the organic matter of oil shale of Pula (Hungary) at 573—773 K. Acta Miner. Petr., Univ., Szeged, XXIV/2, 301—314.
ISHIWATARI, R., ISHIWATARI, M., ROHRBACK, B. G. and KAPLAN, J. R. [1977]: Thermal alteration experiments on organic matter from recent marine sediments in relation to petroleum genesis. Geochimica et Cosmoschimica Acta **41**, p. 815—828.
JÁMBOR, Á. and SOLTI, G. [1976]: Geological conditions of the Upper Pannonian oil shale deposit recovered in the Balaton Highland and at Kemeneshát (Transdanubia, Hungary). Annual Report of the Hungarian Geological Institute of 1974. p. 193—220.
NAGY, E. [1976]: Palynological investigation of transdanubian oil-shale exploratory boreholes. Annual Report of the Hungarian Geological Institute of 1974, p. 247—262.
TISSOT, B. [1969]: Premières données sur les mécanismes et la cinétique de la formation du pétrole dans les sédiments. Simulation d'un schéma réactionnel sur ordinateur. Rev. Inst. Fr. Pét., **24**—4, p. 470—501.
TISSOT, B., DURAND, B., ESPITALIÉ, J. and COMBAZ, A. [1974]: Influence of nature and diagenesis of organic matter in formation of petroleum. AAPG Bulletin **58**, No. 3, p. 499—506.
TISSOT, B. P. and WELTE, D. H. [1978]: Petroleum formations and occurrence. Springer-Verlag.
VITOROVIĆ, D. K. and JOVANOVIĆ, L. J. [1968]: Solubility of Aleksinac oil shale kerogen III. Solubility of preheated kerogen. Glasnik Hemijskog Drustva **33**, No. 8—9—10, p. 581—588.
WEITKAMP, A. W. and GUTHERLET, L. C. [1970]: Application of a microretort to problems in shale pyrolysis. Ind. and Eng. Chem., Process Design. Development **9**, No. 3, p. 386—395.

Manuscript received. July 31, 1981

M. HETÉNYI
Institute of Mineralogy, Geochemistry and Petrography
Attila József University
H-6701 Szeged, Pf. 428.
Hungary

J. TÓTH
and
GY. MILLEY
Reservoir Engineering Research Laboratory of the Hungarian Academy of Sciences
H-3515 Miskolc-Egyetemváros
P.O. Box 2.
Hungary

Acta Mineralogica—Petrographica, Szeged, XXV/2. 147—156, 1982

IR AND NMR CHARACTERIZATION OF OIL GENERATED FROM SOME HUNGARIAN OIL SHALE AT 773 K

L. PÁPAY

INTRODUCTION

Near Pula (Transdanubian Central Mountains, Hungary) oil shale beds were found filling one of the Upper Pannonian basalt crater [JÁMBOR and SOLTI, 1975]. Subsequently to this discovery several oil shale beds were found which can be assigned to two genetic groups [JÁMBOR, 1980]:

1. Beds accompanying the Pliocene basalt volcanism filling the craters: e.g. Pula, Gérce, Várkesző, etc.

2. Oil shales occurring in the areas of Neogene lagoons of foothills: *e.g.* the indications of Várpalota, Budajenő, Kapolcs, etc.

Though these oil shales are of low grade, their organic matter content is higher than that of the sediments of the Great Plain of similar age. Thus, these provide favourable possibility to produce pure kerogen of greater quantities, consequently to carry out investigations serving the more precise knowledge of the kerogen features.

The thermal behaviour of the organic matter of oil shales is significant from two points of view: first of all from that of the industrial utilization since nowadays the aboveground or in-situ retorting are the most common utilization of oil shales [DINNEEN, 1976]; the second reason is the better knowledge of the formation conditions and evolution of the components of organic matter, first of all those of hydrocarbons [TISSOT *et al.*, 1971, 1974, 1978].

In our department the investigation of kerogen characteristics deriving from the Pula oil shale is in progress for several years [GRASSELLY *et al.*, 1977; HETÉNYI *et al.*, 1977, 1978, 1979]. Since the features of kerogen deriving from a given area are affected by numerous factors (quality of precursors, mineral composition, environmental effects, etc.), the researches on kerogen are rather complex, thus all the plus information may promote the knowledge of this inert matter being important not only from the theoretical but also from the economic point of view. Thus, in addition to the investigation of kerogen, the features of the soluble matter suitable to direct analyses and degrading from the kerogen itself, are also studied.

EXPERIMENTAL

Analyses were carried out at different temperatures and durations on some oil shales of Hungary. Their characteristic data are comprehended in Table 1. In the following only the shale oils generated at 773 K during 1 hour will be dealt with.

Thermal treatment was carried out in a Heraeus-furnace controlled by thermoregulator in oxygen-free nitrogen gas flow. The liquid products, i.e. oil and water

TABLE 1

Characteristic data of some Hungarian oil shales

Locality	Age	Bitumen content %	Ash %	CO_2 %	C_{org} %
Várkesző	Pliocene Upper Pannonian	6.80	68.5	2.7	13.4
Pula	Pliocene Upper Pannonian	4.60	46.3	9.7	27.3
Várpalota	Miocene Badenian	6.6	62.4	3.1	20.1
Mecsek	Miocene Carpathian	0.3	71.9	16.8	4.3

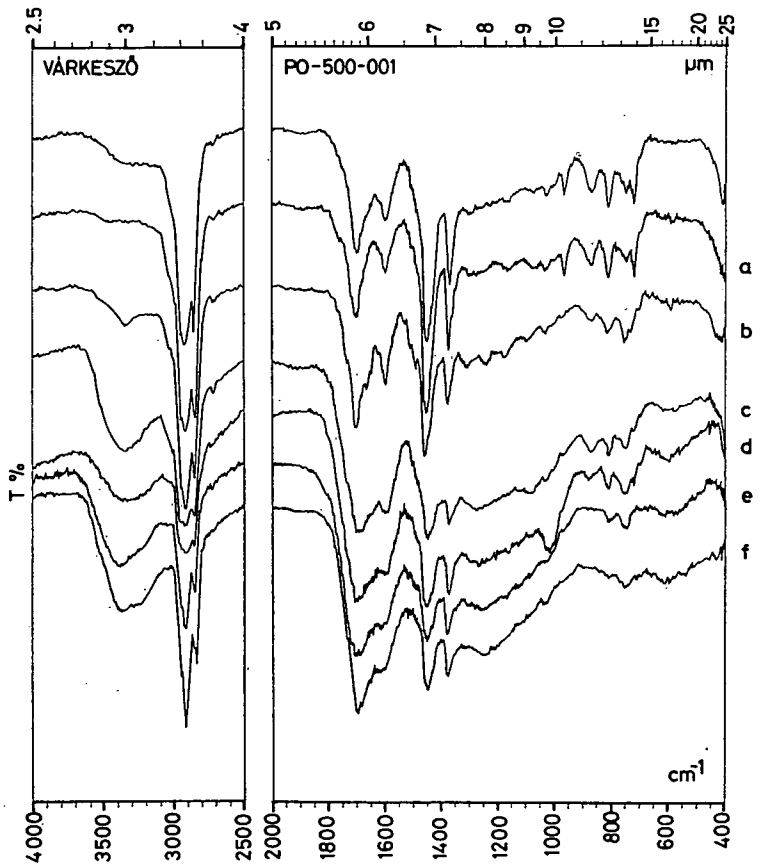

Fig. 1. The IR spectra of crude shale oil from Várkesző and that of its column chromatographed fractions

TABLE 2

Column chromatographic results of some Hungarian shale oils and crude oil from Algyő

Sign of the fraction	Solvent	Várkesző		Pula		Várpalota		Mecsek		Algyő-2	
		Quantity (g) of the fraction	Proportion (%) of the fraction	Quantity (g) of the fraction	Proportion (%) of the fraction	Quantity (g) of the fraction	Proportion (%) of the fraction	Quantity (g) of the fraction	Proportion (%) of the fraction	Quantity (g) of the fraction	Proportion (%) of the fraction
a	hexane	0.4180	73.22	0.6590	73.47	0.6914	62.73	0.5138	78.56	0.6783	72.00
b	hexane: benzene 1:1	0.0127	2.22	0.0710	7.92	0.0600	5.44	0.0307	4.69	0.0150	1.59
c	benzene	0.0272	4.76	0.0580	6.47	0.0879	7.97	0.0275	4.20	0.0450	4.78
d	chloroform	0.0190	3.33	0.0335	3.73	0.0775	7.03	0.0210	3.21	0.0090	0.95
e	acetone	0.0140	2.45	0.0480	5.35	0.0202	1.83	0.0030	0.46	0.0040	0.42
f	methanol	0.0083	1.45	0.0090	1.00	0.0167	1.52	0.0070	1.07	0.0050	0.53
		0.4992	87.43	0.8785	97.94	0.9537	86.52	0.6030	92.19	0.7463	80.27

were trapped in a tank adjusted to the end of the heating tube. The shale oil was separated by shaking in chloroform in a separating filler. The solvent was evaporated at 333 K in drying oven, then the crude shale oil was chromatographed on alumina as reported earlier in the column chromatography of bitumen of the Pula oil shale [PÁPAY, 1979]. The column chromatographic data of different shale oils, as well as of the petroleum deriving from the Algyő-2 Upper Pannonian reservoir are shown in Table 2. (The volatile components of the oil were eliminated at 323 K under water-jet vacuum.) It is characteristic of all the oils that the hexane fraction is of highest amount and, as it has been expected, these fractions consist mainly of apolar compounds, thus the efficiency of chromatography is high.

To determine the qualitative composition of the oils the IR records of the starting oils and fractions was carried out by means of a Specord 75 IR spectrometer in the range of 4000—400 cm^{-1} wavenumber. Spectra were recorded by means of film record of 0.02 mm in case of the crude oils and of the first three fractions, while in case of the fractions *d*, *e* and *f* spectra were recorded by means of the KBr-method (pellets of 20 mm diameter were pressed at about 18 Mp under vacuum).

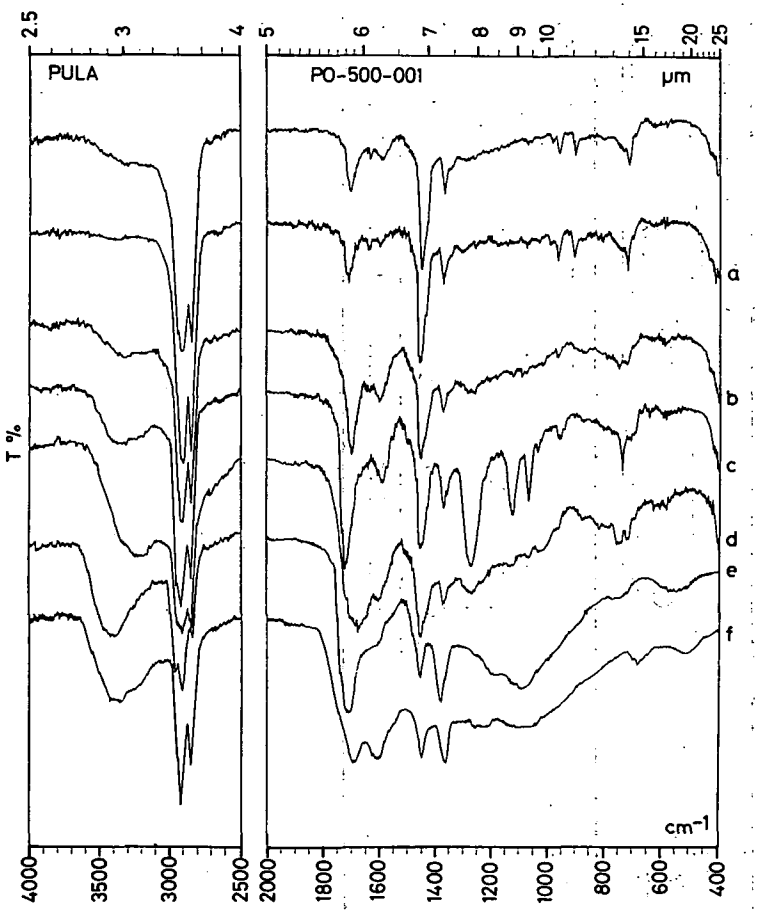

Fig. 2. The IR spectra of crude shale oil from Pula and that of its column chromatographed fractions

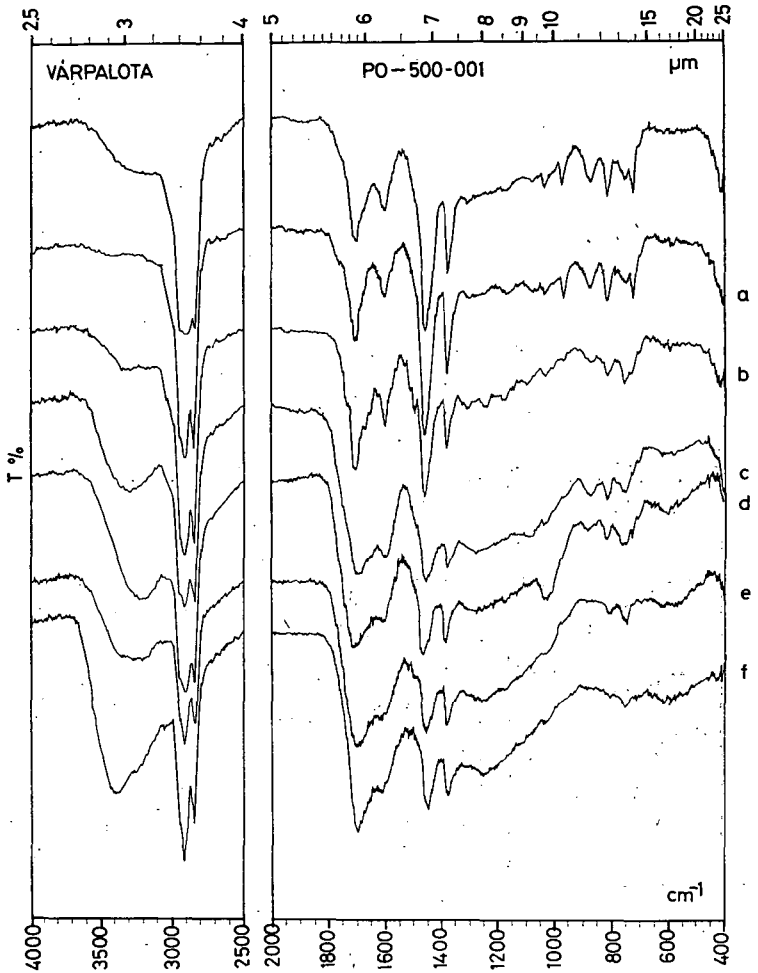

Fig. 3. The IR spectra of crude shale oil from Várpalota and that of its column chromatographed fractions

It is seen in the IR records of shale oils *(Figs. 1—4)* that the crude oils and their hexane fractions are qualitatively rather similar, only the νOH band is lacking in the hexane fractions. Some differences in the intensities of the bands relate to slight quantitative differences. In addition to the long unbranched paraffins ($\nu_s \nu_{as} CH_2$, CH_3 2960—2850 cm^{-1}, $\delta_{as} CH_3$ and $\beta_s CH_2$ 1460 cm^{-1}, $\delta_s CH_3$ 1370 cm^{-1} and β_{as} 720 cm^{-1}) bands relating to the presence of mono- and di-substituted aromatic hydrocarbons are also found in the spectrum (1600—1500 cm^{-1}: aromatic νCC, γ (=CH) 810 and 750 cm^{-1}, γCC 700 cm^{-1}). The νCO band at 1710 cm^{-1} occurs in all records with low intensity, but the quantity of carbonyl is very low. In addition to the bands mentioned above, in the spectra of the shale oils of Pula *(Fig. 2)* and Várpalota *(Fig. 3)* weak νCC at 1640 cm^{-1} and γ ($=CH_2$) at 990, 910 cm^{-1} can be observed being characteristic of the terminal vinyl groups. Taking into account the

relative intensity of the band at 720 cm^{-1} indicating the chain length of paraffins, the shale oil of Várkesző shows the shortest chain.

In fractions *b* (hexane:benzene 1:1) the quantity of oxygen increased indicated by the appearance of slight intensity of the *v*OH and by increase of intensity of the *v*CO band. In the Várpalota sample *(Fig. 3)* small esther bands occur in the "finger print" range (1300—1000 cm^{-1}). The increase of quantity of the aromatic compounds is indicated by the intense band at 750 cm^{-1}. Concerning their quality, in this range also mainly hydrocarbons are found.

In the *c* (benzene) fractions the *v*OH and *v*CO bands are intense. In case of the Mecsek sample *(Fig. 4)* esther bands are found at 1280, 1130 and 1070 cm^{-1}. The proportion of aromatic compounds is considerable.

According to the functional groups in the fraction *d* (chloroform) mostly long-chain alkyl-aryl ketons and alcohols are found. In the Mecsek sample the band of 720 cm^{-1} occurs as a shoulder on the band of 750 cm^{-1} indicating that among the chloroform fractions of the samples the carbon chains of this sample is the shortest.

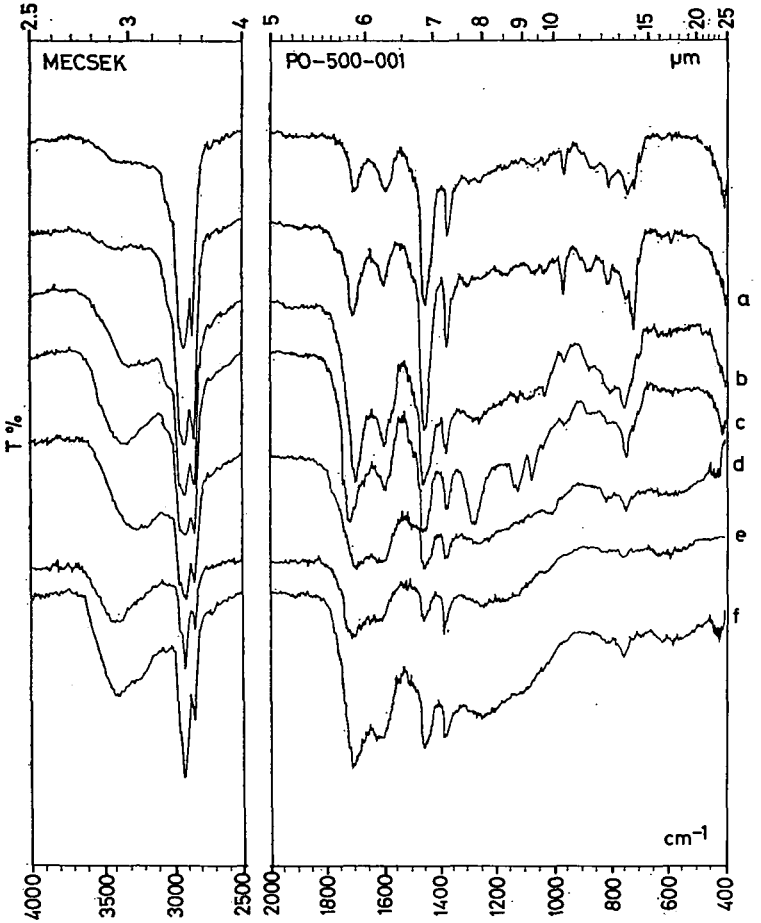

Fig. 4. The IR spectra of crude shale oil from Mecsek and that of its column chromatographed fractions

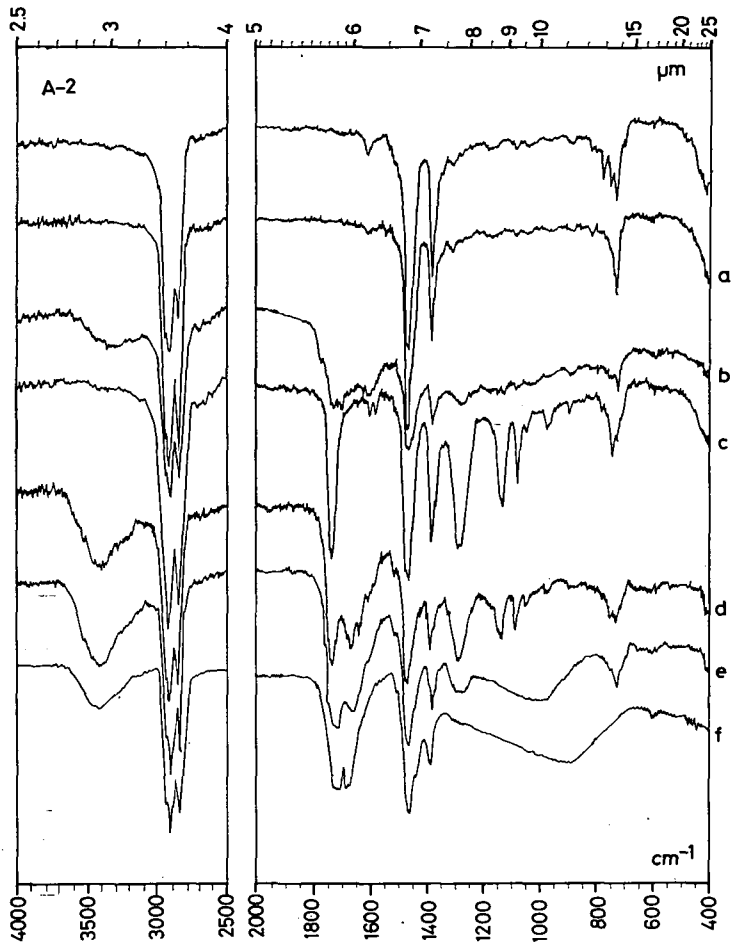

Fig. 5. The IR spectra of crude oil from Algyő and that of its column chromatographed fractions

Spectra of the fractions *e* (acetone) and *f* (methanol) are of similar character. The νOH and νCO bands are intense. In the spectra of both fractions bands relating to the presence of more or less aromatic compounds are found. The band of 720 cm^{-1} is usually absent or appears as a weak shoulder on the aromatic oscillations. The intensity of the band 1370 cm^{-1} is the same or somewhat higher in most of the spectra. Consequently, in these fractions first of all branched as well as aromatic compounds are found.

In *Fig. 5* the IR spectra of the paraffinic oil and of its column chromatographed fractions are shown, the oil deriving from the Algyő-2 Upper Pannonian reservoir. The features described in case of shale oils are valid also of the crude oil, but some differences can also be observed. As compared to the shale oils, in the fractions *a* of the oil and in the oil itself the carbonyl band is absent and occurs only from the *b* (hexane:benzene 1:1) fraction. Consequently, oxygen-bearing compounds occur also in the oil in slight amounts, but their quantity is less than in shale oils.

Further, in the spectra aromatic bands are indicated which is lacking in the hexane fraction and occurs only in the subsequent fractions.

The IR records provide information on the character of the functional groups. Nevertheless, information on the differences, of quality (*e.g.* distribution of the aliphatic and acyclic compounds, the average chain length, the approximate distribution of the quality of carbon chains) can only be obtained by NMR records (POPLE *et al.*, 1959; JACKMAN and STERNHELL, 1969]. NMR records were made by a JEOL C—60 HL type spectrometer, in carbon tetrachloride. The values of crude oils and of their hexane fractions (h.) calculated from NMR records are shown in Table 3.

TABLE 3

Characteristic values of oils and their hexane fractions calculated from NMR records

Locality		Length of the average paraffinic carbon skeleton	Quality of the carbon skeleton		
			Aliphatic %	Alicyclic %	Aromatic %
Várkesző	shale oil	C_{10}	48	31	21
Várkesző h.		C_9	52	26	22
Pula		C_{16}	60,5	30	9.5
Pula h.		C_{13}	60	30	10
Várpalota		C_{13}	55	27	18
Várpalota h.		C_{20}	54	31	15
Mecsek		C_{16}	39	35	26
Mecsek h.		C_{17}	35	35,5	29,5
Algyő-2	crude oil	C_8	80	7	13
Algyő-2 h.		C_9	94	6	—

Accordingly, the average chain length is greater in the shale oils than in crude oils, except the case of Várkesző. The gas chromatographic analyses of some oil proved that data calculated from the NMR records are correct as tendency but the average paraffin chains are somewhat longer. This difference is caused by the fact that the NMR instrument does not make difference between the shorter lateral chains of the aromatic compounds and the paraffins, so the chain length of paraffins is longer by 2 to 4 carbon atoms. When calculating the paraffin content, however, this increase would mean a change of only 3 to 4%. According to the NMR data it is characteristic of the quality of shale oils that these consist of paraffin (40—60%), cycloparaffin (relatively constant value of about 30%) and of aromatic compounds (10 to 26%). The quantity of aromatic compounds is lowest in the oil shale of Pula and highest in the Mecsek sample.

The oil of Algyő is rich in paraffins, the quantities of acyclic and aromatic compounds is subordinated. According to the gas chromatographic analyses the aromatic compounds consist three kinds of xylol isomers and of ethyl-benzene.

SUMMARY

According to the IR and NMR analyses of the oils generated at 773K from oil shales of Hungary, the shale oils consist in 70 to 80% of hydrocarbon mixtures of paraffins, cycloparaffins and aromatic compounds. The other part of shale oils contains hetero-atomic compounds, first of all oxygen, in form of ketons, alcohols, esthers, etc.

When studying the data as a function of geological age, it can be stated in the oils generated from oil shales containing organic matter of the same type that in addition to the alicyclic compounds of relatively constant and high amount the quantity of paraffins is lowest and that of aromatic compounds is highest in the oldest Mecsek sample (Carpathian). As the geological age becomes younger, the quantity of paraffins increases, that of the aromatic compounds decreases. The IR records show that the oxygen content is relatively highest in the Upper Pannonian samples and relatively lowest in the samples of Carpathian stage.

These statements concern the oils containing organic matter of the same type since, in harmony with the investigations carried out so far, the kerogen of the Upper Pannonian oil shales of Pula and Várkesző is of different type. Thus, the oil shale of Pula is assigned to the group I of the VAN KREVELEN diagram (algal origin) while that of Várkesző is presumably a mixed type which contains plant remnants of higher evolution, *i.e.* more humic components, in addition to the ingredients of algal origin (personal communication of M. HETÉNYI).

These results verify the decomposition theory of TISSOT *et al.* which stated that in the course of maturation of the organic matter of sediments first the hetero-atomic bonds are broken, this is followed by the decomposition of the aliphatic chains and the state of aromatization of system increases. Based on our measurements this can be supplemented by the fact that the release of hetero-atoms (first of all of oxygen) proceeds not only by the release of compounds small molecular weight (CO_2, H_2O, etc.), but together with these oxygen-containing compounds of greater molecular weight, *e.g.* ketons may also released. This statement is verified also by the IR records of shale oils in which the carbonyl band is always present.

ACKNOWLEDGEMENTS

I am thankful to DR. Á. JÁMBOR, Head of Department of Hydrocarbon Prognosis for making available the samples, to DR. M. HETÉNYI for the thermal investigations and to DR. GY. DOMBI (Department of Organic Chemistry of the József Attila University) for making the NMR spectra.

REFERENCES

BENCE, G., JÁMBOR, Á., PARTÉNYI, Z. [1979]: Exploration of alginite (oil-shale) and bentonite deposits between Várkesző and Malomsok (Transdanubia, W-Hungary). — Annual Report of the Hungarian Geological Institute of 1977, p. 257—267.

DINNEEN, G. U. [1976]: Retorting technology of oil shale. In: Oil shale. — Edited by T. F. YEN and G. V. CHILINGARIAN. Elsevier Scientific Publishing Company, p. 181—198.

ERŐSS, K. [1974]: Az infravörös spektroszkópia analitikai alkalmazása. (Analytical application of infrared spectroscopy.) Műszaki Könyvkiadó, Budapest.

GRASSELLY, GY., M. BERTALAN and CS. SAJGÓ [1977]: Contributions to the knowledge of the Hungarian oil shale kerogen II. Results of preliminary DTA and IR-investigations on the kerogen of the oil shale occurrence at Pula. Acta Miner. Petr., **XXIII**/1, p. 177—196.

HETÉNYI, M., K. MAITZ and É. TÓTH [1977]: Contributions to the knowledge of the Hungarian oil shale kerogen I. Preliminary report on the results of the pyrolysis and selective oxidation. Acta Miner. Petr., **XXIII**/1, p. 165—175.

HETÉNYI, M. and K. SIROKMÁN [1978]: Structural informations on the kerogen of the Hungarian oil shale. Acta Miner. Petr., **XXIII**/2, p. 211—222.

HETÉNYI, M. [1979]: Thermal degradation of the oil shale kerogen of Pula (Hungary) at 473 and 573 K. Acta Miner. Petr., **XXIV**/1, p. 99—111.

HOLLY, S. and P. SOHÁR [1975]: Absorption spectra in the infrared region. Akadémiai Kiadó, Budapest.

JACKMAN, L. M., S. STERNHELL [1969]: Application of NMR spectroscopy in organic chemistry. Pergamon Press, New York, p. 49—52.
JÁMBOR, Á., G. SOLTI [1975]: Geological conditions of the Upper Pannonian oil shale deposite recovered in the Balaton Highland and Kemeneshát (Transdanubia, Hungary). Acta Miner. Petr., XXII/1, p. 9—28.
JÁMBOR, Á., G. SOLTI [1980]: A magyarországi olajpalakutatások eredményei (1980). (The results of oil shale exploration in Hungary (1980) Földt. Kutatás XXIII/4, p. 5—8.
PÁPAY, L. [1979]: Several features of the oil shale and oil-shale-kerogen bitumen of Pula (Hungary). Acta Miner. Petr., XXIV/1, p. 113—124.
POPLE, J. A., W. G. SCHNEIDER, H. J. BERNSTEIN [1959]: High resolution nuclear magnetic resonance. McGraw-Hill Book Company, New York p. 458—465.
TISSOT, B., Y. CALIFET-DEBYSER, G. DEROO and J. L. OUDIN [1971]: Origin and evolution of hydrocarbons in early Toarcian shales, Paris basin, France. AAPG Bull., **55**, p. 2177—2193
TISSOT, B., B. DURAND, J. ESPITALIE and A. COMBAZ [1974]: Influence of nature and diagenesis of organic matter in formation of petroleum. AAPG Bull., **58**, p. 499—506.
TISSOT, B., G. DEROO, A. HOOD [1978]: Geochemical study of the Uinta Basin: formation of petroleum from the Green River formation. Geochim. et Cosmochim. Acta **42**, p. 1469—1485.
TISSOT, B. P. and D. H. WELTE [1978]: From kerogen to petroleum. In: B. P. TISSOT and D. H. WELTE: Petroleum formations and occurrence. Spinger-Verlag, p. 148—184.

Manuscript received, July 31, 1981

LÁSZLÓ PÁPAY
Institute of Mineralogy, Geochemistry and Petrography
Attila József University
H-6701 Szeged, Pf. 428
Hungary

Acta Mineralogica—Petrographica, Szeged, XXV/2. 157—161, 1982

THE ASSOCIATION OF BARITE VEINS WITH ACID IGNEOUS AND METAMORPHIC ROCKS

A. A. EL SOKKARY and Z. M. ZAYED

ABSTRACT

It was observed that barite veins are invariably associated with acid igneous rocks whether plutonic or volcanic and certain metamorphic rocks which tend to be acidic in composition. The present investigation tries to explain on chemical basis why does this association occur in nature.

The associated acid igneous and metamorphic rocks like granite, granodiorite, porphyrite and gneiss are all characterised by being rich in potash feldspar and biotite, in other words they are feldspar-mica rocks. These two minerals are known to be enriched in the element Ba. Weathering processes release Ba in solution. Once in solution, Ba migrates veinward to regions of sulfate in order to form the well known barite veins.

Another mechanism of forming barite veins depends on the fact that there is considerable Ba mobility and enrichment during metasomatism and granitization. This mobility with the presence of free SO_4^{2-} radical will help in formation of barite veins characteristic of granitized zones.

Magmatic hydrothermal fluids are shown here to be deprived from any significant amount of Ba. Thus hydrothermal origin usually attributed to many barite veins ought to be replaced by a mechanism based on either of the two mentioned models.

INTRODUCTION

Barite is widely distributed in different types of rocks in the world. The importance of studying the occurrence of this mineral is in connection with technological uses. Among these it is used as an absorptive material for radiation.

Barite goes in the construction industry in concrete aggregate to shield stationary nuclear reactors because it absorbs gamma radiation, its use reduces the amount of expensive shielding like for example lead shielding otherwise necessary needed. This makes barite a strategic mineral with expanding use in the field of protection and shielding from hazardous radiation.

It is observed that barite veins has certain affinity to be associated with acid igneous and metamorphic rocks. This association will be discussed here in some detail to find the rules, whether mineralogical or chemical, governing this association. As a matter of fact, the purpose of the present work is to find chemical explanation for the association of barite veins with the mentioned acid igneous and metamorphic rocks.

ASSOCIATION OF BARITE WITH ACID IGNEOUS AND METAMORPHIC ROCKS

As already mentioned, barite occurs in different countries associated with acid igneous and metamorphic rocks. In the following paragraphs the occurrences of the acid igneous and metamorphic rocks in different countries will be mentioned after BROBST [1970].

In South America and in Peru most of the barite has been mined from large hydrothermal deposits associated with andesitic volcanic rocks and diorite to granodiorite intrusive rocks of Tertiary age in the Rimae valley near Lima.

In the continent of Europe and in West Germany, barite veins in the Bad Lauterberg area, western Harz, had reserves of 1 million tons. These vein deposits are associated with granites of Variscan age, but not much is known about their geochemistry or genesis. In the Union of Soviet Socialist Republics, the veins of barite of hydrothermal origin were deposited in tectonic fractures in a tuff porphyry unit of Middle Jurassic age. These deposits are found in Transcaucasus region of Georgia, Armenia and Azerbaidzhan.

In France, barite occurs in hydrothermal veins in metamorphic rock and more rarely in basement granites. Typical vein deposits are in Central Massif and in southern France. Barite veins also occur in the contact aureole around the granite batholith of Mount Lozere in the Lozere and Gard departments. Among many barite veins in the Vosges Mountains of northeastern France, the large barite deposit at Val d'Ajol occurs in a mylonitized granite in the contact zone between the granite and Permian rocks. In Greece veins in granite are mined on Mykones.

The East German occurrences of barite are in metamorphic rocks in the outer contact zone of the Eibenstoker granite of Variscan age. At Huhn Trusetal, on the south western border of the Thuringer Wald, veins containing barite and fluorospar in the ratio of 3:1 occur in old Paleozoic mica schists and gneisses and associated Variscan granite. In Bulgaria barite is abundant in widely distributed deposits of lead and zinc associated with sedimentary and igneous rocks of Tertiary age in the Rhodope massif.

In Czechoslovakia deposits are reported to contain barite with fluorspar and quartz in the crystalline rocks of the Krusne and Smirciny Mountains in north western Bohemia. The deposits composed chiefly of siderite, barite and some sulfides are part of the Zips-Gomorer Erzgebirge in the old Alpine-West Carpathian ore province associated with intensive magmatic activity of the Gemeride granite of Middle Cretaceous age.

In the African continent, major barite resources are associated with the carbonatites of East Africa. In the Republic of South Africa the ore deposits are at or near the contact of recrystallized quartzite and biotite schist on the Gamsberg, a doubly plunging anticline. The origin of deposits is attributed to metasomatic replacement of the country rock from an igneous source. The Egyptian occurrences of barite are mainly in pink granite east of Aswan.

In Liberia six barite veins have recently been described in Precambrian granitic gneisses in an area of about 20 square miles in the Gibi area, eastern Montserrado county. Zambian deposits of barite occur near the contact of granite and schist south of Kafue river about 14 miles east of Kafue Township. Tanzanian barite is reported in carbonatites and occurs in concentrates from kimberlite pipes. In Uganda a considerable tonnage of barite possibly may be recovered from hematite lenses in granitoid gneiss at Muabuzi Hill north west Ankole. The deposit lies only miles from the Kampala-Kasese railway. Barite also occurs associated with the Sukulu carbonatite. Somalian deposits are in the area south of Berbera, in the Bihendula Range, barite fills fractures as much as 2 feet wide in gneiss.

Occurrences of the Near East countries are as follows. In India near Alangayam veins with quartz and 30 percent barite in porphyritic gneiss are several feet thick and have been traced for 7 miles. In the Tikamgarh district of Vindhya Pradesh, grey barite forms 30—45 percent of veins as much as 2.5 feet thick that cut the Bundelkhand

gneiss. In Iran most of the barite is white, although some is red from iron stains, it commonly occurs in relatively thin, structurally controlled veins. The most common host rocks are the volcanic tuffs of the Oligocene and Miocene green beds.

Turkish barite occurrences are in the areas of Bilirkoy, Kizilkilise and Kasorkoy, Mur Province where barite veins as much as 40 m wide occur in schists of early Paleozoic age that generally strike west and dip north.

In the Far East countries like Japan, the Otaru Matsukuva mine in Hokkaido had yielded by the end of 1950, 80 percent of the nation's total production from high-grade ore replecements in volcanic rocks of Tertiary age. In North Korea in the Chaeryong-gang district many barite deposits are known in the limestone, shale, and clay-slate of the Masan-ni (Masanri) beds of the Middle Cambrian Choson system, and in the unconformably overlying succession of three units of porphyrite, breccia, conglomerate, sandstone, quartzite, tuffaceous shale, shale and limestone in the Upper Taedong (Daido) formation of Late Cretaceous age. The deposits in the Masanri beds are commonly lenticular or pocket-like, and those in porphyritic tuff beds are comparatively thick and have substantial reserves.

Finally in Australia barite deposits are known in the Northern Territory, Tasmania, Queensland, Victoria, and New South Wales. In New South Wales, the Kempfield area, about 30 miles south-south west of Bathurst, has yielded about 10 percent of Australia's total barite production from lenticular masses in schistose rocks about 1 mile from a granite mass.

THE MAIN BARITE OCCURRENCES

The foregoing occurrences of barite can be classified according to the type of the associated rock into three classes which are: barites associated with acid igneous rocks, those associated with metamorphic rocks and those associated with carbonatites. The more abundant occurrences are those associated with acid igneous rocks or at the contact of these rocks, these represent about 60% of the studied occurrences. Then comes barites associated with metamorphic rocks and they represent about 30% of the studied occurrences. Finally barites occurring with carbonatites are about 10% of the studied cases.

THE GEOCHEMISTRY OF Ba IN RELATION TO BARITE VEIN FORMATION

NOCKOLDS and ALLEN [1953] mentioned that Ba rises steadily in amount as the more acid rocks are approached. But in the E Central Sierra Nevada series, as in the Scottish Caledonian series, there is a sudden drop in the Ba content at the extreme acid end. KOLBE and TAYLOR [1966] on their study on the granites and granodiorites from Australia and South Africa observed as well a sharp decline of Ba in very acid rocks. EL SOKKARY [1970] during a study on some Egyptian granites and EL BOUSEILY and EL SOKKARY [1975] showed that Ba has a mean value of 770 ppm in normal granites while in strongly differentiated rocks and pegmatites its concentration drops to about 100 ppm. The same authors added that Ba shows definite decrease with extreme fractionation.

In conclusion, it is possible to say that Ba reaches almost maximum concentration in igneous rocks approaching granitic composition (quartz diorite-granodiorite-granite) before it drops out in strongly differentiated rocks and pegmatites. Hydro-

thermal solutions remaining after the pegmatite stage would naturally be deficient in that element.

In any rock which is composed of feldspars, quartz and mica in different proportions, it is understood that the minerals carrying chiefly Ba are the potash feldspar and the mica specially biotite, plagioclase contributes Ba to a much lesser extent than potash feldspar [WEDEPOHL, 1974]. Therefore igneous or metamorphic rocks which carry an abundance of feldspar (particularly potash) and mica (particularly biotite) are liable to liberate much Ba in the weathering solutions.

ROSENQUIST [1939] leached a granite powder with distilled water and he found that BaO was enriched in the residue of the weathering solution to about nine times. Weathering of biotite was observed by BOETTCHER [1966] to lead to a decrease of the BaO content. SOLOMON [1966] reports Ba removal from granites by greisenization. Experimental weathering of K-feldspar in distilled water [PUCHELT, 1967] showed that Ba is preferentially released from this silicate structure into the solution.

Thus Ba tends to be released rather easily from feldspar-mica rocks subjected to weathering solutions. In other words, the weathering solutions from granites and similar rocks become enriched in Ba. LURYE [1963] concluded that all barite and its Sr content originates from the feldspar decomposition in the wall rocks. It seems that the weathering of granites can lead to solutions very rich in their Ba content.

Now if a granitic rock (or a rock rich in feldspars, particularly potash, and mica) contains an original hydrothermal vein which is composed dominantly of quartz plus sulphide minerals such as galena, pyrite or sphalerite. If these sulphides are subjected to weathering near the earth's surface where there is free access to atmospheric O_2 and where the oxidation potential is high, then SO_4^{2-} radical will be formed.

The Ba released from granitic and similar rocks can take the form of soluble $BaHCO_3$ which is an alkaline solution [CLARKE, 1939]. This alkaline solution on moving towards the original quartz-sulphide vein (now containing free SO_4^{2-} radical) can act in two ways: one active in dissolution of SiO_2 and removing it away and the other is the concomitant precipitation of $BaSO_4$. To this result, an evidence is given from the rock texture itself. Some barite specimens from Egypt [EL SOKKARY and ABDEL MONEM, 1977] are observed to contain quartzite remnants composed exclusively of quartz grains and in which barite flows as a plastic material filling cracks and small veinlets, sometimes the quartzite fragments are shattered and barite flows to fill the spaces between the shattered pieces indicating that it is later in its paragenetic sequence than quartz.

TOOKER [1963] was able to show that Ba, and other large ions, normally tends to be removed veinward from all Precambrian and Tertiary metamorphic and igneous rocks he investigated. In solution Ba migrates to the region of sulfate stability and thus is often bound to a narrow zone close to the earth's surface [WEDEPOHL, 1974].

The foregoing model proposed for the formation of certain barite veins associated with granitic and metamorphic rocks seems to be plausible, particularly if it is taken into consideration that magmatic hydrothermal fluids originally do not contain any significant amount of Ba, but obtain this element if possible by leaching suitable rocks.

Another way of formation of barite veins during metasomatism and granitization is as follows. ENGEL and ENGEL [1958] observed that granitized gneisses in the Adirondacks, New York generally showed much higher Ba values than normal gneisses. Thus there is considerable Ba mobility and enrichment during granitization and metasomatism. Any SO_4^{2-} radical present in a fissure or vein will attract the metasomatically mobilized Ba and form barite characteristic of granitized zones.

REFERENCES

BOETTCHER, A. L. [1966]: Vermiculite, hydrobiotite and biotite in the Rainy Creek igneous complex near Libby, Montana. Clay Minerals Bull., **6**, p. 283.

BROBST, D. A. [1970]: Barite: world production, reserves, and future prospects. U.S. Geol. Surv. Bull., **1321**, Govt. Printing Office, Washington.

CLARKE, F. W. [1959]: The data of geochemistry. U.S. Geol. Surv. Bull., **770**, Govt. Printing Office, Washington.

EL BOUSEILY, A. M. and EL SOKKARY, A. A. [1975]: The relation between Rb, Ba and Sr in granitic rocks. Chemical Geology, **16**, p. 207—219.

EL SOKKARY, A. A. [1970]: Geochemical studies of some granites in Egypt, U.A.R. Ph. D. Thesis. Alexandria Univ.

EL SOKKARY, A. A. and ABDEL MONEM, H. M. [1977]: Mineralogical and chemical studies of barites from Gebel El Hudi, Eastern Desert, Egypt. N. Jb. Miner. Abh., **128**/3, p. 285—292.

ENGEL, A. E. J. and ENGEL, C. G. [1958]: Progressive metamorphism and granitization of the major paragneiss, north west Adirondack mountains, New York, Bull. Geol. Soc. Am., **69**, p. 1369.

KOLBE, P. and TAYLOR, S. R. [1966]: Major and trace element relationships in granodiorites and granites from Australia and South Africa. Contr. Mineral. and Petrol., **12**/2, p. 202—222.

LURYE, L. M. [1963]: Migration of barium and strontium during country rock metasomatism in the Zambarak ore field. Dokl. Akad. Nauk SSSR, **149**, p. 1167.

NOCKOLDS, S. R. and ALLEN, R. [1953]: The geochemistry of some igneous rockseries. Geochim. et Cosmochim. Acta **4**, p. 105—142.

PUCHELT, H. [1967]: Zur Geochemie des Bariums im exogenen Zyklus. Sitzungsber. Heidelb. Akad. Wiss. Math.—Nat., Kl. 4.

ROSENQVIST, I. TH. [1939]: Note on leaching of granite with special reference to lead, radium and barium. Norsk Geol. Tidsskr., **19**, p. 110.

SOLOMON, M. [1966]: Origin of barite in the North Pennine ore field. Inst. Mining Met., Trans., **75**, p. 230.

TOOKER, E. W. [1963]: Altered wallrocks in the central part of the Front Range mineral belt, Gilpin and Clear Creek Counties, Colorado. U. S. Geol. Surv. Profess. Paper, **439**.

WEDEPOHL, K. H. [1974]: Handbook of geochemistry. Vol. II/4, Ch. 56 Ba. Springer-Verlag Berlin.

Manuscript received, September 10, 1981

A. A. EL SOKKARY
Z. M. ZAYED
Nuclear Materials Corporation
Cairo, Egypt

Acta Mineralogica—Petrographica, Szeged, XXV/2, 163—167, 1982

IRON-TITANIUM OXIDE MINERALS IN THE HIGH-IRON CONCENTRATION TYPE OF BASALTS IN THE DECCAN TRAPS

A. C. CHATTERJEE

ABSTRACT

The Deccan Trap basalts of Bhopal are high-iron concentration types of tholeiites. Various forms and mode of occurrence is described. The growth of the crystals through stages are discussed. A gradual decrease in the degree of oxidation from the bottom to top flows is noticed. The iron enrichment remaining constant the oxidation ratio show a gradual rise. Studies in reflected light under the ore microscope show the presence of the following types of the iron ores; magnetite, ilmenite, titanomagnetite and scarcely hematite. An account of the paragenesis of these opaques is presented.

INTRODUCTION

The earliest account of the iron-ores of the Deccan Traps was given by FERMOR [1925] who suspected the presence of both magnetite and ilmenite in these rocks. Normative constituents can not explain the actual mineral composition of the rocks. However, the square opaques were taken by him as magnetite while the bars and streaks as ilmenite. Many years later DE [1964] studied the opaques under the reflected light and found that the most abundant and common opaque mineral is titano-

TABLE 1

Some characteristic data of the basalts investigated

Nos.	Sequence of the flows	FeO	Fe_2O_3	TiO_2	H_2O	Oxidation ratio	Degree of oxidation
1.	6th Flow (Et 3)	12.19	3.06	2.11	+2.24	—	0.25
2.	5th Flow (B6)	10.75	4.48	2.90	+1.66 −0.18	27.27	0.42
3.	4th Flow (H5)	10.35	5.22	3.10	+2.64 −0.24	31.22	0.50
4.	3rd Flow (H_{13})	10.18	5.17	3.10	+2.32 −0.36	31.36	0.51
5.	2nd Flow (B_{42})	9.17	6.30	2.90	+3.04 −0.38	38.33	0.68
6.	2nd Flow (B_{15})	9.14	6.47	3.11	—	49.11	0.71
7.	1st Flow (B_1)	8.80	6.27	2.20	+1.26 −0.14	39.08	0.71

Analyst: B. P. GUPTA

magnetite. De subsequently [1974a] demonstrated the occurrence of silicate-liquid immiscibility in the mesostasis of the Deccan Trap basalts. He further documented [1974b] the co-existence of three mutually immiscible liquid phase in the residual magma of the Deccan Traps.

The Deccan Trap basalts are in general moderate iron-concentration type the $FeO+Fe_2O_3$ content being less than 15 per cent. But the various flows studied from near Bhopal range between 17.12 and 15.23 [Chatterjee, 1973] indicating their high iron concentration (Table 1). In the present account the mineralogy of the iron-titanium minerals of these basalts is discussed.

MODE OF OCCURRENCE IN THIN SECTION

Various modes of occurrence and forms are recorded. They are mainly associated with glass. The streaks are found to cut across the plagioclase and pyroxene phenocrysts. Diversity of forms of these opaques often occur in the same section. They are mostly found to occur as follows:

1. Squarish to equidimensional
2. Irregular granules
3. Streaks
4. Tiny needles.

It appears that the squarish, idiomorphic and occasionally equidimensional grains probably did not form by simple enlargement of minute crystals, but many small grains gradually clustered. The growth of the minute crystals in the initial stage might have started at the end of the bars. Such bars which initially had cross arms would change to an equidimensional large crystal. In some of the large grains the sharp octahedral corners, still persisting, confirm this. Talukdar [1963] predicted the formation of the long narrow bands by joining of the squarish or rhomshaped grains. The streaks resulted due to the joining crystallites along a definite direction. The dendrites and skeletal crystals are the results of incomplete growth.

DESCRIPTION OF THE POLISHED SECTIONS

The opaques on the whole do not show much variation from flow to flow. The various minerals identified under the ore-microscope include the following: magnetite, ilmenite, titanomagnetite, hematite, chalcopyrite, etc. A brief description of the above stated occurrences are summarized below.

Magnetite: In a coarse grained non porphyritic flow nearly equidimensional grains of partly martitized magnetite, occasionally containing specks of ilmenite as inclusions are recorded. In a fine grained porphyritic flow the grains are equidimensional euhedral containing silicate inclusions. Some xenomorphic forms interstitial to silicates are also noticed. Prismatic rods are rarely recorded. In this flow the martitization of magnetite is completely absent. In another flow (fine-grained porphyritic) magnetite-ulvospinel intergrowth is very distinct. Here the reflectivity is low, anisotropism weak and the colour is a little more brownish than magnetite. Replacement of grains of magnetite by minor amount of maghemite is recorded in a fine-grained non-porphyritic flow.

Ilmenite: It occurs as coarse-prism and rods or as specks of inclusions. In fine-

grained porphyritic flow this is the most dominating opaque mineral. The colour varies from brownish grey to pale brown, the pleochroism and anisotropism being very strong. Twinning is noticed in the ilmenite of the present flow. Exsolved ilmenite with titan-magnetite is also recorded in certain sections.

Titanomagnetite: Magnetite with dissolved titanium. In some cases exsolved ulvospinel is also visible. Weakly anisotropic. Colour more brownish than that usual with magnetite. Reflectivity slightly low. Exsolved ilmenite with ulvospinel is also found. DE [1964] has deduced that the oxygen fugacity in the Deccan Trap basalts at 1100°C was about 10^{-10} atm when the titanomagnetite crystallized.

Hematite: Numerous small specks of hematite within the pyroxene grains are recorded in a coarse-grained flow. Hematite follows the cleavage planes of the host. The mode of occurrence suggests that this hematite is not primary in origin, but the iron probably was liberated during the break down of the pyroxenes. However, when compared with the thin sections, it is found that the pyroxenes are remarkably fresh, though opaques do occur along the cleavage planes. Since thin section study do not confirm their secondary origin, they must have formed when O_2 in the gases reacted with the iron-bearing minerals under conditions of lower temperature and inequilibrium. This happens when bubbles form in the lavas, since then the vapour does not remain in equilibrium with the crystals and melt [CORNWALL, 1951a].

Chalcopyrite: Besides the iron-titanium oxide minerals this mineral rarely occurs as tiny grains or globules with typical brass-yellow colour. They are frequently replaced by bornite (vein replacement and rim replacement).

CHEMICAL CONSIDERATIONS

Degree of oxidation [BUDDINGTON *et al.* 1963] is based on the ratio of Fe_2O_3 to FeO. Reference to Table 1 will confirm a gradual decrease in the degree of oxidation towards the younger flows. WILKINSON [1957] made the concentration of pressure of water in the melt directly responsible for the state of oxidation. High H_2O, according to him, would result in high Fe_2O_3/FeO ratio. The Bhopal basalts do not bear testimony to this. Since specimen H_{13} shows 2.68 per cent H_2O where the ferric to ferrous ratio is 0,50; as against this the ratio is 0.71 (B_1) for a rock where the water content 1.40. It seems that other major features, such as partial oxygen pressure [OSBORNE, 1959], and the bulk composition might have been responsible for the variation in the degree of oxidation [BUDDINGTON *et al.* 1963].

Gradual rise in the iron-enrichment with the rise of oxidation ratio [DE, 1964, p. 130], is the general trend of Deccan Traps. But the Bhopal basalts on the contrary show a rise in oxidation ratio, the iron-enrichment — remaining constant. Probably a variation in the oxidation ratio takes place in various suites.

ORDER OF CRYSTALLIZATION

In such sections where crystals of opaques are recorded the following features are seen: —

i) Large crudely idiomorphic grains are occurring either interlocking with pyroxenes or are found to have inclusions of pyroxenes in them. Occasionally pyroxene plates are also seen to enclose the grains of opaques.

ii) The plagioclase laths are frequently poikilitically enclosed by the opaques; or

are projecting into the opaques. The skeletal form or the rod like forms of the opaques cut across the earlier formed (more calcic) plagioclase laths.

iii) The opaques are not seen as crystals in high glassy rocks. Under the high power objective numerous black dots are seen along with glass, making the colour extremely dark. A concentration of iron-ores in the residual liquid is the possibility.

iv) A comparison of the percentage of iron-ores with the sum of normative magnetite and ilmenite always indicate a greater percentage of normative ores. This is possible only due to the enrichment of iron at a late stage and thus crystals were not encountered in modal counting. This is quite apparent from the following observations.

Section Nos.	B_1	B_6	B_{42}	H_5	H_{13}
Modal percentage	8.5	7.9	8.1	No crystal	9.4
Norm percentage	13.31	11.97	14.52	13.31	13.59

PARAGENESIS

Depending on degree of crystallization two stages were identified by DE [1974d], which is (*A*) crystallization of plagioclase and augite and (*B*) where crystallization of iron ores (titanomagnetite and ilmenite) comes in a dark brown coloured glass. Naturally a considerable iron-enrichment should take place in the residual liquid before stage *B*. In the present area also titanomagnetite and ilmenite are recorded in the dense black glass of the thin sections. It is reasonable to postulate that they are later than the 'intra-telluric'-crystals. Large idiomorphic and elongated bars of opaques (magnetite) exhibiting inter-locking relationship with pyroxene indicate that they crystallized partly simultaneously [CHATTERJEE, 1973]. Titanomagnetite skeletals in the interstitial space or in the opaque glassy groundmass indicate their later generation. Ilmenite does not occur in the skeletal forms either in the glassy base or in the interstitial glass. The intergrowth relationships, however, suggest that it started crystallizing simultaneously with titanomagnetite and ilmenite must had a shorted period of crystallization. The present writer [1971] has earlier referred to the enrichment of silica and alkali in the last fraction of the cooling magma (glass). More recently DE [1974] predicted that under certain conditions of moderately high oxygen fugacity the residual basalt magma may pass over the immiscibility field at temperature higher than the upper, consolute temperature, crystallizing pyroxene and iron ore (+plagioclase in a natural basalt) giving rise to the above stated conditions.

REFERENCES

BUDDINGTON, A. F., I. FAHEY and A. VLISIDIS [1963]: Degree of oxidation of Adirondack iron-oxide and iron-titanium oxide minerals in relation to petrology. Jour. Petrology **4**, pt. I, pp. 138—169.

CHATTERJEE, A. C. [1971]: On the occurrence of high iron concentration type of basalts in the Deccan Traps near Bhopal, (M. P.). Proc. 58th Ind. Sc. Cong., Sec. V, pt. 3, p. 245.

CHATTERJEE, A. C. [1973]: Order of crystallization of the primary mineral constituents of the Deccan Trap Basalts. Proc. Nat. Acad. Sc., 43, *(A)*, 1 and 2, pp. 27—32.

CORNWALL, H. R. [1951]: Ilmenite, magnetite, hematite and copper in the lavas of the Keweenawan Series. Econ. Geol., **46**, pp. 51—67.

DE ANIRUDHA [1964]: Iron-titanium oxides in alkali-olivine basalts, tholeiites and acidic rocks of the Deccan Trap Series and their significance. Int. Geol. Cong. 22nd Session, pt. 7, pp. 126—138.

De Anirudha [1974]: Silicate liquid immscibility in the Deccan Traps and its petrographic significance. Bull. Geol. Soc. Am., **85**, pp. 471—474.
De Anirudha [1974]: Three immiscible liquid phases in some lunar and terrestrial basaltic rocks. Golden Jubilee Vol. Geol. Min. and Met. Soc. of India.
Fermor, L. L. [1925]: On the basaltic lavas penetrated by the deep borings for coal at Bhusawal. Rec. Geol. Surv. Ind., **58**, pt. 2, pp. 93—238.
Osborn, E. F. [1959]: Role of oxygen pressure in the crystallization and differentiation of basaltic magma. Am. Jour. Sci., **57**, No. 9, pp. 609—647.
Presnall, D. C. [1966]: The joint forsterite-diopside-iron oxide and its bearing on the crystallization of basaltic and ultramafic magmas. Am. Jour. Sc., **264**, pp. 753—809.
Talukdar, S. C. [1962]: Petrology of igneous and metamorphic rocks around Jabalpur. (Unpublished thesis, University Calcutta.
Wilkinson, J. F. G. [1957]: Titanomagnetite from a differentiated teschenite sill. Min. Mag., **31**, No. 237, pp. 443—454.

Manuscript received, December 15, 1981

A. C. Chatterjee
School of Studies in Geology,
Vikram University,
UJJAIN—456 010 (M. P.) India

Acta Mineralogica—Petrographica, Szeged, XXV/2, 169—178, 1982

PETROGRAPHICAL AND GEOCHEMICAL STUDIES OF THE AL-BAYDA GRANITES, SOUTH EASTERN SECTOR, YEMEN ARAB REPUBLIC

ADEL M. REFAAT, MAHMOUD L. KABESH and ZEINAB M. ABDALLAH

ABSTRACT

The study of the Al-Bayda pluton comprises petrography and chemistry of the different granite varieties which are related to the basement rocks in the south eastern sector of the Yemen Arab Republic. According to the modal and chemical data, the present granite can be classified as syeno-granite and kali-granite, respectively. In the Al-Bayda granites, a perthitization had taken place through exsolution and replacement processes.

Generally, the investigated granites were crystallized from an acidic melt during a very limited differentiation stage. Finally, the Al-Bayda granites suffered greatly from metasomatism at a postmagmatic stage producing a type of granite related to the anomalous group.

INTRODUCTION

The present study deals with the behaviour of some major and trace elements in occurrence of Precambrian granitic rocks in the Yemen Arab Republic. The occurrence investigated in the present work is Al-Bayda, which constitutes with

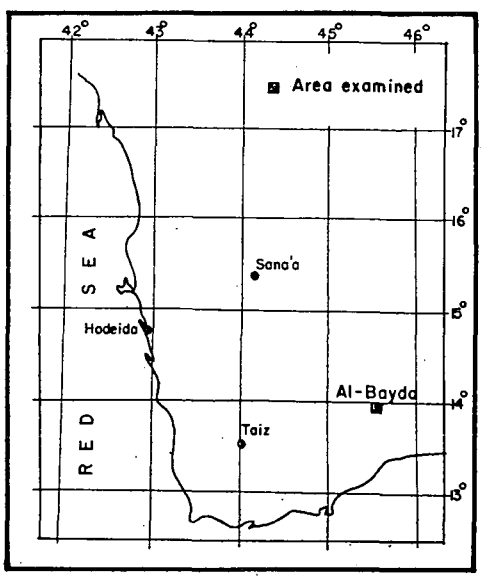

Fig. 1. Location map

others the main granitic outcrops of presumably Precambrian age in the Yemen Arab Republic *(Fig. 1)*.

Broadly, the Precambrian basement rocks cover about 1/4 of the total area of Yemen. These rocks, not yet systematically classified or studied, comprise metamorphics including gneisses, schists, amphibolites, marbles quartzites, intrusives represented mainly by minor mafic masses of diorites and gabbros, ultramafics typified by serpentinites, and finally large granitic massifs.

Generally, detailed studies on the basement rocks of Yemen are scarce. No previous work of significance has been carried out on these rocks in general and the granitic rocks in particular. However, recently, few investigations have been carried out on the Precambrian granitic rocks, as well as some Tertiary alkaline granites of Yemen, [KABESH *et al.* 1979a; KABESH *et al.*, 1979b; REFAAT and KABESH, 1980].

The granitic rocks of Al-Bayda form several hilly outcrops in the south-eastern sector of the Yemen Arab Republic. They are dominantly hard, massive, pink-red and medium-grained. The present work forms part of a research program devoted to the chemical characterisation of the Precambrian granitic rocks of Yemen to elucidate their petrogenesis.

PETROGRAPHY

The Al-Bayda granite rocks consist mainly of pink and red field types. Generally, both types show a slight difference in their mineralogical composition in which quartz, perthite, microcline perthite, orthoclase, plagioclase and biotite form the main minerals in the examined granites. Quartz forms interstitial anhedral crystals reaching up to 2.2 mm in length and 1.6 mm in breadth. Most quartz grains are clear. The alkali feldspars are mainly represented by perthite and microcline perthite in addition to little kaolinized orthoclase crystals. The perthite occurs as elongated crsytals usually with anhedral to subhedral margins reaching up to 2.1 mm in length and 1.21 mm in breadth. Some of the perthite grains enclose small grains of quartz and albite. The plagioclase crystals are mostly albite to oligoclase in composition.

Most of the plagioclase crystals are polysynthetically twinned according to the albite and Carlsbad laws. The albite crystals are characterized by broad uncurved lamellae. A great difference between the direction of lamellae and fractures in the albite crystals is observed. The present authors argue that these albites are characterized by primary twinning resulting from growth nucleation in a liquid magma [SMITH, 1974]. Green and brown biotite flakes are considered the main mafic mineral in the Al-Bayda granites. These biotites vary from short to long flakes. The pleochroic formulae of the green biotite is X=yellow and Y=Z=dark green, whereas the brown biotite is X=straw yellow and Y=Z=brown. Some biotite flakes of the pink granites are corroded by quartz and feldspar and occasionally contain large amounts of sphene. Replacement of biotite by adjacent feldspars and secondary quartz occurs. In one variety of the pink granite, the biotite is associated with little green hornblende crystals. Few primary and secondary muscovite is observed in some varieties of the red biotite granite in which the muscovite flakes are mainly enclosed in the perthite. In some varieties of the red granites, phenocrysts of microcline perthite and quartz are embedded in groundmass of quartz, feldspar and biotite forming porphyritic texture.

Review of perthite mechanism

The microcline perthite and perthite are considered the common feldspars in the pink granite. The microcline perthite originated mainly from exsolution at high temperature and partly from replacement at low temperature. The plagioclase of the pink granites occurs in a coarse interlocking pattern with the microcline, this is ascribed to simultaneous crystallization [ANDERSEN, 1928; BARTH, 1930]. Generally, the simultaneous crystallization of potassium- and sodium-rich feldspar is much less likely and this process is not supported by the crystallization relationships in synthetic feldspar systems [DEER *et al.*, 1966; SMITH, 1974]. As a result, the interlocking texture in the microcline perthite most probably originated through exsolution process. Hair perthite is recognized in the pink granites. ESKOLA [1952] stated that the plagioclase threads, which in the perthites of common granites are comparatively thick and often have curved and tapering flame like forms, are here like extremely thin short hairs. The plagioclase threads in the perthite show that the infiltration of plagioclase into a potash-feldspar involves solution penetrability along directions of weakness or crackes of the host K-feldspar. Also, a replacement is probable, i.e. perthitisation is post-kinematic and metasomatic [AUGUSTITHIS, 1973].

The replacement of microcline by albite produces chessboard albite in which the lamellar lattices of albite and microcline are quasi-parallel [FISHER, 1971]. This process shows that numerous transitions and degrees of replacement had taken place through the formation of chessboard albite texture [MEHNERT, 1968]. In the red granites, the dominant feldspar is the microcline perthites which mainly enclosed small grains of quartz, muscovite and albite along their cracks. The present authors suggest that deposition from external solutions had taken place, *i.e.* the remaining magmatic solutions are communicated with the bulk rocks through the ubiquitous contraction cracks. Initially, these solutions dissolve microcline, and then albite and quartz inclusions are trapped during primary crystallization. Microcline is recrystallized from the solution, facilitating its replacement by albite and forming microcline perthite.

CHEMISTRY

A total of 5 representative samples were analysed from Al-Bayda granite pluton. Two field granite types are recorded in the pluton comprising pink and red granites. The analysed samples were chosen on the basis of petrographic variations in each field type. The major elements of the granite were determined by using the volumetric and gravimetric methods of BENNETT and REED [1971]. These major elements and their normative minerals are listed in Tables 1 and 2, respectively. Some trace elements were detected from the 5 granite samples (Table 3) in which the trace elements were determined by using spectrographic and spectrophotometric methods.

The chemical data show that the pink granites are characterized by SiO_2% ranging from 72.86 to 73.67, whereas the red granites have SiO_2% varying from 73.29 to 74.67.

The SiO_2 values could be used as well as a measure of degree of differentiation in the granites, *i.e.* the drop of SiO_2 between the pink and red granites is caused by internal differentiation within the pluton.

The ternary relation between the Rb, Ba and Sr in granitoid rocks was discussed by EL-BOUSEILY and EL-SOKKARY [1975]. They stated that this relation could be used in tracing differentiation trends in acidic suites. The plots of Rb, Ba and Sr for the

TABLE 1

Chemical analysis of Al-Bayda granites

	1	2	3	4	5
SiO_2	73.67	72.86	74.50	73.29	74.67
Al_2O_3	12.46	11.78	12.56	13.32	12.90
Fe_2O_3	0.85	0.72	0.95	0.95	0.67
FeO	1.26	1.63	1.43	1.41	1.01
MgO	0.83	0.85	0.91	0.99	0.62
CaO	1.61	2.53	1.41	1.32	1.02
Na_2O	1.98	1.51	1.99	2.11	1.36
K_2O	5.51	5.87	5.02	5.11	6.21
P_2O_5	0.21	0.25	0.20	0.22	0.18
TiO_2	0.35	1.21	0.23	0.19	0.11
H_2O	0.82	0.71	0.68	0.55	0.75
Total	99.55	99.92	99.88	99.46	99.50

examined granites on this diagram are shown in *Fig. 2*. All samples are grouped in the anomalous granite zone. The group of anomalous granites cover types that suffered from metasomatism. Generally, most of the investigated granites are clustered near the Ba apex showing that the different varienties of these rocks are crystallized from a limited differentiated acidic magma. Moreover, these granite types are affecte greatly by a metasomatic process at a late stage giving rise to perthitic intergrowths to a large extent.

The present authors argue the K enrichments in the Al-Bayda granites to the strong effect of the metasomatic process in which a solution richer in K than in Na attacked the feldspars particularly the sodic type forming microcline perthits and

TABLE 2

Norm values of Al-Bayda granites

	1	2	3	4	5
q	36.50	36.07	39.23	37.09	39.87
or	32.58	34.71	29.69	30.22	36.72
ab	16.73	12.75	16.81	17.83	11.49
an	6.62	7.97	5.69	5.12	3.88
c	0.79	—	1.75	2.42	2.49
di	—	2.32	—	—	—
hy	3.10	1.41	4.1	3.95	2.66
mt	1.23	1.04	1.37	1.37	0.96
il	0.66	2.29	0.43	0.36	0.20
ap	1.65	1.96	1.57	1.73	1.41
Total	99.86	100.52	100.64	100.09	99.68
or %	58.2	62.6	63.8	62.8	70.4
ab %	29.9	23.0	36.1	37.1	22.0
an %	11.9	14.4	0.1	0.1	7.6
An= =an100/an+ab	28.3	38.4	25.2	22.3	25.2
DI=q+or+ab	85.81	83.53	85.73	85.14	88.08

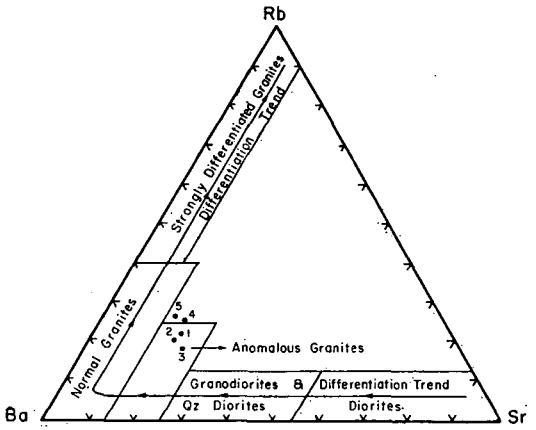

Fig. 2. Relation between Rb, Ba and Sr in granitic rocks [after EL-BOUSEILY and EL-SOKKARY, 1975]

Legend

Pink granites

1. Biotite hornblende granite
2. Biotite granite

Red granites

3. Biotite granite
4. Porphyritic biotite granite
5. Biotite muscovite granite

orthoclase perthite as a dominant feldspar in the Al-Bayda granite pluton. The granite varieties have low values for K/Rb (166.5—235.5) ratios relative to those (K/Rb 620) in the granites of Kongsberg area [KAYODE, 1974]. KAYODE [1974] suggests that the Kongsberg granites could have been formed by a normal crystallization from a granitic melt. It can be concluded that the low K/Rb ratio in the investigated granite is due to the effect of postmagmatic processes (exsolution and metasomatism) which had taken place after the differentiation of the primary granite melt. The low K/Rb ratios in some varieties (samples No. 10, 11 and 17) are mainly due to the enrichment of these varieties in biotites which have large Rb ions [DE ALBUQUERQUE, 1971].

TABLE 3

Trace element analysis in Al-Bayda granites (ppm)

	1	2	3	4	5
Ba	499	550	520	532	575
Sr	146	165	150	147	142
Rb	198	194	180	239	290
Ba/Ca	0.043	0.03	0.052	0.053	0.079
Sr/Ca	0.012	0.009	0.015	0.014	0.019
K/Rb	216.6	235.5	217.2	166.5	166.8
Ba/Rb	0.011	0.012	0.013	0.013	0.011
Ba/Sr	3.41	3.33	3.46	3.61	4.04
Rb/Sr	1.35	1.17	1.21	1.62	2.04
Ba/Rb	2.52	2.83	2.88	2.22	1.97
Ba %	59.1	60.5	61.1	57.9	57.1
Sr %	17.3	18.1	17.6	16.0	14.7
Rb %	23.6	21.4	21.3	26.1	28.2

The norm values of all the examined granites are peraluminous with normative corundum except sample No. 8 in which the diopside exists due to the excess of Ca relative to residual Al. The presence of high amounts of sphene (5%) in addition to the high An content of the plagioclase (88.4%) reflect the cause of enrichments in Ca content in sample No. 8. The short range of differentiation index [THORNTON and TUTTLES, 1960] in the granite rocks (83.53—88.08) reflects that these granites were formed through a very limited differentiated process in which little chemical variations in their major and trace elements had taken place. From Tables 2 and 3, the Ba/Ca, Sr/Ca, Ba/Sr and Rb/Sr ratios increase with differentiation, whereas Ba/Rb shows opposite relation.

CLASSIFICATION

The proposed schemes of classification are based on the modal analysis and chemical composition.

Modal classification

The modal distribution of the mineral constituents of 5 granites varieties was determined using a point counter. A total of 15 thin sections were made 1000 points were taken for each section (Table 4).

The mineralogical variations in the Al-Bayda granite pluton are reflected corresponding differences in their concentrations of major and trace elements.

The increase in the K_2O contents (5.02—6.21%) shows an increase in orthoclase, microcline, microcline perthite and orthoclase perthite. Generally, the examined granite pluton is characterized by low amount of orthoclase (8.7—12.1%) and plagioclase (8.1—11.5%) in which most of the feldspars are concerned in the perthitic type as a result of the metasomatic and exsolution processes.

TABLE 4

Modal analysis of Al-Bayda granites

Modal %	1	2	3	4	5	Explanation
Quartz	37.3	33.3	32.4	36.0	31.4	Pink granite
Perthite	27.1	19.5	22.4	25.3	17.3	1-Coarse-grained
Microcline	—	10.2	11.5	—	14.0	biotite hornblende
Orthoclase	11.2	8.7	9.2	12.1	10.2	granite
Plagioclase	11.5	10.0	8.1	10.1	9.1	2-Coarse-grained
Biotite	6.5	11.2	10.6	12.3	8.5	biotite granite
Muscovite	—	—	—	—	6.4	Red granite
Hornblende	3.0	—	—	—	—	3-Coarse-grained
Accessories	3.4	7.1	5.8	4.2	3.1	biotite granite
Quartz %	42.8	40.7	38.7	43.1	38.2	4-Porphyritic biotite
Alk. Feld. %	43.9	47.0	51.5	44.7	50.6	granite
Plag. %	13.3	12.3	9.8	12.2	11.2	5-Coarse-grained biotite muscovite granite

N. B. Sample numbers referring to various granites are the same throughout the present Tables.

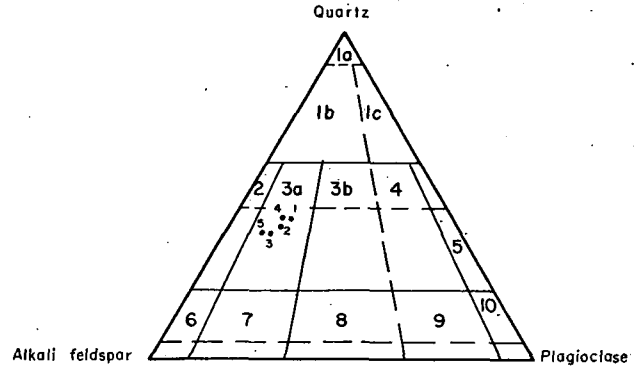

Fig. 3. The investigated granites plotted according to classification scheme by STRECKEISEN [1967]

1a Quartz rocks
1b Quartz granite
1c Quartz granodiorite
2 Alkali granite
3a Syeno-granite
3b Monzo-granite
4 Granodiorite
5. Quartz diorite
6. Alkali syenite
7. Syenite
8 Monzonite
9 Monzo-diorite and Monzo-gabbro
10 Diorite and gabbro
(Index of numbers as in *Fig. 2*)

Fig: 3 illustrates the classification given by STRECKEISEN [1967]. It is obvious that the investigated granite falls within the field of syeno-granite (zone 3a). STRECKEISEN [1967, p. 167] stated that rocks which fall in zone 3b *(Fig. 3)* are granite rocks which are mostly crystallized from a magmatic solution. The present authors argue the unfalling of the investigated granites in zone 3b to the strong suffering of these granites owing to the metasomatic and exsolution processes.

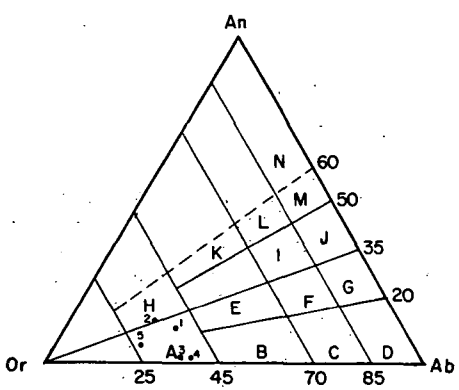

Fig. 4. Triangular diagram for An, Ab, Or normative ratio in the investigated granites [after HIETANEN, 1963]

A Kali-granite
B Granite
C Granite trondhjemite
D Trondhjemite
E Quartz monzonite
F Monzonite
G Tonalite
H Calci-granite
I Granodiorite
J Quartz diorite
K Calci-monzonite
L Granogabbro
M Gabbro
N Mafic gabbro
(Index of numbers as in *Fig. 2*)

Chemical classification

Fig. 4 shows the chemical classification of the investigated granites which are presented on the basis of their normative minerals (orthoclase, albite and anorthite). According to the scheme of HIETANEN [1963], the Al-Bayda granites fall within the kali-granite field due to its low plagioclase contents. One sample only falls in the calci-granite field assuring its enrichment in CaO (2.53%) content due to the high value of An content (38.4) in the plagioclase and also to the presence of fair amounts of sphene (5%) in this rocks (coarse-grained red biotite granite sample No. 8).

PETROGENESIS

The present authors suggest that the Al-Bayda granites were formed through two main stages comprising differentiation and metasomatism. Firstly, the bulk of the Al-Bayda pluton was crystallized early from magma formed due to the melting of salic rocks in the crust as a result of a palingenetic process [KLEEMAN, 1965]. The short range of the DI (83.53—88.08) reflects that the Al-Bayda granites had been crystallized from acidic melt through a very limited differentiation stage.

BOETTCHER and WYLLIE [1968] have observed that albite is converted to a jadeite and quartz assemblage at a depth reaching up to 50 km and under a pressure of 17 kbar. FYFE [1970] remarked that sillimanite is stable in granites formed at a depth less than 30 km in the crust.So the A-Bayda granites are completely free from jadeite and sillimanite, therefore, these granites could have been originated at a depth much less than 30 km and under low pressure.

The normative Or-Ab-An proportions of the present granites have been plotted in a ternary diagram *(Fig. 5)*. All the plots are shown to fall nearer to the Or apex. Most of the plotted points follow the isobaric univariant curve, indicating that crystal-liquid equilibrium was the dominant mechanism involved in the genesis of these granites [JAMES and HAMILTON, 1969].

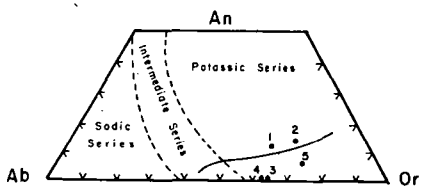

Fig. 5. Triangular diagram for An, Ab and Or normative ratio in the investigated granites. The solid line represents the two feldspar boundary curve for the quartz saturated ternary feldspar system at 1000 bars water-vapour pressure [after JAMES and HAMILTON, 1972]. Sodic and potassic sectors from IRVINE and BARAGAR [1971].
(Index of numbers as in *Fig. 2*)

The variation trend of the Al-Bayda granites fall close to the potassic zone assuring their enrichments in potassium contents. Sodic and potassic sectors in *Fig. 5.* are made by IRVINE and BARAGAR [1971].

Exsolution and replacement are the common process which are responsible for the formation of different types of perthites. Finally, it can be concluded that most of the examined granites had suffered from metasomatism by the action of K-fluids at a postmagmatic stage. As a result, some chemical variations in the Al-Bayda granites took place producing a type of anomalous granite richer in potassic content.

CONCLUSION

The Al-Bayda granites are related to the basement rocks of the south eastern sector of the Yemen Arab Republic. Generally, there are great similarities between the modal and chemical classifications of the examined granites in which both classifications assure their enrichment in microcline perthite (syeno-granite) and their poverty in albite (kali-granite). Microscopically, the perthite intergrowths show different types comprising interlocking, hair and chessboard textures. It can be concluded that a perthitisation had taken place as a result of exsolution and replacement processes.

The short range in the DI (83.53—88.08) indicates that the Al-Bayda granites had been crystallized from acidic melt through a very limited differentiation stage.

The examined granites had suffered from metasomatism. They are therefore, related to the anomalous granite group. The low values of K/Rb ratios in some granite varieties reflect their enrichment of biotite relative to the other types of high K/Rb ratios. But generally, the Al-Bayda granites have low K/Rb ratios. But generally, the Al-Bayda granites have low K/Rb ratios compared to those in the Kongsberg granites [KAYODE, 1974] due to the effect of postmagmatic processes such as metasomatism.

REFERENCES

ANDERSEN, O. [1928]: The genesis of some types of feldspar from granite pegmatites. Norsk Geologisk Tidskrifft **10**, 116—207.

AUGUSTITHIS, S. S. [1973]: Atlas of the textural patterns of granites, gneisses and associated rock type. Elsevier, Amsterdam

BARTH, T. F. W. [1930]: Mineralogy of the Adirondack feldspars. Amer. Miner., **15**, 129—143.

BENNET, H. and R. A. REED [1971]: Chemical Methods of Silicate Analysis. Academic Press, London.

BOETTCHER, A. L. and P. J. WYLLIE [1968]: Melting of granite with excess water to 30 kilobars pressure. J. Geol., **76**, 235—244.

DE ALBUQUERQUE, C. A. R. [1971]: Petrochemistry of a series of granitic rocks from Northern Portugal. Bull. Geol. Soc. Amer., **82**, 2783—98.

DEER, W. A., R. A. HOWIE and J. ZUSSMAN [1966]: An introduction to the rock-forming minerals. Longman, London.

EL BOUSEILY, A. M. and A. A. EL SOKKARY [1975]: The relation between Rb, Ba and Sr in Granitic Rocks. Chemical Geology **16**, 207—219.

ESKOLA, P. [1952]: On the granulites of Lapland. Amer. J. of Sci., Bowen Vol., 133—172.

FISHER, D. J. [1971]: Poikilitic albite in the microcline of granitic pegmatites. Amer. Miner., **56**, 1769—1787.

FYFE, W. S. [1970]: Mechanism of igneous intrusions. Geol. J., Special Issues No. **2**, 15, 187.

HIETANEN, A. [1963]: Idaho batholith near Pierce and Bungalow. Prof. Pap., U. S. Geol. Surv., **344**—D.

IRVINE, T. N. and W. R. A. BARAGAR [1971]: A guide to the chemical classification of the common volcanic rocks. Can. J. Earth Sci., **8**, 523—548.

JAMES, R. S. and D. L. HAMILTON [1969]: Phase relations in the system $NaAlSi_3O_8$—$KAlSi_3O_8$—$CaAl_2Si_2O_8$ at 1 kilobar water vapour pressure. Contr. Miner. Petrol., **21**, 111—141.

KABESH, M. L., M. M. ALY and M. Y. ATTAWIYA [1979]: Petrochemistry and petrogenesis of some posttrap alkaline granite of Gabal Hufash, Surdud Area, Yemen Arab Republic. Acta Miner. Petr. Szeged, XXIV/1, 29—40.

KABESH, M. L., M. M. ALY and M. A. HEIKAL [1979]: Remarks on the petrochemistry of some Precambrian granitic rocks, Yemen Arab Republic. Chem. Erde **38**, 147—159.

KAYODE, A. A. [1974]: Petrography and geochemistry of granites in the Kongsberg area, south Norway. Nor. Geol. Tidsskr., **54**, 269—293.

KLEEMAN, A. W. [1965]: The origin of granitic magmas. J. Geol. Soc. Aust., **12**, 35—52.

MEHNERT, K. R. [1968]: Migmatites and the origin of granitic rocks. Elsevier, Amsterdam.

REFAAT, A. M. and M. L. KABESH [1980]: The chemistry of arfwedsonite and riebeckite from Sabir alkali granites, Taiz area, Yemen Arab Republic, Chem. Erde 39, 37—45.
SMITH, J. V. [1974]: Feldspar Minerals. Springer Verlag, Berlin, Vol. 2.
STRECKEISEN, A. L. [1967]: Classification and nomenclature of igneous rocks. N. Jb. Miner. Abh., 107, 144—240.
THORNTON, C. P. and O. F. TUTTLE [1960]: Chemistry of igneous rocks. I Differentiation index. Am. J. Sci., 258, 664—684.

Manuscript received, April 30, 1982

ADEL M. REFAAT
Teachers' Inst. of Education
El-Odylia, Kuwait
MAHMOUD L. KABESH
National Research Centre
Dokki-Cairo, Egypt
ZEINAB M. ABDALLAH
Teachers' Inst. of Education
El-Odylia, Kuwait

Acta Mineralogica—Petrographica, Szeged, XXV/2, 179—186, 1982

GENESIS OF MANGANESE ORES OF KORAPUT DISTRICT, ORISSA, INDIA

J. S. R. KRISHNA RAO and B. VENKATA NAIDU

ABSTRACT

Manganese ores of Koraput district are typically found in Nishikhal area and occur in association with the khondalite suite of rocks. The manganese ore is high grade in quality with Mn — 59 to 64%. The ores have high phosphorous content, P — 0.30%. The important ore minerals are psilomelane, pyrolusite, braunite, cryptomelane and goethite. Bixbyite, nsutite, hollandite, rhodochrosite and manganite are detected by X-ray. These ores are residual concentration type and suggest enrichment by supergene processes.

INTRODUCTION

The Government of Orissa laid special interest on the exploration of the manganese belt in the Koraput district during its second five year plan period. A number of promising veins of manganese were located in Taldoshi-Upardhoshi, Podkana, Nishikhal, Kinchikhal and Koka areas [MOHAPATRA *et al.*, 1957—58]. Among these Nishikhal is typical having good reserves.

Manganese ores of Nishikhal area (19°13′, 83°13′) is situated 45 kms west of Rayagada town on Rayagada-Kashipur road. The deposit is connected by an unmetalled road of 15 kms to the north of the above mentioned metalled road. Location and geological formations around the deposit are shown in the *Fig. 1*. The area is approachable by foot from Gum village situated about 16 kms from the main

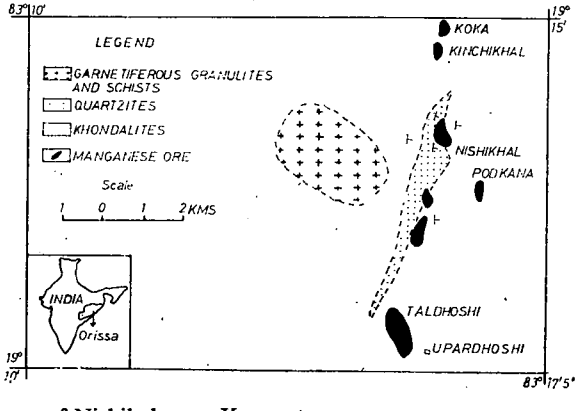

Fig. 1. Geological map of Nishikal area, Koraput

Rayagada-Koraput main road. The area shows extreme climate variations in summer 37,8°C and in winter −1,2°C. The annual rain fall is 100 to 150 cms. The area is thickly forested.

GEOLOGICAL SETTING AND MODE OF OCCURRENCE

Manganese ores are present as irregular veins and lenses in khondalite suite of rocks. The entire manganese belt is found in quartzites and khondalitic gneisses. The ore body is found on the hill slopes, and a few exposures are also seen in the valley region. The general sequence of formations with which the ore is associated intimately is as follows:

Alluvium
Aplites
Quartz-schists, garnetiferous granulites
Khondalitic rocks with manganese ore bodies alternating with the quartzites (quartzites, calc-silicates, garnetiferous and graphite schists)

The manganese deposit is trending N-S and it is 2 to 3 kms long belonging to the upper part of the Khondalite Supergroup of the older Precambrians. The dip of the ore body is 50° to 60° and mostly vertical. The width of the body varies between 1 to 8 metres. The manganese ore is a band, interbedded with garnetiferous quartzite schist or khondalite graphite schist, quartzite and phyllite and the manganese ore has fine intercalations of quartzite.

FIELD CHARACTERISTICS OF THE ORE BAND

Manganese ore occurs in form of lenses, veins, botryoidal and as pockets in khondalites which alternate with quartzites and broadly classified in to three types; 1) brownish black ore, 2) grey massive ore and 3) botryoidal ore. The chemical composition of these types is given an Table 1.

1. *Brown black ore:* Brownish black ore is disconnected from the grey massive ore and botryoidal ore. The ore is hard and compact and in parts brittle. The polished sections show round concentric layers which are colloidal. The structures resemble

TABLE 1

Chemical analyses of the three types of ores

	1 Brownish black ore (average of 3 samples)	*2* Grey massive ore (average of 4 samples)	*3* Botryoidal ore (average of 3 samples)
MnO	34.60	58.50	63.50
Fe_2O_3	31.80	3.20	0.50
Al_2O_3	0.50	1.40	0.50
MgO	4.10	3.00	2.90
CaO	4.50	4.60	4.40
P	0.51	0.26	0.37
V	—	—	—
Ti	0.06	0.31	0.10
Cu	0.0072	0.016	0.011
Ni	0.0032	0.088	0.0088

a nodule. Pyrolusite, bixbyite and goethite are the mineral constituents of such nodular manganese ore.

2. *Grey massive ore:* Grey massive ore occurs as veins and lenses in association with botryoidal manganese ore. The contact between the two types of ore bodies is sharp and sometimes it is not clearly noticeable. The grey massive ore alternates with botryoidal ore and it is discontinuous both in length and widthwise covering about 200 metres in length and 120 metres in width. The essential ore mineral of this type of ore is pyrolusite followed by psilomelane, hollandite, cryptomelane, bixbyite and goethite.

3. *Botryoidal manganese ore:* Botryoidal manganese ore occurs in the area mostly as pockets and lenses sometimes also as veins. It is vug filling type. The botryoidal layers grow towards the centre of the vugs. Botryoidal manganese ore alternates with grey massive ores. The dominating ore mineral is psilomelane followed by hollandite and pyrolusite.

Brownish black ore occurs fareway from the grey massive and botryoidal ore types. Chemical analyses showed low manganese and high iron in the former type of ores and increase of manganese and decrease of the iron content towards the grey massive and botryoidal types of ores. Magnesium content decreases from brownish black type of ore through grey massive ore to botryoidal types, whereas calcium maintains the same throughout. P, Al, Ti, Cu and Ni show some irregularity, however, botryoidal ore types are enriched in these elements. Usually, the dehydrated gels of manganese can adsorb some elements like Cu, Ni and Ca etc. [RAMDOHR, 1969]. Vanadium is found absent in all three types of ores.

The process of formation of manganese ores in the area took place in four stages to reach the high grade ores (type 3) as follows: manganese bearing rocks → brownish black ore → grey massive ore → botryoidal ore. In all the four stages, the manganese is active and enriched. Though the manganese and iron behave geochemically in the same manner they differ sharply in physico-chemical conditions of enrichment.

MINERALOGY

The minerals identified by mineralographic studies of a representative collection of manganese ores are psilomelane, cryptomelane, pyrolusite, hollandite, braunite, nsutite, manganite, bixbyite, rhodochrosite and goethite. Some of these minerals have been identified by X-ray diffraction analyses only. Measured *d* values of individual minerals are given in the Table 2. The values are compared with those of different workers, BERRY and THOMPSON [1962]; SOO JIM KIM [1970]; DESSAI and DESHPANDE [1978]. It may be mentioned that this is the first time that rhodochrosite is identified in the manganese ores of Koraput district.

Psilomelane is the abundant mineral in the manganese ores. It occurs in massive, botryoidal and reniform varieties. Psilomelane is massive and shows colloform textures. It has typical grey colour.

Cryptomelane is found mainly in grey massive ores. It forms colloform bands sometimes with or without alternating pyrolusite layers. The colour is grey and it is fine grained; reflectivity is low, nonpleochroic and isotropic.

Pyrolusite shows metallic lustre and it has a colour varying from iron black to steel grey. Under reflected light, it shows crystalline as well as non-crystalline forms. It is white in colour with yellowish tint; pleochroism is distinct with colour

TABLE 2

X-ray diffraction data of the manganese and iron minerals

Psilomelane		Cryptomelane		Pyrolusite		Hollandite		Braunite	
I	d (Å)	I	d (Å)	I	d (Å)	I	d (Å)	I	d (Å)
6	2.423	28	3.11	47	3.101	31	6.978	22	4.700
20	2.400	21	2.40	31	2.391	25	3.110	34	3.316
17	2.392	17	2.165	18	2.189	6	2.423	20	2.341
5	2.12	8	1.638	19	2.12	17	2.41	16	2.131
6	2.112	10	1.435	10	1.619	9	2.16	17	1.872
11	2.04	18	1.365	13	1.43	26	1.949	14	1.653
15	2.01	16	1.303					21	1.283
10	1.862								
9	1.625								

Goethite		Manganite		Bixbyite		Nsutite		Rhodochrosite	
I	d (Å)	I	d (Å)	I	d (Å)	I	d (Å)	I	d (Å)
13	3.376	27	3.412	32	4.685	17	2.596	40	3.654
23	2.694	32	2.644	20	2.502	13	2.437	28	2.840
17	2.584	41	2.520	13	2.211	27	2.170	13	2.012
21	2.447	33	2.275	10	1.916	19	2.134	17	1.530
15	2.003	24	2.201	18	1.714	9	2.045	15	1.382
17	1.799	16	1.183	15	1.612	44	1.623		
18	1.717			24	1.282	27	1.408		
15	1.688								
16	1.658								
15	1.421								

changing from yellowish white to white. Anisotropism is present in shades of yellowish white.

Braunite is one of the important constituents of the ores. FERMOR [1909] considers braunite as the most important manganese mineral of the Indian manganese ores. Generally, braunite occurs in all manganese ores irrespective of the grade of metamorphism [ROY, 1966]. In the ores, it is fine grained and it has variable colour from dark to grey. The anisotropism is feeble.

Goethite is usually found in association with colloform cryptomelane and pyrolusite. In many cases, it forms the core around which concentric layers of cryptomelane and pyrolusite are deposited and also vice versa. Occassionally, stalactitic forms of manganese oxides are formed around a central core of goethite. Under reflected light, goethite is observed as layered and needle like forms or more often, it forms the nucleus around which manganese oxides form concentric layers. Needle-like crystals are often replaced by cryptomelane.

The minerals like nsutite, manganite, hollandite, bixbyite and rhodochrosite are identified only by X-ray studies.

TEXTURES

Colloform texture: The term 'colloform' is in other words called as colloidal or gel texture [EDWARDS, 1954]. The ores showing colloform textures are composed of layers of cryptomelane, pyrolusite and rarely nsutite *(Figs 2—4)*. Colloform layers

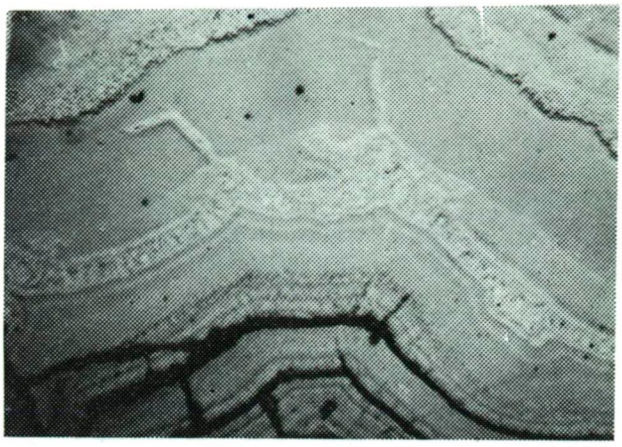

Fig. 2. Colloform bands of pyrolusite (white) alternating with cryptomelane (dark grey), psilomelane (grey) and gangue (black). Pyrolusite (white) is replacing the psilomelane (grey) ×70.

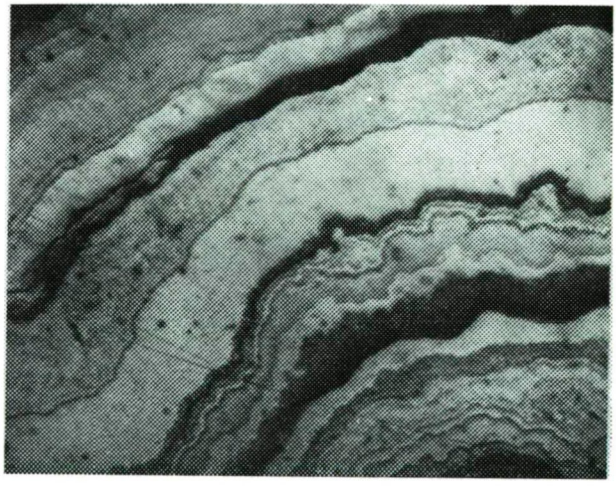

Fig. 3. Colloform texture. Alternating bands of gangue (black), cryptomelane (grey) and pyrolusite (white) ×90.

may be monomineralic or may consist of more than one mineral. Concentric layers of different mineral composition often enclose small nuclei of the ore or gangue at the centre *(Fig. 5)*.

Fracture fillings: Fractures generally develop in the brittle minerals like quartz and later these fractures are filled with one or several minerals. The fractures may localize later deposited ores or serve as channel ways to initiate the replacement of the fractures mineral by younger minerals [EDWARDS, 1954]. The fractures may form a net work or may show bifurcations *(Fig. 6)*. Some of the segmented veins found at different parts of fracturing may filled with crystals of pyrolusite, psilomelane or gangue.

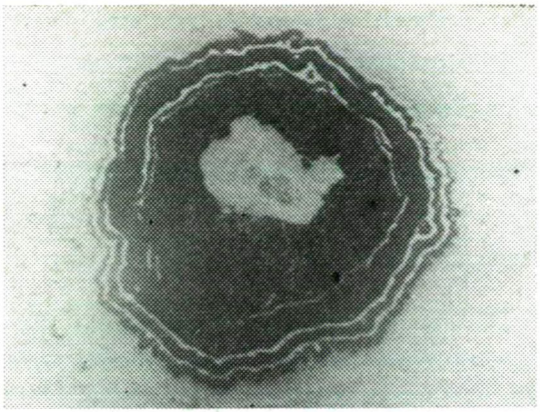

Fig. 4. Pyrolusite (white) at the centre surrounded by layers of goethite (dark grey) and pyrolusite (white) ×70.

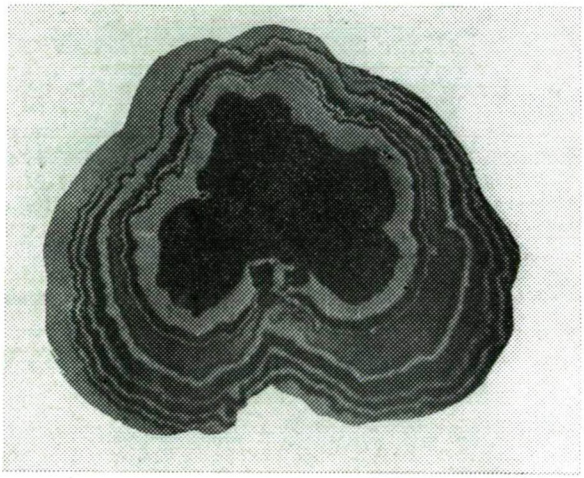

Fig. 5. Gangue (black) surrounded by layers of pyrolusite (white) and goethite (grey) ×100.

Replacement texture: Replacement texture is the dominant mechanism in the process of downward enrichment of ores, which is of major economic importance [BASTIN, 1950]. The replacement is mainly confined to fractures, mineral cleavages, contacts between mineral grains etc. Many replacements have taken place at ordinary temperatures equal to the waters of surface origin. Some replacements also occur at high temperatures ranging up to 500° and even more. In the present ores the replacement is mainly seen between pyrolusite — braunite, cryptomelane — gangue, and pyrolusite — psilomelane. The replacement of braunite and pyrolusite is common *(Fig. 7)*. Cryptomelane is seen as patches in a ground mass composed of braunite and gangue, the gangue is mostly quartz and sometimes the ore replaces the gangue.

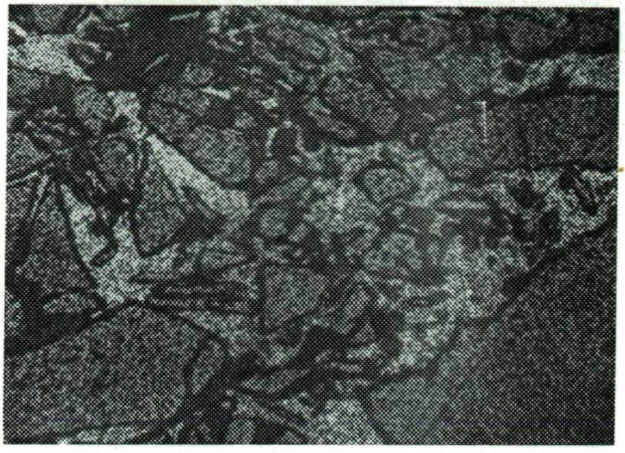

Fig. 6. The fractured veins showing the pyrolusite (white) in quartz (grey) ×70.

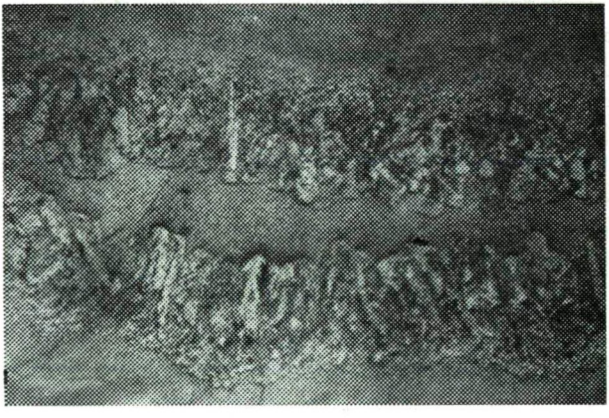

Fig. 7. Scaly forms of pyrolusite (white) replacing braunite (grey) ×70.

GENESIS

The primary minerals are rare, the reasons may be topographic relief. The deposit mainly consists of supergene enriched secondary oxides derived from primary syngenetically metamorphosed oxide and silicate assemblages. Most of the primary minerals have undergone supergene alteration.

The ore consitutes both the higher and lower oxide minerals that indicate the change of oxygen during deposition. SOKOLOVA [1964] applied the physico-chemical methods on the formation of ore minerals. According to her, higher oxide minerals like pyrolusite, psilomelane, cryptomelane have the highest Eh and considerably low pH values. The lower oxides like manganite have low Eh and pH values and intermediate minerals like hollandite, braunite have intermediate values between two above. Thus, the change of oxygen and acidity varies from low-intermediate-high, then the formation of minerals in the area may be written as follows:

1. Manganite → Nsutite → Pyrolusite
   Psilomelane
   Cryptomelane

2. Manganite → Nsutite → Hollandite → Pyrolusite
   Braunite Psilomelane
   Cryptomelane

Thus, the manganese ores form by chemical reshuffling of the manganese bearing rocks in sediments under suitable conditions of temperature, pressure, Eh and pH. The manganese ores of Nishikhal area are essentially originally syngenetic sedimentary resulted from a set of systematically metamorphosed oxide and silicate assemblages by supergene enrichment.

ACKNOWLEDGEMENT

The co-author expresses his gratitude to the Council of Scientific and Industrial Research, New Delhi for providing a Post-Doctoral Fellowship during the investigations.

REFERENCES

BASTIN, S. EDSON [1950]: Interpretation of ore textures. Geol. Soc. America, Memoir, **45**.

BERRY, L. G. and R. M. THOMPSON [1962]: X-ray powder data for ore minerals: The Peacock Atlas, New York., Geol. Soc. America, Memoir **85**.

DESSAI, A. G. and G. G. DESPHANDE [1978]: Mineralogy and paragenesis of the manganese ore deposits of Snguem District, Goa, India. Recent researches in geology (Vol. 5). A collection of papers in honour of Professor M. R. Sahni.

EDWARDS, A. B. [1954]: Textures of the ore minerals and their significance. Melbourne, Australian Institute of Mining and Metallurgy (Inc), 2nd edn.

FERMOR, L. L. [1909]: The manganese deposits of India. Geol. Surv. India, Vol. **37**.

MAHAPATRA, S. K., V. G. SHESH and S. SOMNATH [1958]: Geological report on the manganese belt between Upardhoshi and Sirlijod, including deposits at Taldhoshi, Podkana, Nishikhal, Kinchikhal, Koka and Liligumma (Unpublished).

RAMDOHR, P. [1968]: The ore minerals and their intergrowths. Pergamon Press, 3rd edn.

ROY, S. [1966]: Syngenetic manganese formations of India. Jadavpur University, Calcutta.

SOO JIM KIM [1970]: Mineralogy and genesis of manganese ores from Junggun Mine, Korea. Jour. Geol. Soc. Korea, **6**, No. 3, pp. 135—186.

SOKOLOVA, E. I. [1964]: Physico-chemical investigations of sedimentary iron and manganese ores and associated rocks. Oldbourne Press, 1—5, Portpool Lane, London, E. C. I.

Manuscript received, September 20, 1981

J. S. R. KRISHNA RAO
and
B. VENKATA NAIDU
Dept. of Geology, Andhra University
Waltair, India

Acta Mineralogica—Petrographica, Szeged, XXV/2, 187—192, 1982

THE STRUCTURE OF THE HOST MINERAL AS DETERMINING FACTOR IN ACCOMODATION OF TRACE ELEMENTS

A. A. EL SOKKARY and M. W. EL REEDY

ABSTRACT

A discussion of the current distribution rules of elements in rocks and minerals is given here. The criticism of the rules and the continuous trials of different authors to improve them is presented as well. Such discussion revealed the general dissatisfaction of the GOLDSCHMIDT-rules.

The authors found from their experience that the factor of the structure of the host mineral is very important in the fate of an element during magmatic crystallization. We recommend the following rule to be added to the existing rules for the distribution of elements: "The structrure of the host mineral is one of the determining factors in the allowance of elements into minerals". Various evidences from the analyses of coexisting mineral pairs are discussed in order to support this conclusion.

INTRODUCTION

The search for rules governing the distribution of elements in rocks and minerals is going on since GOLDSCHMIDT [1937]. The subject is still far from being settled and as a matter of fact much work is needed in this field. The present work exposes the old rules of GOLDSCHMIDT and RINGWOOD followed by criticizm of these rules in order to reveal their general dissatisfaction and at the same time presents the continuous trials of different authors to formulate new rules or to improve the old ones.

The present authors found from their experience with the analytical chemistry of rocks and minerals that the factor of the structure of the host mineral is an important criterion in the fate of an element during magmatic crystallization. Evidence on the importance of the structure of a crystal in allowing elements to enter will be given. The evidence includes six examples from the analytical chemistry of coexisting mineral pairs partly taken from the first authors own work or from the available literature. The following rule should be added to the existing rules for the distribution of elements: *"The structure of the host mineral is one of the determining factors in the admission of elements into minerals".*

THE GOLDSCHMIDT- AND RINGWOOD-RULES

The accomodation of an element into the crystal structure in a multicomponent system according to GOLDSCHMIDT [1937] is governed by the following rules:

1) If two ions have the same radius and the same charge, they will enter a given crystal lattice with equal facility.

2) If two ions have similar radii and the same charge, the smaller ion will enter a given crystal lattice more readily.

3) If two ions have similar radii and different charges, the ion with the higher charge will enter a given crystal lattice more readily.

Despite that GOLDSCHMIDT's rules are a significant tool toward the explanation of the distribution of the different elements during the sequence of magmatic crystallization, yet they are not completely valid and are seriously criticized [MASON, 1964]. The GOLDSCHMIDT-rules ignored the bonding character of minerals and this was considered by RINGWOOD [1955] who showed that the electronegativity of an element is a measure of its tendency to form covalent bonds and hence has an important influence on the extent to which it will replace another element of similar size.

CRITICISM AND AMENDMENT OF THE DISTRIBUTION RULES

By careful examination of subsequent literature, it is important to conclude that some modifications of GOLDSCHMIDT-rules have very important influence on interpretations of trace element geochemistry [MASON, 1964; TAYLOR, 1964]. However, the GOLDSCHMIDT-rules have again been found to lack generality, particularly with regard to the transition metal ions, with the result that dissatisfaction has been expressed, over the utility of the "rules" for accounting for element distribution [FYFE, 1964; NASSAU, 1964].

Some writers have abandoned the GOLDSCHMIDT-rules and have endeavoured to interpret trace element geochemistry by adsorption phenomena, kinetics of crystal growth and disequilibrium processes. Some aspects of transition metal geochemistry have been interpreted by crystal field theory. Other writers have formulated new rules using bond energy criteria. Adherents to the rules have proposed complex explanation for anomalous cases. As a result considerable confusion has developed in the geological literature over the nature of chemical bonding in geologic media and in minerals [BURNS and FYFE, 1967].

KRAUSKOPF [1967] mentioned that the GOLDSCHMIDT-rules of substitution give some insight into the distribution of elements in igneous rocks but leave many distinct anomalies unexplained. These anomalies can be grouped on the basis of bond character and differences in differentiation trends. KRAUSKOPF *(op. cit.)* adds that two further reasons for deviation from the rules are the tendency of some trace elements to form very stable minerals of their own and the preference of some trace elements for certain silicate structures rather than others.

BURNS and FYFE [1967] evaluated various criteria which have been used to interpret trace element geochemistry and chemical bonding in minerals. They concluded that in all cases single rules fail in simple cases and they suggested that attention must be focussed on the thermodynamic parameters governing the free energy of distribution on differences in two states, and not the parameters of any single state.

JIYAMA and VOLFINGER [1976] assumed that a foreign atom fixed in a crystal causes local lattice deformation, the deformed zone does not prohibit foreign atoms, but that the number of foreign atoms acceptable in this region depends on the total numbers of foreign atoms already fixed in the crystal.

EVIDENCE ON THE IMPORTANCE OF THE STRUCTURE OF THE HOST MINERAL

Six evidences from the analyses of coexisting mineral pairs are given here to illustrate the preference of certain elements toward specific mineral phases:

1) *The spessartine-plagioclase feldspar pair;* KHALIL and EL SOKKARY [1971] during a study on an yttrian spessartine from a pegmatite in the South Eastern Desert of Egypt mentioned that the partition coefficient Y-garnet/Y-feldspar=74, which reflects great preference of Y toward the Mn-bearing garnet rather than toward the Ca-bearing plagioclase. The authors were of the opinion that the geochemical relation between Y and Mn is not quite clear and worth more detailed investigation. Accordingly it is obvious that Y prefers the cubic spessartine structure which carries Mn and Fe more than the coexisting triclinic oligoclase which is a Ca-bearing feldspar. This is an example of the deviation from the strict GOLDSCHMIDT-rules.

Such rules predict that the trivalent Y^{3+} ion (r=0.93 Å) would replace the divalent Ca^{2+} ion (r=0.99 Å) in the plagioclase structure more readily than substituting divalent Mn^{2+} (r=0.80 Å) or divalent iron Fe^{2+} (r=0.76 Å) in the cubic garnet structure.

2) *The fluorite-calcite pair;* Table 1 gives the analyses of some trace elements in fluorite and coexisting calcite lying as a vein in an amphibolite body present in the central Eastern Desert of Egypt [EL SOKKARY and ABDEL MONEM, 1980].

TABLE 1

Analyses of some trace elements (ppm) in fluorite and calcite from the Central Eastern Desert of Egypt

Element	Fluorite	Calcite	D (C/F)*
La	11	68	6.2
Ce	10	107	10.7
Nd	7	69	9.9
Y	89	111	1.2
Zr	10	9	0.9
Nb	12	12	1.0

* D (C/F= Distribution factor which is simply taken as the concentration of an element in calcite divided by the concentration of the same element in fluorite.

Table 1 shows clearly that the elements La, Ce and Nd are enriched in the trigonal calcite more than in the cubic coexisting fluorite lattice. Yet both calcite and fluorite are Ca-bearing minerals in which Ca is a major constituent. The enrichment factor of the three mentioned elements in calcite ranges between 6 to 11. However, with respect to the other three elements Y, Zr and Nb they are almost equally distributed between calcite and fluorite, their distribution factor ranges between 0.9 to 1.2. Thus certain rare earth elements prefer the trigonal calcium carbonate structure.

3) *The barite-calcite pair;* SALEEB RAUFAIEL *et al.* [1976] on the study of the barite-fluorite-calcite mineralization at Hammash, Egypt presented some analyses for barite and the coexisting calcite (Table 2).

TABLE 2

Some trace elements (ppm) in barite and coexisting calcite from Hammash, Egypt

Element	Barite[1]	Calcite[2]	D (B/C)
Sr	8090 8275 Av.=7715 7020	1970 2750 Av.=2360	3.3
Li	13 22 Av.=16 13	34 44 Av.=39	0.4

1. Barite samples are pure
2. Samples are taken from calcite-sphalerite and calcite-barite bands

Unfortunately, the given analyses of Sr and Li are not for pure calcite samples but from calcite-sphalerite and calcite-barite mixture. The Sr of the calcite-sphalerite mixture comes mainly from calcite, while the diminutive effect of calcite on the total Sr content of the calcite-barite sample is quite clear. The lower quantity of Sr in these samples reflects the impoverishment of this element in calcite relative to barite. That Sr of calcite is in smaller quantity compared to the Sr of coexisting barite is confirmed from the statement of the authors mentioned: "the low Sr content in the lode of the calcite-barite band is due to the presence of relatively small amount of barite which is the main carrier of Sr". This assures clearly that the orthorhombic Ba sulphate mineral present as barite is more enriched in Sr than the coexisting trigonal Ca carbonate mineral which is calcite in this case. The simple distribution coefficient D(B/C) for Sr equals 3.3 tells in a numerical way that barite is enriched more than three times in Sr with respect to coexisting calcite.

The element Li is enriched in the calcitic samples, its D(B/C)=0.4. These samples are contaminated by either barite or a sulphide phase identified as sphalerite.

Analyses of pure barite samples give an average Li content of 16 ppm which is definitely lower than its value in the calcitic samples that give an average Li content of 39 ppm. Therefore the effect of barite on a barite-calcite mixture is to lower the Li content of the mix.

With respect to the effect of sulphides, GOLDSCHMIDT [1954] mentioned that Li does not occur in sulphide minerals, in sulphides of magmatic origin or in sulphides from hydrothermal solutions. The contaminating sphalerite in the calcitic material does not contribute significantly to Li. The increase in the Li content of the calcitic material comes mainly from calcite which according to Table 2 is more enriched in Li than its coexisting barite.

4) *The muscovite-potassium feldspar pair;* DE ALBUQUERQUE [1975] during a study on the partition of trace elements in coexisting muscovite and potassium feldspar of granitic rocks of Northern Portugal presented some interesting data concerning these two minerals which are reproduced in Table 3. Table 4 on the other hand gives the simple distribution coefficient for each element in the two mineral pair of the four quoted samples, beside the average distribution coefficient for each element in the four samples.

Table 4 shows that the element Ga has definite enrichment in muscovite (Av. D.=12.49) besides the element Cs tends to show certain rising trends in muscovite (Av. D.=1.92).

TABLE 3

Some trace elements (ppm) in muscovite and coexisting potassium feldspar in granitic rocks of Northern Portugal

Element	Muscovite (M)				K-Feldspar (F)			
	8	9	11	12	8	9	11	12
Ga	85	100	110	150	15	11	8	7
Sr	14	13	6	7	1200	800	440	160
Pb	9	5	5	—	46	65	38	23
Ba	1250	660	510	220	4750	2250	2350	1500
Rb	500	410	525	750	400	430	700	550
Cs	17	20	25	115	19	20	21	25

TABLE 4

Simple distribution factor (D) of each element in muscovite (M) and coexisting K-feldspar (F) of the granitic rocks of Northern Portugal

D	8	9	11	12	Av. D
Ga M/F	5.67	9.09	13.75	21.43	12.49
Sr M/F	0.01	0.02	0.01	0.04	0.02
Pb M/F	0.20	0.08	0.13	—	0.14
Ba M/F	0.26	0.29	0.22	0.15	0.23
Rb M/F	1.25	0.95	0.75	1.36	1.08
Cs M/F	0.89	1.00	1.19	4.60	1.92

On the other hand Rb is an element of almost equal distribution in both muscovite and the coexisting K-Feldspar (Av. D.=1.08 and it ranges between 0.75 to 1.36). With respect to the three elements Sr, Pb and Ba, there is definite enrichment in the coexisting potassic feldspar (Av. D Sr=0.02, Av. D Pb=0.14 and Av. D Ba= =0.23). Thus Ga is surely enriched in the monoclinic phyllosilicate structure of the muscovite while Sr, Pb and Ba develop rising trends in the coexisting triclinic tectosilicate K-feldspar structure, yet both minerals are KAl-silicates.

5) *The olivine-pyroxene pair;* KRAUSKOPF [1967, p. 590] mentioned that Cr and V are generally much more concentrated in pyroxene than in coexisting olivine, while Ni and Co favour the olivine, although on the basis of ionic radii alone the same possibility of substitution should be available in both minerals.

6) *The hornblende-biotite pair;* The partition coefficient of an element among pairs of coexisting minerals according to WEDEPOHL [1971] depends on the crystal chemical properties of the element. In coexisting amphiboles and biotites, Mn for instance prefers the amphiboles and Ni the biotite structure. WEDEPOHL continues that analyses of this type may be useful in testing the mineral assemblage of a certain rock for internal equilibrium.

CONCLUSION

The foregoing investigation shows that the structure of the host mineral which in most of the studied cases is a silicate mineral is an important factor in controlling the distribution of elements during magmatic crystallization. This is primarily based

on both experimental work on the analyses of mineral pairs as well as analyses taken from literature. It is already seen that GOLDSCHMIDT-rules have their shortcomings in interpreting the fate of minor elements during magmatic crystallization. These rules can be more useful if another factor is added to them concerning the structure of the host mineral which is necessary to explain the distribution of elements in certain cases.

A question arises here, why the structure of a mineral is a profound determining factor in acceptance of trace elements? The answer is just tentative. It may be due to the nature of the regular arrangement of the anionic groups together with the cations, it may be due to the extent of randomness of the trace element in the host structure or otherwise may be due to the fixation of the trace element either in interstitial, vacant or deformed sites of the mineral.

These substitution reactions are always interpreted on thermodynamic basis, namely the free energy change associated with change of state of the trace element say from magma into solid solution with the host.

REFERENCES

BURNS, R. G. and W. S. [1967]: Trace Element Distribution Rules and Their Significance. Chem. Geol., **2**, p. 89—104.

DE ALBUQUERQUE, C. A. R. [1975]: Partition of Trace Elements in Coexisting Biotite, Muscovite and Potassium Feldspar of Granitic Rocks, Northern Portugal. Chem. Geol., **16**, No. 2, p. 89—108.

EL SOKKARY, A. A. and H. M. ABDEL MONEM [1980]: Mineralogy and Geochemistry of Some Fluorites from Egypt. Under Preparation.

FYFE, W. S. [1964]: Geochemistry of Solids. Mc Graw-Hill, New York, N. Y. 199 pp.

GOLDSCHMIDT, V. M. [1937]: The principles of distribution of chemical elements in minerals and rocks. J. Chem. Soc., p. 655—672.

GOLDSCHMIDT, V. M. [1954]: Geochemistry. Clarendon Press, Oxford

IIYAMA, J. T. and M. VOLFINGER [1976]: A model for trace element distribution in silicate structures. Min. Mag., **40**, p. 555—564.

KHALIL, S. O. and A. A. EL SOKKARY: An Yttrian Spessartine from a Pegmatite in the South Eastern Desert of Egypt. Bull. Faculty of Science, Alexandria Univ, p. 61—69.

KRAUSKOPF, K. [1967]: Introduction to Geochemistry .Mc Graw-Hill Book Company.

MASON, B. [1964]: Principles of Geochemistry. John Wiley and Sons, INC.

NASSAU, K. [1964]: On the Distribution of Minor Components during Formation of Minerals. Amer., Mineral. **28**, p. 575—581.

RINGWOOD, A. E. [1955]: The Principles Governing Trace Element Distribution During Magmatic Crystallization. Geochim. et Cosmochim. Acta **7**, o. 189—202 and 242—254.

SALEEB ROUFAIEL, G. S. M. E. HILMY and N. T. AWAD [1976]: Metallogenic and Geochemical Studies of Barite—Fluorite—Calcite Mineralization at Hammash, Egypt. Bull. MRC., **1**, p. 106—119.

TAYLOR, S. R. [1964]: The Application of Trace Element Data to Problems in Petrology. Phys. Chem. Earth, **6**, p. 133—214.

WEDEPOHL, K. H. [1971]: Geochemistry. Holt, Rinehart and Winston Inc.

Manuscript received, January 20, 2981

A. A. EL SOKKARY
and
M. W. EL REEDY
Nuclear Raw Materials Authority
Cairo, Egypt.

Acta Mineralogica—Petrographica, Szeged, XXV/1, 193—195, 1982

URANIUM-THORIUM MINERALIZATION AND ALBITIZATION (A GEOCHEMICAL NOTE)

A. A. EL SOKKARY and M. W. M. EL REEDY

ABSTRACT

This work sheds some light on the relation between albite-bearing or alkaline rocks and U—Th anomaly. Various local and international examples are given. The chemical basis for this association is briefly outlined. Rocks tending to show a trend of albitization or a trend of alkalinity should receive intensive prospection program for U and Th.

INTRODUCTION

The geochemistry of U has been so long known to be controlled mainly by the oxidation of U to the hexavalent mobile state or reduction to the precipitating tetravalent state [GOLDSCHMIDT, 1962]. On the other hand, there is certain crystallochemical and geochemical relationships between uranium and thorium. The present investigation shows the importance of the albitization process in igneous and metamorphic environments as a medium of U-Th mobility and concentration. Thus the albitization process is connected in many cases with U-Th mineralization. This fact is of equal importance in the geochemistry of the two elements particularly U as the fact of the latter's oxidation and reduction and should receive much more attention by U-Th explorers.

EXAMPLES ON ANOMALOUS ALBITE-BEARING ROCKS

Seven examples are given here to illustrate the association of albite-bearing igneous and metamorphic rocks with U and Th anomalies. These include both local and international cases.

1) *Abu Garadi locality:* The most outsanding example comes from Abu Garadi locality of the Eastern Desert of Egypt [EL SOKKARY, 1970]. A suite of samples from Abu Garadi locality was chemically analysed and was analysed as well for U and Th. It was found that changes in the contents of Na_2O and K_2O reflect clearly changes in modal analysis. Na_2O is enriched in certain samples of the suite while K_2O drops out in the same samples. This process of increase of Na_2O with a consequent reduction in K_2O is related to a process of albitization. Again the albitized samples show considerable enrichment in U and Th (up to 186 and 1253 ppm, respectively).

2) *Wadi El Atshan locality:* ABDEL GAWAD [1964] mentioned the case of some volcanic rocks occurring in the Eastern Desert of Egypt which carry uranium mineralization. He says that the volcanic rocks are of two distinctive types, acidic por-

phyries with no associated mineralization and alkaline bostonites which were found to be favourable host rocks for uranium. These bostonites exemplified by the type locality at Wadi El Atshan are intruded in metasediments of the Hammamat series of Upper Algonkian age.

Essential minerals composing these bostonites are sodic feldspar (albite) and orthoclase together making 80 per cent of the rock. Albite with very fine polysynthetic twinning prevails in the groundmass but orthoclase (sanidine) occurs both as microphenocrysts and in the groundmass. The predominance of albite is shown by optical and X-ray diffraction studies.

3) *Abu Rusheid locality:* Another important example is Abu Rusheid locality of the south Eastern Desert of Egypt [SABET, *et al.*, 1976]. Abu Rusheid has contents amounting to 0.02 % Ta_2O_5 and 0.14% Nb_2O_5, respectively. The tantalum-niobium mineralization is associated with Sn, Li, Zr, U (up to 0.80%) and Th (up to 1.43%). The mineralization is located in a sill-like body of albitized and amazonitized granite called apogranite intruded along the contact of the schist and gneiss of the Hafafit series.

4) *The White Mountain locality:* LARSEN and PHAIR [1957] believed that the Southern California batholith contains about the average amount of uranium for batholithic rocks in general. By way of contrast, the Carboniferous White Mountain rocks in New England contain on the average about twice as much uranium as do the comparable rocks from the Southern California batholith. The White Mountain rocks are, however, more sodic than their western counterparts, and underlie a very much smaller area.

5) *Three more international localities:* LARSEN and PHAIR [1957] stated that nearly all samples of alkali granite end syenite tested to date exceed the average uranium and thorium content of calc-alkalic granite not uncommonly by a several-fold factor. All three most radioactive rocks so far reported are alkalic granites *e.g.* the albite granite from Nigeria gives an average U content 130 ppm, the quartz bostonite from Colorado gives 33 ppm U while the Conway biotite granite from New Hampshire yields 9 ppm U.

All three are the silicic end members of predominantly sodic series, the intermediate members of which are monzonites and syenites. All three rocks contain aboundant albite, but in addition to phenocryst of high temperature alkali feldspar, potash-rich cryptoperthite is common in the quartz bostonite. The highly radioactive quartz bostonites from the Colorado Front Range belong to a predominantly sodic series.

RELATION BETWEEN ALKALINITY AND URANIUM MOBILITY

GOLDSCHMIDT [1962] found that in neutral or slightly alkaline solutions uranate ions are also present in increasing proportion with increasing alkalinity. KRAUSKOPF [1967, p. 526] on discussing oxidation of uranium ores mentioned that uranyl hydroxide is slightly soluble in alkaline solutions as well as in acid, solubilities become appreciable only in strongly alkaline solutions.

The same author concluded from the Eh-pH diagram for uranium and vanadium compounds at 25°C and 1 atm. total pressure, that at both sides of the diagram (pH from 0—2 and pH from 12—14 *i.e.* at both the acid and alkaline sides) uranium shows a total solubility exceeding 10^{-4} M, on the acid side taking the form chiefly of uranyl ion and on the alkaline side appearing chiefly in the carbonate complexes.

There is no doubt that alkaline media enhance the solubility and mobility of the uranium ions. It is understood that the albitization process which is connected mainly with the mobilization of Na^+ ions under water vapor pressure provide the alkaline medium suitable for U wandering. Since the geochemistry of uranium particularly the quadrivalent state has much in common with the geochemistry of Th, it is expected that the same alkaline media are suitable as well for Th mobility. This explains the chemical basis for the association of albitized rocks with U-Th anomaly.

CONCLUSION

It is thus plausible to say that albitization in igneous and metamorphic environments tends to be always associated with U-Th anomaly. This fact can find wide application during geochemical prospection or in areas which are studied geochemically in a sense that whenever the chemistry of rocks shows a trend of albitization, then these rocks might be favourable sites for U and/or Th concentrations and they should receive intensive prospection program because it may lead finally to the discovery of U or Th ores.

REFERENCES

ABDEL GAWAD, A. M. [1964]: Mineralogy, geochemistry and radioactivity of El Atshan No. 1 uranium deposit, Eastern Desert, U. A. R. Internal Report. Geology and Raw Materials Dept., UAR A. E. E.

EL SOKKARY, A. A. [1970]: Geochemical studies of some granites in Egypt. U. A. R. Ph. D. D. Thesis, Alexandria Univ.

GOLDSCHMIDT, V. M. [1962]: Geochemistry. Clarendon Press, Oxford

KRAUSKOPF, K. B. [1967]: Introduction to geochemistry. McGraw-Hill Book Co., New York.

LARSEN, E. S. and G. PHAIR [1957]: The distribution of uranium and thorium in igneous rocks. In: Nuclear Geology. Ed. by H. FAUL, John Wiley and Sons, Inc.

SABET, A., V. B. TSOGOEV V. P. BORDONOSOV R. G. SHABLOVSKY and M. KOSA [1976]: On the geologic structure, laws of localization and prospects of Abu Rusheid rare metals deposit. Geological Survey of Egypt, Annal 6, Cairo.

Manuscript received, August 25, 1981

A. A. EL SOKKARY
and
M. W. M. EL REEDY
Nuclear Materials Corporatian
Cairo, Egypt.

Acta Mineralogica—Petrographica, Szeged, XXV/2, 197—201, 1982

AN UNUSUAL CARBONATE MINERAL FROM THE SCHISTS OF WADI UM KABU, SOUTH EASTERN DESERT, EGYPT

A. A. EL SOKKARY

ABSTRACT

An unusual carbonate mineral is associated with the schists of Wadi Um Kabu in the South Eastern Desert of Egypt. It is subjected here to detailed mineralogical and chemical studies. It is revealed that the brownish and rhombic carbonate material under study is composed of: dolomite with MgO partly replacing CaO and the mineral retaining the structure of its predecessor ferroan dolomite, calcite, goethite which is amorphous to poorly crystalline and possible brucite.

It is suggested that the former ferroan dolomite was subjected to a thermal metamorphic pulse by means of which major part of Fe and some Ca and Mg were exuded while the original ferroan dolomite is modified in chemical composition to the present dolomite. The expelled elements formed goethite, calcite and brucite, respectively. Both the dolomites and their schistose country rocks underwent differential mobilization of the three cations: Fe, Ca and Mg under thermal metamorphic environment.

INTRODUCTION

The schists of Wadi Um Kabu lying in the South Eastern Desert of Egypt were referred to by EL SOKKARY [1960] and certain members of these schists were studied in some detail from mineralogical and chemical points of view by EL SOKKARY [1977]. These schists particularly the muscovite-talc schist are associated with unusual coarse crystals of a carbonate mineral which is the subject matter of the present investigation.

The schists of the studied area belong to muscovite-talc members which are veined by a great vein composed of anthophyllite-actinolite schist, the succession runs from down upwards as follows:

1) Country rock schists of muscovite-talc character.
2) Vein of anthophyllite-actinolite schist, grading downwards to graphite mica schist.
3) Country rock of muscovite-talc schist.

The whole succession is associated with this unusual carbonate mineral which takes the form of small isolated and scattered pockets.

MINERALOGY

The carbonate mineral under study develops very coarse rhombohedral crystals with varying sizes such as: $5\times4\times4$ and $3.5\times3.5\times3.5$ cm, crystal faces are almost complete, in other words crystals are almost euhedral, brown in color, with distinct

cleavage traces. The solid material gives weak reaction with dilute HCl. The powdered material effervesces after a while with dilute HCl and the reaction is not vigorous. This excludes the bulk carbonate mineral under study to be calcite.

A sample of the carbonate mineral was ground to pass 150 mesh size, afterwards it was subjected to X-ray differaction analysis. The used instrument is a Russian diffractometer working with Cu radiation with wave length 1.5418 Å, Ni filter, current 8 mA, 35 kV. Sample data which are given in Table 1 are compared with the important lines of some standard ASTM minerals.

The diffraction pattern as given in Table 1 shows that the carbonate material under study is composed mainly of dolomite as a principal constituent, with minor calcite, goethite which is poorly crystalline to amorphous and possible brucite $Mg(OH)_2$. Anthophyllite and actinolite are present as impurity from the host country rock carrying the carbonate mineral.

The three principal lines of goethite (α-FeOOH) are: 4.21 (100), 2.69 (80) and 2.44 (70). Only one of them 2.42 (52) is present in the diffraction pattern of the analysed carbonate material. This is interpreted on the basis that the present hydrated iron oxides are poorly crystalline to amorphous.

TABLE 1

Partial diffraction pattern of the carbonate sample under study as compared with standard dolomite and calcite

Sample		Dolomite[1]		Calcite[2]		Others
d Å	I/I_0	d Å	I/I_0	d Å	I/I_0	
9.51	31					An[3]
6.81	25					?
4.44	42					?
4.06	56	4.02	1	3.86	12	
3.45	29	3.69	2			
3.12	23					Ac[4]
3.04	21			3.04	100	
2.83	100	2.88	100	2.85	3	
2.62	35	2.66	4			
		2.53	4	2.50	14	
2.42	52					G[5]
2.40	50	2.40	4			B[6]
2.28	27			2.29	18	
2.16	63	2.19	12			
2.10	31			2.10	18	
2.06	40	2.06	2			
1.97	40	2.01	7	1.93	5	
1.90	33			1.91	17	
		1.84	2	1.88	17	
1.78	52	1.80	13			B[6]
1.77	48	1.78	14			
1.70	44					An[3]
1.67	38			1.63	4	
1.57	35	1.56	1			
1.53	25	1.54	2			
1.52	25	1.49	1			
1.41	25	1.41	1			
1.38	27	1.39	2			

(1): ASTM Card No. 5—0622.
(2): ASTM Card No. 5—0586.
(3): Anthophyllite ASTM Card No. 9—455.
(4): Actinolite ASTM Card No. 7—336.
(5): Goethite ASTM Card No. 8—97.
(6): Brucite ASTM Card No. 7—239.

It is worthy to note that the diffraction lines of the present identified dolomite do not accord precisely with the standard dolomite lines of the ASTM cards, a matter indicating the presence of certain substitutions in the unit cell. However, this might be explained as follows. The present dolomite with brownish rhombic crystals and shifted diffraction lines has acquired the structure of its predecessor which was ferroan dolomite, the latter was subjected to a thermal metamorphic pulse by means of which major part of its Fe and some of its Ca and Mg were exuded while the original ferroan dolomite is modified in chemical composition to the present dolomite.

This kind of pseudomorphism (dolomite after ferroan dolomite) is discussed by BETEKHTIN [1968] who explained the phenomenon of pseudomorphism as being replacement of crystal by a certain constituent in such a way that the resulting mineral retains not only the external shape but sometimes also the peculiar internal structure of the original mineral.

The mentioned metamorphic pulse has happened in the presence of carbon dioxide (CO_2) and water vapour (H_2O) atmosphere. Thus the exuded Ca formed calcite while the expelled Fe and Mg formed amorphous to poorly crystalline goethite beside possible brucite, respectively. The expelled iron takes at first the ferrous form and then oxidized to give Fe_2O_3 which is subsequently hydrated. DEER *et al.* [1972] mentioned that the commonest alteration product of siderite ($FeCO_3$) is a hydrous ferric oxide generally goethite often known loosely as limonite. It seems that the alteration of $FeCO_3$ to goethite is valid whether the former takes the form of an independent mineral like siderite or forms part of a more complex carbonate mineral like dolomite or ankerite.

CHEMISTRY

Table 2 presents complete chemical analysis of the investigated carbonate material from Um Kabu as expressed in weight per cent of the oxides.

TABLE 2

Chemical analysis of the carbonate material under study

Oxide	Wt. %
SiO_2	16.99
Al_2O_3	2.55
Fe_2O_3	22.41
FeO	2.22
MnO	0.81
MgO	14.26
CaO	8.82
Na_2O	1.88
K_2O	0.48
TiO_2	2.17
P_2O_5	0.12
CO_2	23.56
H_2O^+	2.94
H_2O^-	0.38
Total	99.59

Silica and alumina originates mainly from some anthophyllite (hydrated silicate of Mg, Fe) and actinolite (hydrated silicate of Ca, Mg, Fe) impurity associating the carbonate mineral.

It is to be noted that excessive amount of Fe_2O_3 is present up to 22.41% probably as free phase in the form of fine disseminated particles imparting a brownish coloration to the rhombohedral dolomite. On the other hand, a small part of the combined water ($H_2O^+ = 2.94\%$) is attributed to anthophyllite-actinolite impurity while the main part should be associated with Fe_2O_3 to make goethite or lepidocrocite constituting about one quarter by weight of the analysed carbonate material. Thus iron oxides are present mainly in the form of hydrated iron oxides. As it is clear from X-ray diffraction, these iron hydroxides are either poorly crystalline or amorphous because the characteristic diffraction lines of both goethite and lepidocrocite are almost wanting. It looks that these iron hydroxides firstly precipitated in a colloidal sooty form and then partly started to change with time to cryptocrystalline character.

Both MnO and TiO_2 are somewhat enriched in this carbonate material, being present up to 0.81% MnO and 2.17% TiO_2 respectively.

The remaining important ions in the analysis of the carbonate material are: Mg, Ca, Fe^{2+} and CO_2 which amount to MgO = 14.26%, CaO = 8.82%, FeO = 2.22% and CO_2 = 23.56%. No doubt that the anthophyllite-actinolite impurity contributes, though to a small extent, to the MgO, CaO and FeO contents. Its contribution to the MgO content is greater because the impurity itself contains more anthophyllite, this explains why the MgO content is much higher than the CaO content. However, the bulk of these elements comes from the analysed carbonate material. Thus, this carbonate material is composed mainly of Mg, Ca, some Fe^{2+} and CO_2 which belong to dolomite. To sum up, hand specimen investigation, X-ray diffraction and chemical analysis all tend to prove the investigated carbonate mineral to be dolomite.

The two alkali elements $Na_2O = 1.88\%$ and $K_2O = 0.48\%$ substitute for Ca in the dolomite structure. This is apparent from the ionic radii of the three cations which are: $Na^+ = 0.95$, $K^+ = 1.33$ and $Ca^{2+} = 0.99$ Å. Because of the close similarity of the ionic radii between univalent sodium and divalent calcium, more Na than K is incorporated in the dolomite trigonal structure.

In order to get a more detailed insight in the composition of this dolomite, the MgO, CaO, FeO and CO_2 (the main constituents of dolomite) contents as given in Table 2 are recalculated to 100 and compared with the corresponding values of normal dolomite $CaCO_3 . MgCO_3$ [DANA, 1949] as given in Table 3.

TABLE 3

Recalculated analysis (wt. %) of dolomite of the studied carbonate sample as compared with normal dolomite

Oxide	Calculated dolomite	Normal dolomite
MgO	29.19	21.70
CaO	18.05	30.40
FeO	4.54	—
CO_2	48.23	47.90
Total	100.01	100.00

It is evident from Table 3 that the MgO content of the investigated dolomite is higher while the CaO content is lower than normal dolomite. DANA *(op. cit.)* continues that the carbonates of iron and manganese also frequently enter replacing the magnesium carbonate and grading to ankerite, limited amounts of lime may replace the magnesia and vice versa. It appears in the present case that magnesia is replacing part of the lime.

Concerning the chemistry of dolomites, DEER, *et al.* [1972] say that although the composition is normally fairly close to pure $CaMg(CO_3)_2$, many dolomites contain small amounts of Fe^{2+} replacing Mg, giving the mineral a brownish tinge in hand specimen. It is seen from Table 2 and Table 3 that the investigated dolomite contains certain amount of FeO partly replacing MgO.

CONCLUSION

The investigated rhombohedral and brownish carbonate material proved on the basis of megascopic description, X-ray diffraction and chemical analysis to be composed of the following components: dolomite, calcite, goethite and possible brucite. The dolomite has some MgO replacing part of CaO. The goethite is amorphous to poorly crystalline.

It is argued that the present dolomite has acquired the structure of its predecessor which was ferroan dolomite, the latter was subjected to a thermal metamorphic pulse by means of which major part of Fe and some of the Ca and Mg were exuded while the original ferroan dolomite is modified in chemical composition to the present dolomite. The expelled elements formed goethite, calcite and possible brucite, respectively.

This study illustrated the mobility of certain cations like Fe, Ca and Mg during thermal metamorphic environment. It is already shown [EL SOKKARY, 1977] that the schist of Wadi Um Kabu, the country rocks of the present carbonate material, are also the place of differential mobilization of certain elements particularly Ca and Fe during thermal metamorphism. Thus both the schists and their dolomites underwent differential mobilization of the three cations: Fe, Ca and Mg under thermal metamorphism.

REFERENCES

BETEKHTIN, A. [1968]: A course of mineralogy. Peace Publishers, Moscow.

DANA, E. S. [1949]: A textbook of mineralogy. 4nd ed. John Wiley and Sons, Inc.

DEER, W. A., R. A. HOWIE and J. ZUSSMAN [1972]: An introduction to the rock-forming minerals. Longman.

EL SOKKARY, A. A. [1960]: The geology and mineralogy of Wadi Um Kabu area, Eastern Desert, Egypt. Unpublished report.

EL SOKKARY, A. A. [1977]: Mineralogical and chemical studies on anthophyllite-actinolite schist from Wadi Um Kabu, south Eastern Desert, Egypt. Acta Miner. Petr., Szeged, **23**/1, 71—76.

Manuscript received, July 25, 1981

A. A. EL SOKKARY
Nuclear Materials Corporation
Cairo, Egypt

Acta Mineralogica—Petrographica, Szeged, XXV/2, 203—210, 1982

ON PLACER ILMENITE COMPOSITION

L. A. GUIRGUIS and S. N. WASSEF

ABSTRACT

A selected pure sample of fresh ilmenite was examined by activation analysis technique to study its complete chemical composition. The method produced a very wide spectrum which cannot be obtained by any other methods. About 20 trace elements have been estimated against the standard W1. Before activation analysis of the sample an infrared spectrogram was obtained in order to confirm its purity. The studied ilmenite sample was found to contain high chromium content. This could reveal in a decisive way its origin from the basaltic rocks of Ethiopia, Sudan, and Upper Egypt.

INTRODUCTION

The importance of ilmenite stems from its major abundance in the beach sands of the delta on the Mediterranean Sea. The sands originally transported by the River Nile and when reaching the outlet to Mediterranean Sea the abrupt change in water current velocity gives the conditions to deposit the heavy minerals along the continental shelf. The heavy minerals were subjected to different natural, physical and chemical sorting during transportation. This process led to the concentration of insoluble minerals which underwent a second concentration process mainly by specific gravity [FARAG, 1958]. The beach sands are enriched in heavy minerals by undertow action of the waves and at the River mouth a further elutriation takes place by the north westerly winds which spread the beach sand over the spit [SHUKRI, 1980].

The content of the Egyptian black sands shows: ilmenite 0—37.6%, magnetite 0.2—15.20%; zircon 0.02—3.00%, monazite 0.01—0.40%, rutile 0.06—0.70%, garnet 0.05—1.7%, spinel 0—0.2%, amphiboles 4.4—14.8%, pyroxenes 1.58—7.4%, biotite 0.30—1.7%, epidote 0.60—1.24%, staurolite 0—0.65%, sillimanite 0.05—0.20%, olivine 0—0.04%, tourmaline 0—0.40%, sphene 0—0.63%, quartz 15—87.3%, feldspars 0.88—3.9%, glauconite 0—0.27%, calcite 0—1.0% [WASSEF, 1964].

Ilmenite is mostly black with bluish or violet tint. Some of altered grains are dull black. In case of leucoxene grains the yellowish white colour is predominant.

According to EL HINNAWI [1964] the chemical composition of the Egyptian placer ilmenite using the emission spectrography was as follows:

SiO_2 0.25%, TiO_2 43.73%, Fe_2O_3 24.04%, FeO 30.63%, MnO 0.20%, MgO 0.65%. The trace element are estimated by the figures: Al 400 ppm, Ca 300 ppm, Co 200 ppm, Cr 400 ppm, Cu 30 ppm, Mn 1500 ppm, Nb 600 ppm, Ni 100 ppm, Pb 250 ppm, Sn 50 ppm.

The ilmenite optical properties are highly affected by its chemical composition. This ilmenite with appreciable amounts of Fe_2O_3 in solid solution has a lighter col-

our and weaker reflection pleochroism and anisotropism than normal ilmenite. On the other hand ilmenite grains which probably contain geikielite in solid solution show a darker colour [BOCTOR, 1966].

Most of ilmenite grains are irregular in shape angular to subangular and some grains are rounded. The ilmenite grains show the L/B (Length—Breadth) ratio between 2:1, among them the majority have L/B ratio between 1:1, and 2:1. The fresh or homogeneous ilmenite may reach about 61.14% of the total ilmenite present in the black sand deposits [MIKHAIL, 1971].

HAMMOUD [1975], in his study on a highly purified dry ilmenite sample and by X-ray fluorescence has mentioned that the composition of this sample shows: Fe_2O_3 18.63%, FeO 31.18%, TiO_2 46.24%, MnO 1.35%, MgO 0.64%, Al_2O_3 0.87%, Cr_2O_3 0.28%, V_2O_5 0.14%, CaO 0.12%, SiO_2 0.32%, P_2O_5 0.04%, and trace of Nb, Co, Ni, Zn, Mo and Zr. Traces of chromospinel sometimes with ilmenite exsolution bodies and hematite with pseudobrookite intergrowth are present [EL GORESY, 1962].

EXPERIMENTAL

Sample preparation

The ilmenite sample presently investigated was separated from the black sand deposit on the Mediterranean Sea beach. Frantz isodynamic separator was used in 0.1 amp., 3° tilt, and 15° slope. After separation the fraction was purified by bromoform (2.85) to reject the highly altered grains. Moreover, the foreign grains were rejected by picking under the stereomicroscope. The purity of the sample was confirmed by its infrared pattern *(Fig. 1)*.

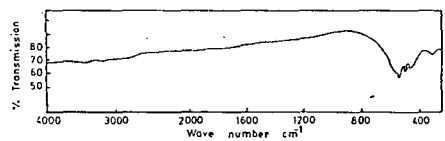

Fig. 1. Infrared spectrogram of the ilmenite

Activation analysis

A known weight of the sample was packed in a thin aluminium sheet together with the standard sample and irradiated in the vertical dry channel of ET RR-1 reactor of Nuclear Research Center at Inshas. Short irradiation time of 4 hours favour the shorter life isotopes. On the other hand, by irradiating long enough for 32 hours to induce sufficient activity of the longer life isotopes and by deferring examination time until the shorter life isotopes has decayed, the longer life product can be favoured. For the very short half-life isotopes as ^{28}Al, ^{52}V, ^{27}Mg, and ^{51}Ti a rabbit system should be used. Unfortunately this system is unavailable at our reactor. Accordingly these elements were determined spectrophotometrically [SHAPIRO and BRANNOCK, 1962].

An international United States Geological Survey (USGS) standard sample (W_1) was used. Its complete chemical analysis is shown in Table 1.

TABLE 1

Chemical analysis of standard sample W1

Element	W1	Element	W1	Element	W1 (ppm)
SiO_2	52.58	CaO	10.92	Ba	130
Al_2O_3	14.94	Li_2O	—	Be	1
TiO_2	1.08	Na_2O	2.15	Bi	n.d.
ZrO_2	0.022	K_2O	0.63	Co	44
SnO_2	0.0003	Rb_2O	0.0022	Cr	110
V_2O_5	0.045	BaO	0.00006	Cs	5
Cr_2O_3	0.016	SrO	0.021	Cu	110
R.E.ThO_2	—	H_2O^+	0.45	La	n.d.
UO_2	—	Ignition		Li	—
NiO	0.0097	loss	0.08	Mn	1320
CuO	0.0138	(H_2O^-)		Ni	76
BeO	0.0003	P_2O_5	0.14	Rb	20
CoO	0.0056	CO_2	0.07	Sc	34
PbO	0.0006	F	0.03	Sr	180
ZnO	0.014		—	Ti	6500
As_2O_3	—		100.02	V	250
Fe_2O_3	1.38			Y	19
FeO	8.71			Yb	3
MnO	0.17			Zn	110
MgO	6.52			Zr	160

The identities of the detected elements producing γ-rays when activated were established by measurements of γ-rays energy and of half-life, whereas the concentrations of the elements were calculated for all principal γ-lines by reference to the standard according to the following equation:

$$W_2 = \frac{W_1 A_2 M_1}{A_1 M_2} \tag{1}$$

Where:

W_1 = the known concentration of certain isotope in the standard,
W_2 = the unkown concentration of the same isotope to be determined,
A_1 = the calculated area under the known peak after subtracting the background in the standard,
A_2 = the calculated area under the same peak after subtracting the background in the sample,
M_1 = the weight in gms of the standard samle,
M_2 = the weight in gms of the examined sample.

In case of elements which are absent or not quantitatively given in the international standard, spectrally pure elements were added as internal standard. In this case equation (1) is also valid after computing A_1 for the standard.

For elements which are absent in the standard and the addition of their spectrally pure grade was impossible, the general equation of decay and growth [TAYLOR, 1964] has been modified to suit our application. A correction factor K_2 which takes into consideration the change in the absolute value of neutron flux at the position of irradiation has been added [GUIRGUIS *et al.*, 1979]. This resulted in the following expression:

$$W_2 = \frac{A_2 K_2 M}{E}\left(1/Na\Phi\delta CB(1-e^{\frac{-0.693t_{ir}}{T1/2}} \cdot e^{\frac{-0.693t_d}{T1/2}}) \right) \tag{2}$$

where:

W_2 = unknown concentration,
A_2 = area under the peak after subtracting the background,
M = molecular weight,
E = relative efficiency of the Ge(Li) detector taken from the efficiency curve [Essa et al., 1974],
N = Avogadro's No (6.023×10^{23}),
a = percent abundance [Ledrer and Hollander, 1967],
Φ = thermal neutron flux (10^{12} neutron cm^{-2} sec^{-1}),
δC = neutron capture reaction cross sections in barns ($10^{-24} cm^2$),
B = branching ratio [Peakfind and Isoquam, 1975],
t_{1r} = irradiation time in minutes,
t_d = decay time in minutes,
$T1/2$ = half life in minutes [Peakfind and Isoquam, 1975].

RESULTS AND DISCUSSION

Nuclear data for the elements determined is shown in Table 2 and their concentration are given in Table 3. Gamma spectra obtained from standard W1 and the studied ilmenite sample are shown in *Figs 2, 3,* and *4.*

The infrared spectrogram of the ilmenite sample is shown in *Fig. 1.* The strong absorption band around 530 cm^{-1} may be due to TiO linkage while the two medium absorption bands at 460—440 cm^{-1} and 325 cm^{-1} may be due FeO linkage. In fact

Table 2

Nuclear data of the elements detected

Element	Product	Half life		Photo peaks used in keV
Scandium	^{46}Sc	83.9	d	889.3, 1120.5
Chromium	^{51}Cr	27.8	d	320.1
Iron	^{59}Fe	44.6	d	1099.3, 1291.6
Cobalt	^{60}Co	5.26	y	1173.2, 1332.5
Strontium	^{85}Sr	64.5	d	514
Zirconium	^{95}Zr	68.6	d	724.2, 756.9
Niobium	^{94}Nb	20 000	y	871.1
Silver	^{110}Ag	260	d	763.9
Barium	^{131}Ba	11.6	d	373.1
	^{133}Ba	1.62	d	56.8, 275.9
	^{133}Ba	7.2	y	160.7
Lanthanum	^{140}La	1.672	d	328.8, 815.8, 1596.6
Europium	^{154}Eu	7.8	y	1274.8
	^{152}Eu	12.7	y	1407.9
Ytterbium	^{175}Yb	4.21	d	112.4, 122.9, 144.9
				153.1, 396.3
	^{169}Yb	32	d	61.2, 86.2, 196
Lutetium	^{177}Lu	155	d	204.3
Hafnium	^{181}Hf	42.5	d	133.0, 482.2
	^{175}Hf	70	d	343.6
Tantalum	^{182}Ta	115	d	1189, 264.4
Gold	^{198}Au	64.8	h	412
Terbium	^{160}Tb	72.3	d	879.3
Cerium	^{143}Ce	33.0	h	57.4, 664.2
Silicon	^{31}Si	2.62	h	1266
Copper	^{64}Cu	12.80	h	511
Manganese	^{56}Mn	2.28	h	848
Nickel	^{65}Ni	2.569	h	1114

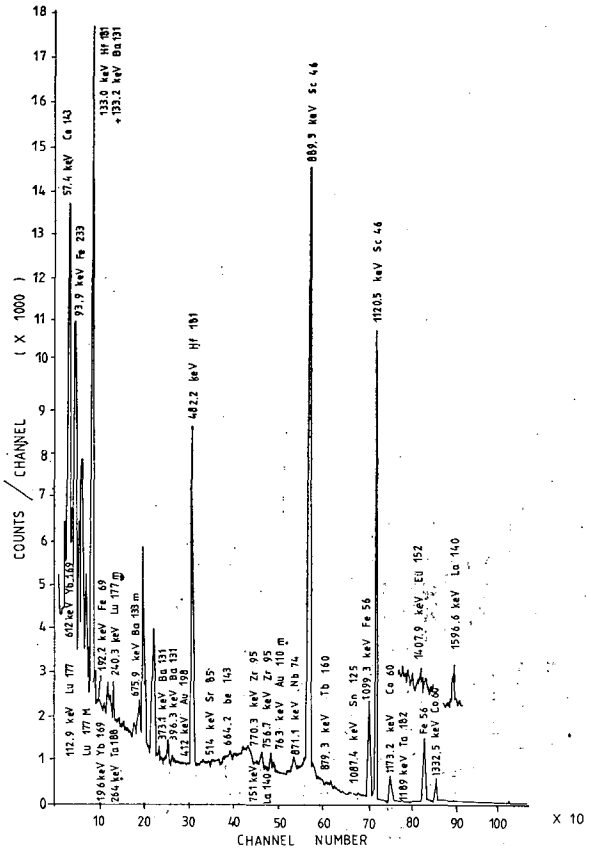

Fig. 2. Gamma-ray spectrum of irradiated standard sample W1 (irradiation time 35 hours, decay time 48 hours)

the spectrum is that of a typical ilmenite and is in good agreement with that given by CLAREMCE [1975]. Thus the fresh ilmenite sample used in the present study is very pure.

Major elements

In the present work TiO_2 was found to assay 84.04% while HAMMOUD [1975] and EL HINNAWI [1964] reported a value of 46.25 and 43.73%, respectively. Accordingly the iron content estimated by the activation represents the lowest value (46.98%). It has been concluded from DEAR *et al.*, [1966] that ilmenite is a titanate of ferrous iron ($Fe^{2+}Ti^{2+}O_3$) rather than a double oxide of ferric iron and titanium ($Fe^{3+}Ti^{3+}O_3$). In the present study MnO assays 0.064% indicating a sharp decrease from 1.35 and 0.20%, the value previously reported by HAMMOUD [1975], and EL HINNAWI [1964], respectively. This can be explained by the fact that the elements Ca, Mg, Ni, Cu, Co and Mn can substitute the Fe^{2+} ion in ilmenite [HAMMOUD, 1966] the formula may be fully expressed as (Fe, Mg, Mn) TiO_3 with only limited amount of Mg and

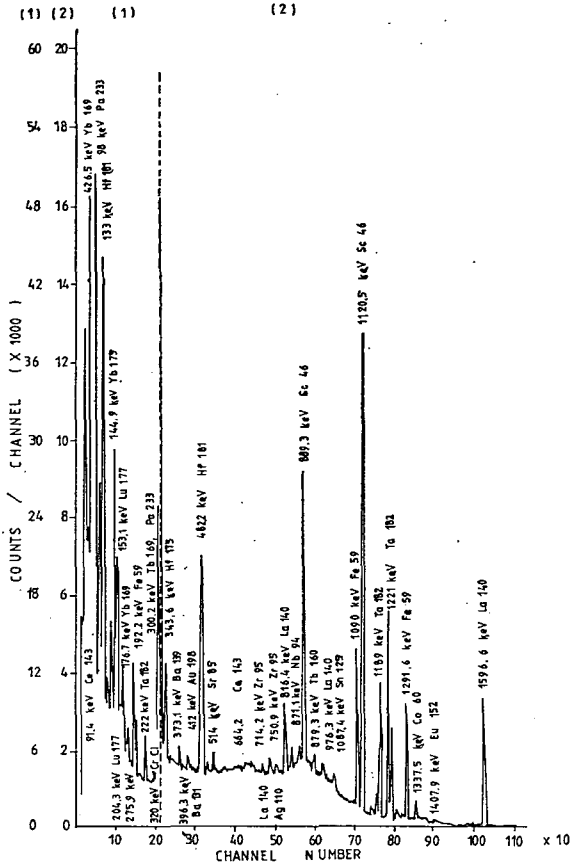

Fig. 3. Gamma-ray spectrum of irradiated ilmenite (irradiation and decay time as in *Fig. 2*)

Mn [DEER *et al.*, 1966]. MgO has actually not been detected in the present work although both HAMMOUD [1975] and EL HINNAWI [1964] ascertained its presence at a value of 0.65 and 0.64%, respectively. HAMMOUD [1975] gave an average concentration of 0,87% Al_2O_3, 0.14% V_2O_3 and 0.04% P_2O_5, However, this study reveals the complete absence of them.

The analysis of ilmenite showed the presence of 0.34% of Cr_2O_3 indicating the relation between ilmenite and the probable source of the basic rocks. This chromium oxide is estimated as 0.28% by HAMMOUD [1975], and as 400 ppm chromium by EL HINNAWI [1964].

SiO_2 in the studied ilmenite sample assays 0.27%. The figure is actually of the some order of magnitude as that found by EL HINNAWI [1964], while its amount up to 0.32% [HAMMOUD, 1975].

Trace elements

The concentration of trace elements is shown in Table 3. According to BRAUNLOW, [1979] the distribution of most trace elements is controlled by substitution for the major elements in crystallizing minerals, thus the divalent ions Ca, Mg, Ni,

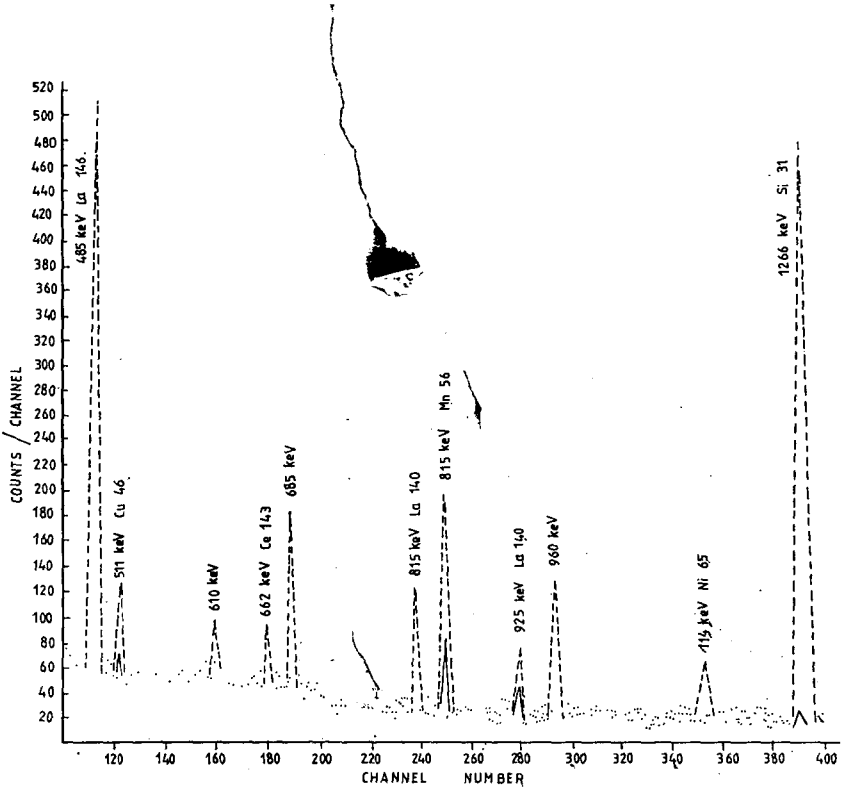

Fig. 4. Gamma-ray spectra of irradiated ilmenite (——) and the standard W1 sample (– – –) (irradiation time 4 hours, decay time 5 hours)

Cu, and Co may substitute Fe^{2+} in space lattice of ilmenite whereas trivalent ions of chromium and vanadium substitute mainly for ferric iron. The concentration of platinoid metals occurs as direct magmatic segregations in layered mafic intrusions [BRAUNLOW, 1979].

TABLE 3

Chemical composition of ilmenite by activation analysis

Element	Concentration %	Element	Concentration (ppm)	Element	Concentration (ppm)
FeO	46.980*	Co	76	Tb	17.713
TiO_2	48.040			La	328.20
SiO_2	0.270	Cu	20	Ta	416.62
Al_2O_3	—	Mn	500	Hf	89.73
V_2O_3	—	Nb	409	Au	0.504
MnO	0.064	Ni	50		
MgO	—			Eu	31.96
Cr_2O_3	0.430	Zr	211.46	Ba	50.00
CaO	—	Sc	34.304	Sr	76.16
P_2O_5	—	Yb	5.97	Ce	80.20
		Lu	0.076		
		Ag	0.036		

* Determined as Fe and calculated as FeO

CONCLUSION

Instrumental neutron activation analysis is a powerful non destructive technique for the determination of elements particularly the earths and platinum metals. As shown from the result a fraction of ppm lutetium and silver could be analysed. The presence of 0.430% chromium oxide have be[illegible] attributed to the origin of ilmenite as explained by SHUKRI [1950]. The authors [illegible]gest that this ilmenite is derived from the basic rocks of Upper Egypt, Sudan and Ethiopia, as the ilmenite segregates in gabbros and norites [RAGUIN, 1961].

REFERENCES

BOCTOR, N. Z. [1966]: Ore microscopic studies of the opaque minerals in Rosetta-Damietta black sands. M. Sc. thesis, Cairo Univ.

BRAUNLOW, A. H. [1979]: Geochemistry. Prentice-Hall Inc. Englewood Cliffs. N. J., p. 384.

CLAREMCE, K. JR. [1975]: Infrared and RAMAN spectroscopy of lunar and terrestial minerals. Academic Press, N. Y., San Francisco, London, p. 202.

DEER, W. A., R. HOWIE and J. ZUSSMAN [1966]: Rock forming minerals, **5**, J. Willey.

EL GORESY, A. A. [1962]: Mineragraphic study of ilmenite and magnetite from the Egyptian black sands. Cairo Centrel Lab. for Mineral Research. (Internal Report.)

EL HINNAWI, E. E. [1964]: Mineralogical and geochemical studies on Egyptian black sands. Beiträge zur Mineralogie und Petrographie **9**, p. 519.

ESSA, E. M., N. B. ROFAIEL, A. A. EL KADY, A. M. HASSAN and H. M. ABU ZEID [1974]: Response characteristics of Ge (Li) detector for thermal neutron capture. Gamma Ray Spectroscopy, ARE AEE./Rep. 192.

FARAG, A. M. [1958]: Stratigraphy of Egypt. Faculty of Science, Cairo University.

GOLDSCHMIDT, V. M. [1954]: Geochemistry, Clarendon Press, Oxford.

GUIRGUIS, L. A., T. M. NOWEIR and A. A. EL KADY [1979]: A rapid instrumental neutron activation method for multielement content of some Egyptian phosphate minerals. ARE. AEE/Rep. 239.

HAMMOUD, N. S. [1966]: Concentration of monazite from Egyptian black sand employing industrial techniques. M. Sc. thesis, Cairo University Egypt.

HAMMOUD, N. S. [1975]: A process for recovery low-chromium high grade ilmenite from north Egyptian beach deposits. Proccedings of the 11th International Mineral Processing Congress. Regione Autonoma Delta Sardegna, Italy.

MIKHAIL, M. A. [1971]: Distribution and sedimentation of ilmenite in black sands west of Rosetta. M. Sc. thesis, faculty of Science, Cairo University.

LEDERER, M., J. M. HOLLANDER [1967]: Tables of isotopes. Sixth edition, University of California, Berkeley.

PEAKFIND and ISOQUAM [1975]: Gamma ray library listing by energies with branching ratios and half lives. Oakridge, TN, USA.

RAGUIN, E. [1961]: Géologie des Gites Mineraux. Troisieme édition. Masson & Cie., Paris.

SHAPIRO, L. and W. W. BRANNOCK [1962]: Rapid analysis of silicates, carbonates and phosphate rocks. U. S. Geol. Survey. Bull. **1144**A.

SHUKRI, N. M. [1950]: The mineralogy of some Nile sediments. Quarterly Journal of the Geological Society of London, **105**, p. 511.

WASSEF, S. N. [1964]: Correlation of the sedimentation conditions of the Mediterranean beach east of Damietta to Suez canal by heavy minerals and isotopes applications. M. Sc. thesis. Faculty of Science, Ain Shams University, Cairo, Egypt.

Manuscript received, September 10, 1981

L. A. GUIRGUIS
and
S. N. WASSEF
Nuclear Materials Corporation
Cairo, Egypt

Acta Mineralogica—Petrographica, Szeged, XXV/2, 211—221, 1982

MINERALOGY AND GEOCHEMISTRY OF THE LEAD-ZINC MINERALIZATION AT RANGA, RED SEA COAST

M. RASMY and A. A. YONAN

ABSTRACT

The mineral association of Ranga lead-zinc deposit is microscopically described. The trace elements assemblage in cubic and zonal galena is quantitatively determined. Besides, the trace elements in other minerals associated with galena were semiquantitatively estimated. The deposit is attributed to the exhalative sedimentary processes by which other Egyptian Miocene lead-zinc ores were similarly formed.

INTRODUCTION

The Egyptian lead-zinc deposits of Miocene age occur in a narrow strip extending along the Red Sea coast between Qoseir and Ras Benas. They are mainly confined to the Middle Miocene formations which unconformably overlie the Precambrian

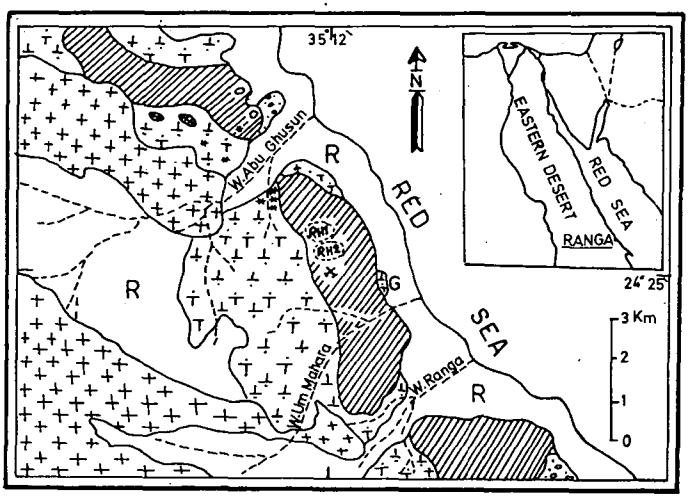

Fig. 1. Geological map of Wadi Abu Ghusun — Wadi Ranga area [after BEADNELL, 1924 with modifications after SAMUEL and SALEEB ROUFAIEL, 1977]

igneous and metamorphic rocks of the Basement Complex. The most important localities are Zug El Bohar, Wadi Essel, Wadi Wizr, Um Gheig, Abu Anz, Gabal El Rossas and Ranga [AMIN, 1955; SABET, *et al.*, 1966; EL SHAZLY, 1966 and HILMY, *et al.*, 1972].

EL SHAZLY and ABDALLAH [1964] described the mineralization at Ranga and recorded its occurrence as small lenticular masses within the gypseous rocks of the area. SOLIMAN and HASSAN [1969] gave the results of geochemical prospection along a 600 m profile section passing through the main lead-zinc deposit. SALEEB, ROUFAIEL and SAMUEL [1975] described some of the ore minerals of the deposit.

This mineralization occurs in a dolomitic bed intercalated within the gypsum-anhydrite horizon of Abu Dabbab Formation *(Figs 1, 2)*. A faulting system is believed to have played a principal role in the deposition of this deposit. As other Egyptian Miocene Pb-Zn deposits, it is thought to be stratigraphically, lithogically and structurally controlled [HILMY, *et al.*, 1972].

The aim of this work is to record the mineralogical and geochemical characteristics of the deposit. Its probable mode of occurrence is also suggested.

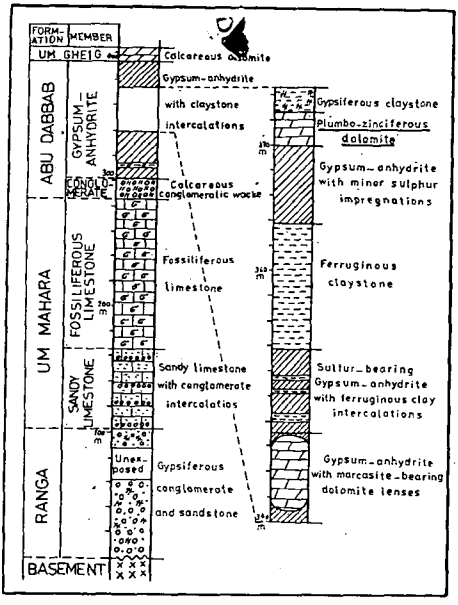

Fig. 2. Lithostratigraphic columnar section of Middle Miocene succession at Ranga area including Abu Dabbab Formation [after SALEEB ROUFAIEL & SAMUEL, 1975 & 1977]

SAMPLING

Galena, marcasite and zinc-rich samples were collected from old pits at two main sites at Ranga. Ferruginous samples were also collected in a network system

from the blanket-like "plane" gossan near the asphaltic road. The two red hills RH1 and RH2 were also sampled at 10 m intervals on the only accessible western slopes. Details of the sampling process are given in RASMY, *et al.*, [1981].

MINERALOGICAL STUDY OF THE DEPOSIT

The mineral assemblage, related to Ranga mineralization, is summarized in the following list:

I *Primary minerals:*

A Sulphide minerals: galena, sphalerite and marcasite.
B Gangue minerals: barite, fluorite and celestite.

II *Secondary minerals:*

A Lead-zinc minerals: cerussite, anglesite, smithsonite, hemimorphite and gloslarite.
B Associated minerals: native sulphur, jarosite, limonite, selenite and secondary quartz.

Galena occurs in two major forms. The first is "pisolitic" galena which exhibits a zonal structure. The pisolites are either spherical, oval, pear-shaped or eye-like and may reach 2 cm in mean diameter. The zonal structure is partially disclosed by rim-alteration to zonal cerussite *(Fig. 3)*. This form of galena is common in the dolomite band exposed in the pit nearest to the main sulphur mine. It indicates a very low temperature of formation [RAMDOHR, 1969]. The second form of galena exhibits the normal cubic crystal borders with cleavage planes parallel to (100). It has a slightly higher reflectivity than pisolitic galena. The cubic galena was recorded in a selenitic band exposed in a pit near the foot of the hill RH2. It is impregnated by coarse crystalline selenite which seems to have replaced older dolomite. Cubic galena is probably formed by the crystallisation of older colloform galena as the former replaces and encloses relics of the latter *(Fig. 4)*. Cubic galena is also later than melnicovite pyrite *(Fig. 5)*.

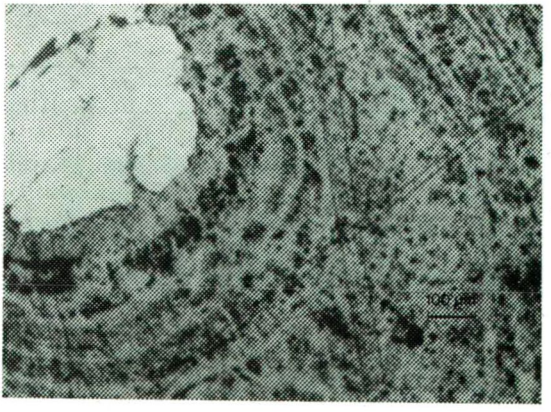

Fig. 3. Part of a "pisolitic" grain of galena (white) showing rim oxidation to cerussite (different shades of gray), reflected plane polarized light

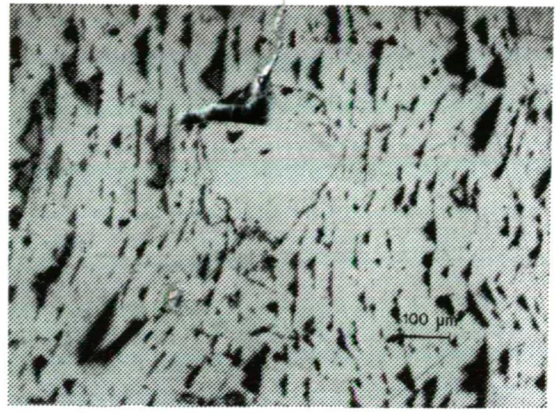

Fig. 4. Cubic galena showing the triangular pits and enclosing a grain of "pisolitic" galena, reflected plane polarized light

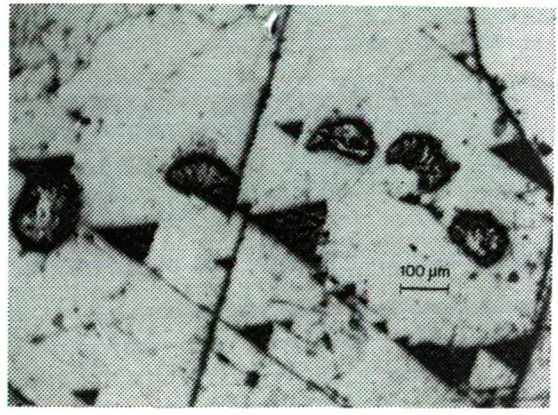

Fig. 5. Galena (white) enclosing parts of melnicovite spheres, black are triangular pits, reflected plane polarized light

Alteration of galena to anglesite is rather uncommon. It occurs along cracks and cleavage planes of galena. Galena is usually oxidized to cerussite in a way that the old texture of galena is still preserved *(Fig. 6)*. Besides, cerussite may invade galena giving rise to caries texture [EDWARDS, 1954] as shown in *Fig. 7*.

Remnants of fine solitary sphalerite dodecahedrons, which may cluster into aggregates, are occasionally observed within zincian and ferruginous rock masses. Sphalerite may also exhibit a framboidal form. Its low reflectivity and honey yellow internal reflection indicate its low Fe content.

Massive colloform bodies of marcasite usually replace dolomite at different sites in the area. It is partially recrystallized to radial star-like aggregates. Sometimes, it encloses rounded bodies of melnicovite pyrite which exhibits a rhythmic zonal texture *(Fig. 8)*. Marcasite is occasionally altered to jarosite and commonly to goethite and limonitic material. Massive colloform vein-like pitch-black bodies of

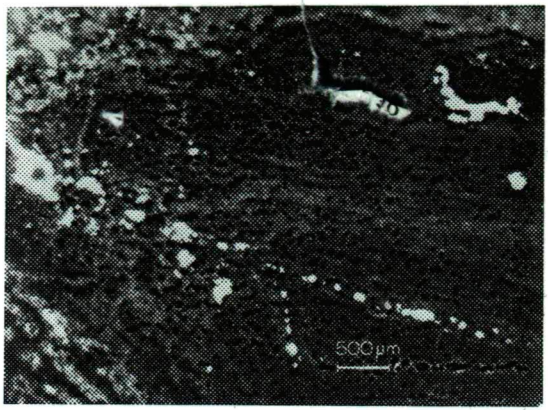

Fig. 6. Rim oxidation of cubic galena (black) to cerussite (different shades of gray), transmitted plane polarized light

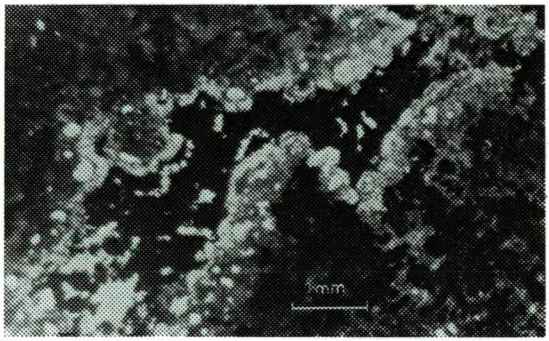

Fig. 7. Colloform aggregates of cerussite enclosing black fragments of goethite and replacing an elongated grain of galena (black) giving rise to caries texture, transmitted plane polarized light

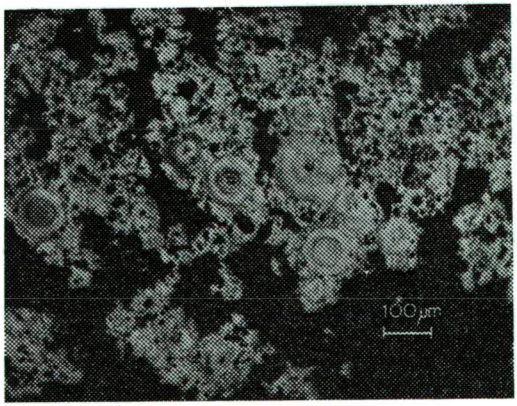

Fig. 8. Marcasite (white) enclosing spherulitic bodies of melnicovite, black is dolomite, reflected plane polarized light

goethite, after marcasite, are recorded at the top of the red hills where arid conditions of oxidation prevail.

Appreciable amounts of barium and strontium, indicated by spectral analysis, indicate the possible presence of barite and celestite which could not be microscopically distinguished. Traces of fluorite were chemically detected.

Cerussite, either as a direct oxidation product of galena or a recrystallisation form, is the most common secondary lead mineral *(Fig. 9.)*. Smithsonite usually forms cellular or saccharoidal crystals which fill cracks and incrust dolomitic and limonitic bodies. Sometimes it shows oolitic form. Radial, feathery or sheaf-like blades and rosettes of hemimorphite, in zinc-rich limonitic masses are not uncommon *(Fig. 10)*. It usually encloses relics of sphalerite and replaces limonite, cerussite and dolomite. Occasionally, very fine acicular crystals of goslarite, or probably epsomite, protrude from the massive zinc-rich limonitic bodies.

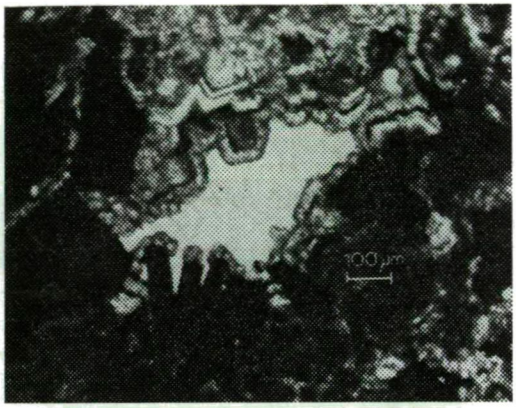

Fig. 9. Euhedral crystals of cerussite (gray) replacing iron oxides (black) and filling cavities, transmitted plane polarized light

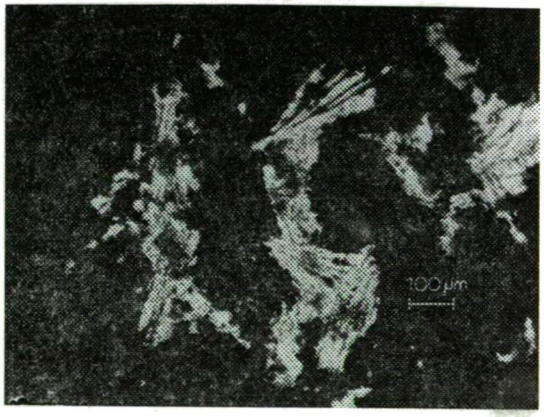

Fig. 10. Sheaf-like hemimorphite (white) replacing goethite (black), transmitted plane polarized light

The greenish-yellow aggregates of sulphur, associated with gypsum in several horizons of Abu Dabbab Formation, show no direct contact with the sulphide mineralisation. It is most probable that sulphur is produced through bacterial or hydrocarbonic reduction of sulphuric acid developed during wet oxidation of iron sulphides. Limonites, produced by oxidation of pyrite, are responsible for pigmenting most of the rock bodies at Ranga. Euhedral crystal aggregates of selenite, probably related to percolating ground water, fill cavities in aggregates of cubic galena and associated rocks. Secondary quartz is occasionally recorded.

PARAGENETIC STAGES

Three paragenetic stages could be identified at Ranga area:

1) *The mineralization stage:* This stage began with the deposition of melnicovite pyrite followed by marcasite, sphalerite and lastly colloform galena. The latter was later crystallized to cubic galena.

2) *The oxidation stage:* The oxidation of iron sulphides, by the action of percolating water, has led to the liberation of sulphuric acid responsible for the formation of anglesite, goslarite and sulphur. The sulphate minerals were later altered to cerussite and smithsonite by the action of natural water charged with calcium bicarbonate. The oxidized minerals were later subjected to partial recrystallisation.

3) *The silicification stage:* Hemimorphite and secondary quartz were formed by the action of silica-rich solutions on earlier zincian minerals.

GEOCHEMICAL STUDY OF THE DEPOSIT

This study includes the determination of trace elements in Ranga galena and the associated mineral phases which are related to the process of mineralization.

A) Trace elements in Ranga galena

Details of the emission spectrographic technique, used for the quantitative determination of trace elements in Ranga galena, are given in RASMY and YONAN [1981]. A summary of the analytical conditions is given here:

Apparatus:	Jena grating spectrograph PGS—2 and arc generator ABR 3. Slit width is 14 microns.
Excitation:	AC 220 V, 12 Amp.
Electrodes:	JMC 21/39 for sample and 21/19 for counter.
Carrier:	Specpure PbI_2 mixed as 20% with each of the samples and synthetic standards.
Arcing time:	57 sec., the first 10 sec. are not exposed.
Internal standard:	Background intensity in vicinity of lines.
Plates:	Gevaert Scientia 23D56 9×24 cm.
Calibration:	Jena microphotometer GII was used. Calibration curves were constructed by the 6 step diminisher method.

Detection limits are: 0.3 ppm for Ag; 1 ppm for Sn, Cu, Mo, In, V; 3 ppm for Cd, Bi, Tl; 10 for Zn, Sb; 30 for As and 300 ppm for Te. The concentration of trace elements in Ranga galena is shown in Table 1. The maximum content, arithmetic

TABLE 1

Trace elements content of Ranga pisolitic galena (samples 1—19) and cubic galena (samples 20—30) (values are in ppm)

Sample No.	Ag	Zn	Cd	Tl	Bi	Sn	Cu
1	1	15	10	16	—	—	5
2	2	14	17	48	—	—	1
3	4	24	11	17	15	1	3
4	—	29	14	25	—	—	3
5	2	92	15	19	11	—	1
6	—	14	22	30	—	—	1
7	6	100	11	5	7	1	15
8	2	15	10	23	—	2	3
9	—	225	19	25	—	—	3
10	3	28	5	22	31	—	3
11	—	100	23	27	10	2	1
12	2	—	13	18	15	—	2
13	5	25	10	33	8	—	1
14	2	27	8	22	12	—	3
15	17	14	12	11	4	—	15
16	2	18	8	40	5	—	1
17	—	16	8	5	9	—	30
18	17	14	11	26	—	—	40
19	1	42	3	32	5	—	10
20	1	15	10	100	4	—	5
21	—	15	15	80	9	3	1
22	4	13	32	45	3	1	2
23	2	—	15	78	7	—	4
24	2	100	17	39	13	1	3
25	2	110	15	75	3	—	1
26	—	100	15	40	12	—	3
27	4	—	8	134	13	2	25
28	1	18	12	52	13	—	1
29	2	20	11	76	13	—	5
30	2	25	15	45	10	—	1

mean and the interquartile range of Ranga galena, together with those of Um Gheig galena [RASMY, 1981], are given in Table 2. In calculating the arithmetic mean, dashes are considered to contribute with values equal to the half of the corresponding detection limits. The interquartile range is the range considered after excluding the first and fourth quartiles which may contain extremely low or high values.

It was observed that thallium is the most common guest element in Ranga galena. Its interquartile range is 22—52 ppm and is replacing lead isomorphously [ATANASOV and ESKENAZI, 1964]. Cubic galena contains more Tl than zonal galena. The Cd content is low, however, it cannot be solely attributed to sphalerite inclusions in galena. This is proved by the fact that some samples of galena contain more cadmium than zinc. Silver, bismuth, antimony, arsenic and other trace elements are either recorded in minor amounts or absent.

The impoverishment of silver and bismuth, and the irregular distribution of other trace elements, indicate low temperature, shallow and telethermal conditions of formation of galena [HERTEL, 1966; KAUTZSCH, 1967]. From Table 2, it can be concluded that Ranga galena, which occurs within gypseous rocks, is poorer in trace elements than Um Gheig galena occurring in lime grits.

TABLE 2

Maximum content (MC), arithmetic mean (AM) and interquartile range (IQR) of Ranga and Um Gheig galena. Total number of analysed samples is given in parenthesis (values are in ppm)

	Ag	Zn	Cd	Tl	Bi	Sn	Cu	Sb	As
Ranga galena (30):									
MC	17	225	32	134	31	3	30	10	30
AM	3	41	13	41	8	—	5		
IQR	1—3	14—28	10—15	23—52	3—12	—	1—5		
Um Gheig galena (38):									
MC	300	1300	840	410	203	32	8	100	1200
AM	41	254	154	85	21	1	—	18	148
IQR	4—52	18—118	21—220	16—124	0—15	—	—	0—18	31—130

N.B. Dashes indicate that the concentration of the elements is beyond their detection limits. The elements Mo, In, V, Sb, As & Te were not recorded in Ranga galena.

B. Trace elements in other minerals and rocks associated with galena

Owing to its disguising character, sphalerite could not be separated from mineralized rocks even under a binocular microscope. Actually, 27 zinc-rich samples were prepared for analysis, together with 6 samples of fresh marcasite and about 120 ferruginous samples enriched in both lead and zinc. The ferruginous samples were collected from the plane gossan and the two red hills *(Fig. 1)*.

The semiquantitative spectrographic technique used [RASMY and YONAN, 1981] is rather similar to the quantitative technique used for galena. The standard matrix was composed of 10% $CaCO_3$ and 90% SiO_2. Standards and samples were buffered by a synthetic mixture of graphite, silica and $CaCO_3$. Arcing time was 105 sec. Detection limits are: 1 ppm for each of Ag, Mo, Cu, Sn, Pb, Ga, Ni and Cr, 3 for Tl and V, 10 for Mn, Cd, Bi, Ge and In, and 30 ppm for As, Sb, Zn and Ba. Values of lead and zinc were checked by the dithizone wet chemical method.

From the analytical results, which are given in Table 3 A—C, the following can be observed:

1. The zincian minerals are enriched in Mn, poor in Cd and nearly devoid of Ga and Ge.

2. Marcasite contains minor amounts of lead and zinc which are probably attributed to submicroscopic inclusions of galena and sphalerite. Manganese is a major constituent in marcasite while arsenic is not detected.

3. The ferruginous samples show a small content of V, Mo, Cr and Cu. This may be attributed to the occasional presence of minute crystals of vanadinite $Pb_5(VO_4)_3Cl$, descloisite $Pb(Zn, Cu)(VO_4)OH$, wulfenite $PbMO_4$ and/or crocoite $PbCrO_4$.

4. In the oxidized ferruginous samples, some elements are generally impoverished, *e.g.*, silver and cadmium. On the other hand, some other elements were introduced to the area during or directly after the mineralization process. These elements include Ba, Mn, Mo, V, Cr, Ni and Cu. They are either in the form of independant minerals, *e.g.* barite, pyrolusite, etc., or they were captured during the precipitation of iron oxide and hydroxide minerals.

TABLE 3A

Maximum content, arithmetic mean and interquartile range of elements in 27 samples of Zn-rich minerals associated with Ranga galena (values are in ppm)

	Pb	Mn	Cd	Cu	Ag	Mo	Tl	Sn
MC	1500	10 000	200	300	8	10	5	10
AM	470	2 027	68	20	3	2	3	4
IQR	300—700	1200—2000	50—100	2	3	2	2	4

N. B. The elements As, Sb, Bi, In, Ge, V & Ga are present in values beyond their detection limits.

TABLE 3B

Maximum content, arithmetic mean and interquartile range of trace elements in 17 marcasite samples from Ranga (ppm)

	Pb	Zn	Mn	Cd	Cu	Ag	Mo
MC	300	5000	25 000	50	10	1	10
AM	130	1200	10 000	17	2	1	3
IQR	50—200	200—1000	3000—10 000				

N. B. The elements As, Sb, Bi, Ge, Tl, V, Sn & Ga are beyond their detection limits.

TABLE 3C

Maximum content, arithmetic mean and interquartile range of trace elements in Zn- and Pb-rich ferruginous samples from Ranga (ppm)

	Pb	Zn	Mn	Ba	Cu	Ag	Mo	V	Cr	Ni	Ga
Samples from plane gossan (79):											
MC	1200	1500	2000	4000	50	5	100	100	100	100	15
AM	465	500	670	770	10	1	9	27	34	6	4
IQR	400—500	300—600	200—1000	400—1000	7	—	7	20	25	5	3
Samples from red hill RH1 (16):											
MC	2300	1000	1000	3000	30	5	50	10	100	20	10
AM	683	416	144	400	8	1	8	5	25	3	2
Samples from red hill RH2 (21):											
MC	3000	1800	1000	5000	100	1	150	100	80	10	100
AM	852	629	78	293	22	1	38	28	24	4	17

N B. The elements As, Sb, Bi, In, Ge, Tl & Sn are beyond their detection limits.

ORIGIN OF THE DEPOSIT

The poor content of trace elements in Ranga galena may be attributed to the low temperature and shallow depth conditions of formation, to local factors and to the nature of the enclosing gypseous rocks. Remobilization of older lead, derived from the underlying crystalline rocks of the basement, may be the source of this galena. Sulphur, as a constituent of the sulphides, may be contributed by local reduc-

tion of gypsum, probably by the action of preexisting hydrocarbons. The whole process is a part of the exhalative sedimentary processes responsible for the deposition of other Miocene lead-zinc deposits [HILMY, *et al.*, 1972]. Post mineralization processes may be responsible for the introduction of some elements like barium, vanadium, molybdenum and chromium.

REFERENCES

AMIN, M. S. [1955]: Geological features of some mineral deposits in Egypt. Bull. Inst. Desert D'Egypte, **5**, 209—239.

ATANASOV, A. and G. ESKENAZI [1964]: Rare elements in galena from the Madjarovo deposit (Bulg.), Condishnik Sofiskiya Univ., Kniga, 1-Geol., **57**, 185—196 (1962—63).

EDWARDS, A. B. [1954]: Textures of the Ore Minerals and their Significance, 2nd ed., Austral. Inst. Min. Metall., Melbourne, 200 p.

EL SHAZLY, E. M. [1966]: Lead deposits in Egypt, Ann. Mines et Geol., Tunisie, **23**, 245—275.

EL SHAZLY, E. M. and A. M. ABDALLAH [1964]: The geology of the sulphur occurrence of Ranga, Eastern Desert, Geol. Surv. Egypt. Paper No. **31**.

HERTEL, L. [1966]: Die Fremdelementführung der Bleiglanze als Hilfe zur Bestimung der Bildungstemperatur. Erzmetall **19**, 632—635.

HILMY, M. E., F. M. NAKHLA and M. RASMY [1972]: Contribution to the mineralogy, geochemistry and genesis of the Miocene lead-zinc deposits in Egypt. Chem. Erde, **31**, 373—390.

KAUTZSCH, E. [1967]: Genesis of stratiform lead-zinc deposits in Central Europe. Econ. Geol., Monograph **3**, 133—137.

RAMDOHR, P. [1969]: The Ore Minerals and their Intergrowths, 3d ed., Pergamon, London.

RASMY, M. [1981]: Trace elements content of galena and associated minerals in Miocene lead-zinc deposits near Red Sea coast, Egypt. Geol. Rundschau **70** (in press).

RASMY M., G. S. SALEEB-ROUFAIEL and A. A. YONAN [1981]: Distribution of lead-and zinc at Ranga sulphur mine. Egypt. J. Geol., (in press).

RASMY, M. and A. A. YONAN [1981]: Development of some geochemical techniques used for the analysis of some Egyptian lead- and zinc-rich rocks. Bull. NRC, Cairo, (in press).

SABET, A. H., *et al.* [1966]: Geochronology of the lead-zinc mineralisation of Egypt, Assoc. Africa Geol. Surv., Tunisia Meeting.

SALEEB ROUFAIEL, G. S. and M. D. SAMUEL [1975]: Iron-lead-zinc sulphide mineralization and related sulphur in Miocene sediments at Ranga, Red Sea coast, Egypt. N. Jb. Geol. Paläont., Mh., **11**, 682—692.

SAMUEL, M. D. and G. S. SALEEB ROUFAIEL [1977]: Lithostratigraphy and petrographical analysis of the Neogene sediments at Abu Ghusun — Um Mahara area, Red Sea coast. Egypt. Freiberger Forschungshefte C **323**, 47—56.

SOLIMAN, S. M. and M. M. HASSAN [1969]: Contribution to the geology and geochemistry of lead-zinc and sulphur deposits of Gabal El Rossas, Ranga and Abu Anz localities, Eastern Desert. 6th Arab Sci. Congr., Part **4**, 591—660, Damascus.

Manuscript received, December 20, 1981

MOKHTAR RASMY
and
ADEL A. YONAN
Earth Sciences Lab.
National Research Centre
Dokki, Cairo
Egypt

Acta Mineralogica—Petrographica, Szeged, XXV/2, 223—230, 1982

ABOUT THE PLATE TECTONIC PATTERN OF THE MIDDLE EAST

G. M. SALLOUM and I. ABU EL-LEIL

ABSTRACT

The area of the Middle East and specially the Gulf of Suez, Gulf of Aqaba, Red Sea and Gulf of Aden are interesting from the tectonic point of view. The work presents the different theories formulated by many workers on this area, and gives new evidences and theory about the plate tectonics of the area under consideration based mainly upon the correlative studies of geographic continuity, petrography, geochemistry and structural trends.

The authors proposed the presence of three main tectonic plates, these are the African, Sinai (Levantine) and Arabian plates. The African plate tends to move in NW direction while the Arabian plate tends to move in NE direction. The dynamic resultant of these two (nearly perpendicular) trends was the separation of the Sinai plate. The geochronological events in the area were as follows: The presence of two major plates which are the African and Arabian, during the early Paleozoic, then the formation of the Gulf of Suez, which is dated back as Carboniferous or even older, then the opening of the Red Sea which actively take place during Eocene-Miocene period and finally the formation of the Gulf of Aqaba which is proposed to be formed mainly during Pliocene.

INTRODUCTION

Many theories had been proposed to explain the tectonic development of the Middle East. The geophysical data played the most important role and as a matter of fact sometimes, we get data which are not in harmony with the previous fixed data. The area of the Middle East is composed mainly of the African, Arabian, Levantine (Sinai) and Turkish plates. These plates were located south of the Paleozoic Tethys, as part of the northern margin of Gondwanaland.

The present work is an attempt to explain the plate tectonics of the African, Sinai and Arabian plates i.e. the plates surrounding the Egyptian area.

Sinai Peninsula plate is regarded by many investigators as the geographic and geologic extension of both the Eastern Desert of Egypt and the western part of the Saudi Arabia. However, this continuity is interrupted by the presence of the Suez and Aqaba Gulfs *(Fig. 3)*.

BALL [1911] concluded that, the Gulf of Suez ows its origin to erosion and secular oscillation rather than local subsidence by trough faulting. SWARTZ and ARDEN [1960] postulated that at the end of the lower Eocene the Sinai block moved towards the SE direction along NW-SE faults. SAID [1962] considers the Gulf of Suez as a rift valley. YOUSSEF [1968] arrived at a conclusion that the Gulfs of Suez and Aqaba have the trends of two complementary sets of wrench faults. MCKENZIE, *et al*,. [1970] visualized the Red Sea area with three tectonic plates: The Arabian, the Nubian and Sinai. The Arabian plate is moving in a NE direction, while the Nubian takes a westward direction. LE PICHON *et al.*, [1973] consider that, at the Gulf of

Suez there is a predicted right lateral strike slip with minor extension of about 30 kms. The Gulf of Suez is a north western branch of the Red Sea, which was subjected to an intense geological and geophysical researches, explaining that, the Red Sea is formed by a series of transcurrent faults [GIRDLER, 1966; ABDEL GAWAD, 1969], which are associated with the addition of new oceanic crust in the axial parts [PHILLIPS, 1970] and the drifting of Arabian to the NE direction [DAVIS and TRAMONTINI, 1970].

EL SOKKARY [1976], explain that, Sinai Peninsula underwent a rotational movement of 6° in an anticlockwise direction and over a distance of about 45 km during most probably Cretaceous Tertiary times in order to take the present day setting; while EL SHAZLY [1980], distinguished five NNW-SSE segments or old plates in the Egyptian Basement, these plates act alternatively as highs and lows.

The proposed theory and evidences

The purpose of this work is to present the pertinent geologic data, to consider it in relation to prior tectonic hypothesis and to deduce from it revised concepts of plate tectonics and evolution of this interesting region.

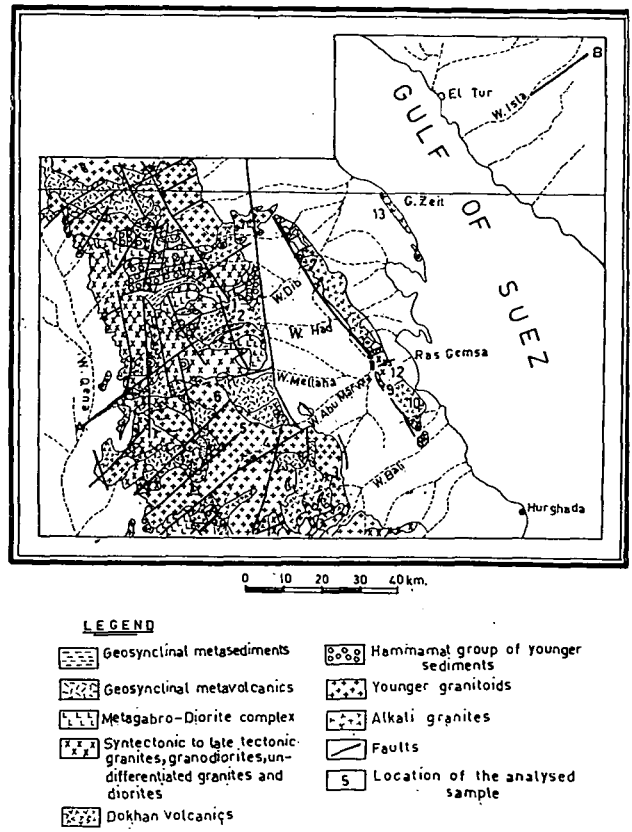

Fig. 1. Geologic map of main basement mass, Esh Mellaha and G. Zeit blocks [after EL RAMLY, 1972]

The correlation of the geographic position, petrography, structural trends and geochemistry of Esh Mellaha block comparable with the main basement mass lying to the west *(Fig. 1)*, shows a very close genetic similarity and both are controlled by deep-seated faults. Esh Mellaha block has about 80 km length and 5 km width. It is stretched in NNW-SSE direction.

The Esh Mellaha block is composed mainly of schists, metavolcanics, serpentinites, diorites, Dokhan volcanics, Hammamat mollasses and granites which are the same rock units outcropped in the opposite part of the main mass of the basement rocks (lie to west) [KABESH, *et al.*, 1970; FRANCIS, 1972].

Table 1 shows correlation of the geochemical analyses of some rocks sampled from the main mass of the basement rocks, Esh Mellaha block and Gabal Zeit (laying east of Esh Mellaha). The samples of rocks collected from each mass are very close in their petrographic composition and their geochemical analyses.

The detailed petrographic studies of the different rock units outcropping in the main basement mass, Esh Mellaha block and G. Zeit [SCHURMANN, 1966; KABESH *et al.*, 1970; FRANCIS, 1972; ABU EL-LEIL, 1980], reveal an addition evidence about their similarity and that they belong to one single mass (which later on drifted in separate blocks) and even belong to the same magmatic activity. We can summarize the main petrographic characteristics of the different rock units sampled from different blocks in the following from the oldest unit:

1. The metasediments are of low grade metamorphosed greywackey rocks, consist mainly of quartz and plagioclase feldspars in fine quartzo-feldspathic matrix having chlorite, biotite composition.
2. The Dokhan volcanics are ranging from intermediate to acidic rocks having the composition of andesite and rhyolite. The porphyrites predominate in all cases.
3. The granitic rocks are ranging from medium to coarse grained and from pale pink to red colour. They have the composition varying from granodiorites to leucocratic granites.

The close coincidence of the major Precambrian structural trends in the main mass of the basement rocks, Esh Mellaha, G. Zeit and the western part of Sinai Peninsula which are NNW-SSE in different blocks suggests the same opinion, that they form a single mass [EL RAMLY and SALLOUM, 1974; ABDALLAH and SALLOUM, 1978].

From the above mentioned data, the present authors came to the conclusion that, the main basement mass, Esh Mellaha block, G. Zeit and Sinai Peninsula were linked together during the Precambrian, and this Afro-Arabian plate would be moving north-north eastwards during the period 100—45 Ma in response of seafloor spreading in the south Atlantic and Indian oceans [SHELTON and GASS, 1979], in other words complex drifting was initiated in this area during mid-Triassic time and seas gradually invaded the subsiding block-faulted terrain.

The Esh Mellaha block was drifted from the main basement mass lying to the west, for a distance ranging from 10 kms in the northern part to about 25 kms in the southern part. Esh Mellaha block was twisted as a result of the drifting and so it is not parallel to the main mass of the basement complex but makes about 25° with its intersection. The resulting configuration is closely similar to the shape of the two coasts of the Gulf of Suez. In the first case the depressed area in between was filled by Meso-Cenozoic sediments, having thickness about 5 kms, which unconformably overlying the rocks of the basement complex. The oldest rock unit of this sedimentary sequence belong to the Carboniferous.

HAILWOOD and TARLING [1973] studied the Upper Devonian — Lower Carboni-

TABLE 1

Comparative average geochemical analyses

	Main mass of basement rocks						Esh El Mellaha Block						* G. Zeit
Contents / Sample No.	1	2	3	4	5	6	7	8	9	10	11	12	13
SiO_2	76.70	61.145	67.95	71.51	67.91	72.24	76.90	60.19	69.99	71.78	67.45	74.98	76.11
Al_2O_3	12.53	17.43	15.52	14.57	16.60	14.43	12.53	16.065	14.19	12.18	15.73	14.20	12.87
Fe_2O_3	1.67	4.00	1.83	2.55	1.86	1.17	1.59	4.29	1.42	1.55	2.39	0.93	0.96
FeO	0.37	1.19	1.94	0.43	1.69	1.34	0.25	1.49	0.55	0.78	1.88	0.61	0.74
MnO	0.01	0.155	0.04	0.04	0.07	0.24	0.01	0.135	0.06	0.08	—	—	—
MgO	0.19	2.26	0.27	0.67	1.13	0.29	0.18	2.675	0.45	1.04	1.31	0.34	0.60
CaO	0.67	3.80	2.81	1.23	1.87	0.85	0.81	4.00	3.99	1.73	1.72	1.38	0.33
Na_2O	4.56	2.875	4.67	4.41	4.33	3.32	4.39	3.67	5.07	4.73	4.34	3.60	4.18
K_2O	2.46	1.285	3.02	4.82	4.41	5.32	3.16	1.663	1.94	2.97	4.81	6.27	3.97
H_2O^+	0.15	1.97	1.11	0.18	0.10	0.46	0.31	2.06	0.78	1:16	0.29	0.47	—
H_2O^-	0.05	0.20	0.10	—	—	—	0.10	0.10	0.02	0.02	—	—	—
CO_2	0.16	2.39	—	—	—	—	0.37	1.91	—	—	—	—	—
TiO_2	0.22	1.34	0.55	0.10	0.10	0.10	0.14	0.895	0.51	0.68	trace	—	—
P_2O_5	0.05	0.275	0.32	—	—	—	0.05	0.30	0.41	0.17	trace	trace	—
Total	99.99	100.015	99.87	100.46	100.13	100.56	100.23	99.476	99.57	98.87	99.87	99.78	99.76

1 and 7 average geochemical analyses of keratophyre [after SCHURMANN, 1966]
2 and 8 average geochemical analyses of dark grey quartz porphyrite [after SCHURMANN, 1966]
3 and 9 average geochemical analyses of granodiorite [after SCHURMANN, 1966]
4 and 10 average geochemical analyses of pink leucocratic granites [4 after ABU EL-LEIL, 1980 and 10 after SCHURMANN, 1966]
5 and 11 average geochemical analyses of granodiorite-adamelite [5 after ABU EL-LEIL, 1980 and 11 after SCHURMANN, 1966]
6, 12 and 13 average geochemical analyses of coarse grained granites [6 after ABU EL-LEIL, 1980, 12 after KABESH *et al.*, 1970 and 13 after SCHURMANN, 1966]

* G. Zeit i e. G. = Gabal (arabic) = mountain

ferous pole positions and it has been indicated that during these periods Africa moved over the South Pole in a north westerly direction. During the Carboniferous, Sinai was linked to the Eastern Desert [EL SOKKARY, 1964; ANVAR and EL SOKKARY 1970; HUSSEIN, *et al.*, 1971].

DRAKE and GIRDLER [1964], deduced that Arabia suffered from an anticlockwise rotational movement relative to Africa by some 6° to 9°. It seems that drifting had occurred during Cretaceous and later times and was accompanied by the volcanic activity of the area [ANDREW, 1937; FARIS, *et al.*, 1953].

VAN DER PLOEG [1953] divided the Gulf of Suez into four structural provinces separated by three NNE-SSW fault zone *(Fig. 3)*. The provinces constitute two uplifted (I and III) and alternating with two depressed (II and IV). The Esh Mellaha and G. Zeit blocks lie within the uplifted province III.

VAN DER PLOEG's cross disturbances, SAID's shifting tectonic activity from west to east and the presence of seismicity at the mouth of the Gulf of Suez [FAIRHEAD and GIRDLER, 1971] all tend to suggest, that the disturbance represent a series of parallel strike slip faults along which active fracture zones tend to move progressively as an echelon taking a general eastwards direction.

The correlation of the geographic continuity, petrographic studies, geochemical analyses and structural trends of samples from the main basement complex, Esh Mellaha block, G. Zeit block and W. Araba block (Sinai), shows that they are strikingly similar.

The Red Sea indicates a strong positive gravity anomaly beneath a central deep trough some 50—70 kms wide, which indicates, that basic rocks occupy much of this narrow central zone [GIRDLER, 1958; GASS and GIBSON, 1969; ROBERTS, 1969]. So the Arabian sialic block has moved away from the African, the basic rocks in the fracture representing sub-sialic or oceanic crust. Such major structures with parallel sides have been called Rhombochasms [CAREY, 1958].

So, it is well known, that the Middle East region, particularly around the Egyptian territory is mainly controlled by the dynamics of three moving plates. The eastern Arabian plate is supposed to move in NE direction [DAVIS and TRAMONTINI, 1970]. The Western (African) plate is supposed to move in NW direction [HAILWOOD

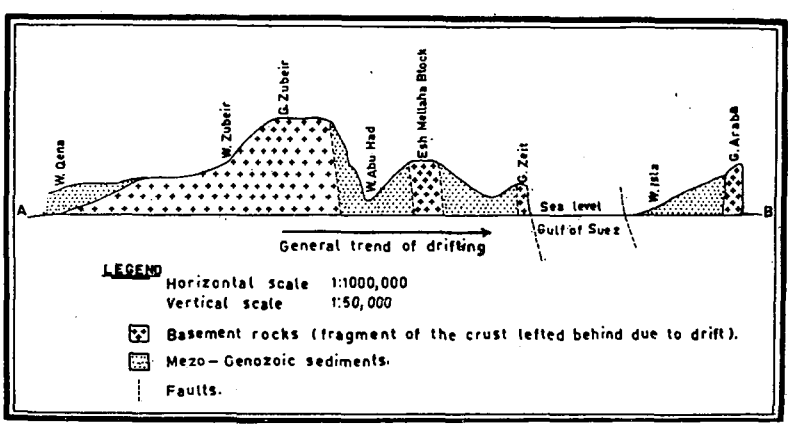

Fig. 2. Topographic profile along the area showing location of fault zones and the basement rocks

and TARLING, 1973]. Concerning the third Sinai (Levantine) plate, it was bounded by active system of transcurrent faults dominating along both the Gulf of Suez and Gulf of Aqaba (and extends further north up to the Dead Sea).

Admittedly, this region lies under the effect of three plates and the tectonics of the Middle East area will be explained on this basis.

During the early Paleozoic times were persisted only the African and Arabian plates. Sinai (Levantine) plate at these periods was behaving as a linked part to the Arabian plate. As stated above, the Arabian plate tend to move in NE direction, in the mean time, the African plate tend to move in NW direction.

The dynamic resultant of such nearly perpendicular trends is the splitting of the Sinai plate and the formation of NNW—SSE VAN DER PLOEG's transcurrent faults.

The supposed geochronological tectonic sequence of events in the area is as follows: the presence of two major African and Arabian plates during the early Paleozoic, then the formation of the Gulf of Suez, which is dated back as Carboniferous or even older as a result of sea floor-spreading. Then the opening of the Red Sea which actively took place during Eocene-Miocene period. Finally the formation of the Gulf of Aqaba which is proposed to be formed mainly during Pliocene and being still active.

It seems also, that Esh Mellaha block and G. Zeit block are fragments of crust which were left behind when the African and Arabian plates were drifted and separated as a result of sea floar spreading *(Fig. 2)*.

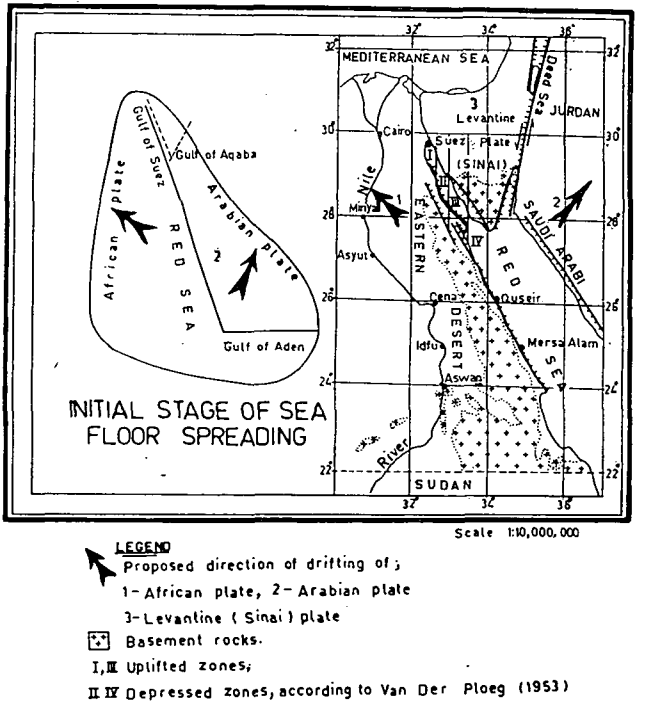

Fig. 3. Proposed plate tectonic map of the Middle East area

REFERENCES

ABDALLAH A. and G. M. SALLOUM: Precambrian structural trends in Eastern Desert and Sinai Peninsula, Egypt. (Under Public.)

ABDEL GAWAD, M. [1969]: New evidence of transcurrent movements in Red Sea area and petroleum implications. Am. Assoc. Petrol. Geol. Bull., **53**, No. 7. p. 1466—1479.

ABDEL GAWAD, M. [1970]: The Gulf of Suez, a brief review of stratigraphy and structure. Phil. Trans. Roy. Soc. London, **267**, No. 1181, p. 41—48.

ABU EL-LEIL, I. [1980]: Geology, petrography and geochemistry of some granitic rocks in the northern part of the basement complex, Egypt, Ph. D. Thesis, Faculty of Science, Al-Azhar Univ., Egypt.

ANDREW, G. [1937]: The late Tertiary igneous rocks of Egypt. Bull. Fac. Science, Cairo Univ., No. 10.

ANWAR, Y. M. and A. A. EL SOKKARY [1970]: Geochemical and paragenetic studies of Mn—Fe ores of west central Sinai, Egypt. Bull. Fac. Science, Alexandria Univ., **10**, p. 239—251.

BALL, J. [1911]: The Gulf of Suez. Geol. Mag., **VIII**, No. 1, p. 1—10.

CAREY, S. W. [1958]: The tectonic approach to continental drift, symposium on continental drift, Hobart, p. 177—355.

CHOUBERT, G. and A. FAURE MURET [1968]: Tectonic map of Africa Scale 1:15 000 000 UNESCO.

CLOOS, M. [1932]: Zur mechanik grosser Bruche und Graben. Centrabl. f. Min., p. 273—286.

DAVIS, D. and C. TRAMONTIRI [1970]: The deep structure of the Red Sea. Phil. Trans. Roy. Soc. London, **267**, No. 1181, p. 181—189.

DRAKE, C. L. and R. W. GIRDLER [1964]: A geophysical study of the Red Sea. Geophys. J. R. Astr. Soc., **8**, p. 473—495.

DIXEY, F. [1956]: The East African Rift system. Colon. Geol. and Min. Res., Suppt. Bull., No. 1.

EL RAMLY, M. F. and G. M. SALLOUM [1974]: The tectonic regioning of the Basement Rocks of the Eastern Desert of Egypt. Acta Miner.—Petr., Szeged XX1/2, p. 173—181.

EL SHAZLY, E. M. [1980]: Correlation and evolution of the Precambrian in Northeast Africa and Southwest Asia. Earth Science Review **16**, p. 303—312.

EL SOKKARY, A. A. [1964]: Geologic and mineralogic studies of some radioactive deposits in West Central Sinai. M. Sc. Thesis, Facult. of Science, Alexandria Univ.

EL SOKKARY, A. A. [1976]: Drifting of Sinai Peninsula, Egypt. Proc. Egypt. Acad. Sci., **XXIX**, p. 243—250.

EYAL, M., Y. BARTOU, A. E. SHIMRON and Y. K. BENTOR [1980]: Sinai Geological Map Geol. Surv. of Israel.

FAIRHEAD, J. D. and R. W. GINDLER [1971]: The seismicity of Africa. Geophys. J. R. Astr., **24**, p. 271—301.

FARIS, M. I. and I. KAMEL [1953]: Mid-Tertiary volcanicity of Egypt. Bull. Volcanologique, Serie II, **XIII**, p. 99—104.

FRANCIS, M. H. [1972]: Geology of the Basement complex in the north Eastern Desert between Latitudes 27° 30' and 28° 00' N. Annals **II**, Geol. Surv. of Egypt, Cairo.

GASS, I. G. and I. L. GIBSON [1969]: Structural evolution of the Rift zones in the Middle East. Nature Vol. 221, p. 926—930.

GIRDLER, R. W. [1958]: The relationship of the Red Sea to the East African rift system. Quart. Journ. Geol. Soc., **114**, p. 79—105.

GIRDLER, R. W. [1966]: The role of translational and rotational movements in the formation of the Red Sea and Gulf of Aden. Symposium on the world rift system. Geol. Surv., Ottawa, Canada, p. 65—77.

GIRDLER, R. W. [1969]: The Red Sea — a geophysical background. In: Hot brines and recent heavy metal deposits in the Red Sea. p. 38—58. New York, Springer-Verlag.

GIRDLER, R. W. [1970]: An aeromagnetic survey of the junction of the Red Sea, Gulf of Aden and Ethiopian rifts. A preliminary report. Phil. Trans. Roy. Soc. London, p. 359—368.

HAILWOOD, E. A. and D. H. TARLING [1973]: Paleomagnetic evidence for a proto-Atlantic Ocean. Implications of Continental Drift to the Earth Sciences, Vol. **1**, p. 37—46.

HEIRTZLER, J. R. [1937]: The evolution of the North Atlantic Ocean. Implications of Continental Drift to the Earth Sciences, Vol. **1**, p. 191—196.

HILLS, E. SH. [1975]: Elements of structural geology. Chapman and Hall Ltd.

HUSSIEN, H. A., Y. M. ANWAR and A. A. EL SOKKARY [1971]: Radiogeologic studies of some Carboniferous rocks of west central Sinai. UAR. J. Geol., **15**, No. 2, p. 119—127.

KABESH, M. L., A. M. LOTFY and A. M. REFAAT [1970]: Geology of Wadi El Mellaha area, Esh El Mellaha range, Eastern Desert, Egypt, J. Geol., **14**, No. 2, p. 53—84.

LE PICHON, X., J. FRANCHETEAU and J. BONNIN [1973]: Plate tectonics. Elsevier Scientific Publ. Co.

McKenzie, D. P. [1970]: Plate tectonics of the Mediterranean sea region. Nature, **226**, p. 239—243.
McKenzie, D. P., D. Davis and P. Molnar [1970]: Plate tectonics of the Red Sea and East Africa. Nature, **226**, p. 243—248.
Neev, D. [1975]: Tectonic evolution of the Middle East and the Levantine basin. J. Geology **3**, p. 683—686.
Neev, D. *et al.* [1973]: The geology of south eastern Mediterranean Sea. Israel Geol. Surv. Dept. M. G. 73—5—43 p.
Phillips, J. D. [1970]: Magnetic anomalies in the Red Sea. Phil. Trans. Roy. Soc. London, **267**, No. 1181, p. 205—217.
Roberts, D. G. [1969]: Structural evolution of the rift zones in the Middle East. Nature, **223**, p. 55—57.
Robson, D. A. [1970]: Suez Rift., Nature, **228**, p. 1237.
Said, R. [1962]: The geology of Egypt. Elsevier Publ. Co.
Schurmann, M. H. E. [1966]: The Precambrian along the Gulf of Suez and northern part of the Red Sea. E. J. Brill. Leiden.
Shelton, A. W. and I. G. Gass [1979]: Rotation of the Cyprus microplate. Ophiol. Proc. Intern. Ophiol. Symposium, Cyprus.
Swartz, D. H. and D. D. Arden [1960]: Geologic history of Red Sea area. Bull. Am. Ass. Petrol. Geol., **44**, p. 1621—1637.
Van Der Ploeg, P. [1953]: The world's oilfields — the eastern hemisphere. In the Science of Petrol. pt. **1**, p. 151—157. Oxford Univ. Press.
Yanshin, *et al.* [1966]: Tectonic Map of Eurasia. Scale 1:5 000 000, Moscow.
Youssef, M. I. [1968]: Structural pattern of Egypt and its interpretation. Bull. Am. Ass. Petrol. Geol., **52**, No. 4, p. 601—614.

Manuscript received, December 20, 1981

G. M. Salloum and J. Abu-El-Leil
Dept. of Geology, Faculty of Sciences
Al Azhar University
Cairo, Egypt

CONTENTS

Felelős kiadó: Grasselly Gyula
Készült: monószedéssel, íves magasnyomással, 9,1 A/5 ív terjedelemben,
az MSZ 5601—59 és 5602—55 szabvány szerint
Példányszám: 625
82-3265 — Szegedi Nyomda — Felelős vezető: Dobó József igazgató

NOTE TO CONTRIBUTORS

General

The Acta Mineralogica—Petrographica publishes original studies on the field of geochemistry, mineralogy and petrology, first of all studies of Hungarian researchers, papers resulted in by co-operation of Hungarian researchers and those of other countries and, in a limited volume, papers from abroad on topics of global interest.

Manuscripts should be written in English and submitted to the Editor-in-chief, Institute of Mineralogy, Geochemistry and Petrography, Attila József University, H-6701 Szeged, Pf. 428, Hungary.

The authors are responsible for the accuracy of their data, references and quotations from other sources.

Manuscript

Manuscripts should be typewritten with double spacing, 25 lines on a page and space for 50 letters in a line. Each new paragraph should begin with an indented line. Underline only words that should be typed in italics.

Manuscripts should generally be organized in the following order:

Title
Name(s) of author(s) and their affiliations, in foot-note the address of the author to whom the correspondence should be sent.
Abstract
Introduction
Methods, techniques, material studied, description of the area investigated, etc.
Results
Discussion or conclusions
Acknowledgement
Explanation of plates (if any)
Tables
Captions of figures (drawings, photomicrographs, etc.)

Abstract

The abstract cannot be longer than 500 words.

Tables

The tables should be typewritten on separate sheets and numbered according to their sequence in the text, which refers to all tables.

The title of the table as well as the column headings must be brief, but sufficiently explanatory.

The tables generally should not exceed the type-area of the journal, i.e. 12.5×18.5 cm. Fold-outs can only exceptionally be accepted.

Illustrations

Figures should be used only where they are essential to elucidate the text.

The illustrations should be numbered according to their sequence in the text, and in the text references should be made to each figure.

All illustrations should be given separately, not stuck on sheets and not folded. The number of the figure and the authors name should be noted on the reverse side of the photographs and on the lower frontside of drawings, indicating at the same time the top of the figure where it is necessary.

Captions for all figures should be given typewritten on a separate list at the end of the manuscript. Drawn text in the figures should be kept to a minimum.

Drawings should be made on tracing paper by Indian ink. The thickness of the lines and the size of the lettering should be big enough to allow a necessary reduction.

Photographs of good contrast and intensity on glossy paper are only acceptable. Colour photographs or drawings cannot be accepted.

Use bar scale on all illustrations instead of numerical scales that must be changed if reduction is necessary.

References

All references to publications made in the text should be made by quoting the author's name (without initials) and year of publication in parenthesis.

The list of references at the end of the manuscript should be arranged alphabetically by author's names and chronologically per author.

If the referred publications are written by more than two authors, in the text only the name of the first author should be indicated, the other co-authors are denoted by "et al.", however, in the list of references the names of authors and all co-authors should be mentioned.

In the list of references all references should be written, e.g. Balogh, K., A. Barabás [1972]: The Carboniferous and Permian of Hungary. Acta Miner. Petr., Szeged, XX/2, 191—207.

At references to books beside the author's name, year of publication, title and the publishing house should also be mentioned.

In the case of references for symposium volumes, special issues or multi-authors books, the following system should be used: Roser, B. P., C. W. Childs, and G. P. Glasby [1980:] Manganese in New Zealand. In: I. M. Varentsov and Gy. Grasselly (Editors): Geology and Geochemistry of Manganese, Vol. II. Akadémiai Kiadó, Budapest, 199—211.

Manuscripts that are not adequately prepared will be returned to the author(s).